2011-07-07

Prediction of Fluid Dielectric Constants

Jiangping Liu
Brigham Young University - Provo

Prediction of Fluid Dielectric Constants

Jiangping Liu

A dissertation submitted to the faculty of
Brigham Young University
in partial fulfillment of the requirements for the degree of

Doctor of Philosophy

Richard L. Rowley, Chair
Vincent W. Wilding
Dean R. Wheeler
Kenneth A. Solen
Thomas A. Knotts

Department of Chemical Engineering

Brigham Young University

August 2011

ABSTRACT

Prediction of Fluid Dielectric Constants

Jiangping Liu
Department of Chemical Engineering, BYU
Doctor of Philosophy

The dielectric constant (ε) or relative static permittivity of a material represents the capacitance of the material relative to a vacuum and is important in many industrial applications. Nevertheless, accurate experimental values are often unavailable and current prediction methods lack accuracy and are often unreliable. A new QSPR (quantitative structure-property relation) correlation of ε for pure organic chemicals is developed and tested. The average absolute percent error is expected to be less than 3% when applied to hydrocarbons and non-polar compounds and less than 18% when applied to polar compounds with ε values ranging from 1.0 to 50.0.

A local composition model is developed for mixture dielectric constants based on the Nonrandom-Two-Liquid (NRTL) model commonly used for correlating activity coefficients in vapor-liquid equilibrium data regression. It is predictive in that no mixture dielectric constant data are used and there are no adjustable parameters. Predictions made on 16 binary and six ternary systems at various compositions and temperatures compare favorably to extant correlations data that require experimental values to fit an adjustable parameter in the mixing rule and are significantly improved over values predicted by Oster's equation that also has no adjustable parameters.

In addition, molecular dynamics (MD) simulations provide an alternative to analytic relations. Results suggest that MD simulations require very accurate force field models, particularly with respect to the charge distribution within the molecules, to yield accurate pure chemical values of ε, but with the development of more accurate pure chemical force fields, it appears that mixture simulations of any number of components are likely possible. Using MD simulations, the impact of different portions of the force field on the calculated ε were examined. The results obtained suggest that rotational polarization arising from the permanent dipole moments makes the dominant contribution to ε. Changes in the dipole moment due to angle bending and bond stretching (distortion polarization) have less impact on ε than rotational polarization due to permanent dipole alignment, with angle bending being more significant than bond stretching.

Keywords: Jiangping Liu, dielectric constant, dipole moment, QSPR, molecular descriptors, NRTL, molecular dynamics simulations, polarization

ACKNOWLEDGMENTS

I would like to thank my wife Xuefei who has supported me throughout my studies. I also wish to thank my research advisor, Dr. Richard Rowley, for his constant encouragement and advice throughout my graduate research at Brigham Young University.

TABLE OF CONTENTS

LIST OF TABLES

LIST OF FIGURES

Chapter 1

Introduction

The dielectric constant (ε, DC) or relative static permittivity represents the capacitance of a material relative to that of a vacuum. The capacitance enhancement of a dielectric material arises from the orientation of charges within the material in response to an applied electrostatic field. Charge orientation within molecules is often thought of in terms of two constituent polarization modes: orientation or rotation polarization in which molecules with permanent dipoles experience an increase in dipole alignment from the thermally-driven random orientation, and distortion polarization in which atomic and electronic polarizations occur due to the effect of the applied field on bond lengths, bond angles and electron distribution within the molecule. Values of ε therefore characterize the polarizability of the material. Because they are a measure of polarizability, ε values have become important in industrial design processes for not only typifying the dielectric nature of the material, but also for providing solubility and separation information useful in separation designs, chemical equilibrium, and chemical reactivity analysis.

The dielectric constant of a material is directly related to charge separation within the constituent molecules and the mobility of the charges, both through rotational motion of any permanent charge separation (e.g., the dipole moment) and through electronic distortion or polarization of the molecule. The permanent dipole moment (μ, DM), associated with an

isolated molecule with no external field is an important physical property of materials in its own right, and has direct bearing on the dielectric nature of the fluid.

1.1 Dipole Moments

Dipole moments result from electronegativity differences of the atoms within a molecule. Although the sum of positive and negative charges in a neutral molecule is zero, local regions of net positive and negative charges created by the distribution of electrons in the molecule create an electric dipole. Specifically, molecules become dipolar when the electron density is higher toward the more electronegative atoms, leaving less electronegative atoms with a partial (relative to the charge on an electron) positive charge and the more electronegative atoms with a partial negative charge.

The permanent dipole moment of an isolated molecule, μ can be defined as

$$\mu = \left\langle \left| \sum_i e_i r_i \right| \right\rangle \ . \tag{1.1}$$

where the summation extends over all charges e_i (nuclei and electrons) in the molecule.[1] The position vector r_i may be referred to any origin as long as the molecule has no net charge. The expectation value shown in Eq. (1.1) implies a stationary state because theoretically the values of r_i could depend upon the vibrational, rotational and electronic states. At present there is no evidence of significant variation of dipole moment with rotational state.

The basic unit of dipole moment is the debye (D). One debye equals 10^{-18} electrostatic units-cm (esu·cm). Typically, dipole moments of organic molecules fall in the range of 0 to 5 D,

but some polymethine dyes have dipole moments around 20 D, and some proteins have DM values in the range of several hundred D. Gas-phase water has a dipole moment of about 1.85 D. It is commonly accepted that the dipole moment of liquid or solid water is enhanced relative to the gas phase, leading to values around 2.3-3.0 D[2]. The magnitude of the dipole moment depends on the size and symmetry of the molecule. Molecules having a center of symmetry are non-polar; molecules with no center of symmetry are polar to some extent.

1.1.1 The Application of Dipole Moments

Dipole moment is a fairly significant parameter used to characterize and aid in the determination of molecular structure, bond angles, and resonance.[3,4] For instance, the fact that carbon dioxide is symmetric around the carbon and has no dipole moment leads one to conclude that the molecule is linear. Water, on the other hand, which is also symmetric around the oxygen, cannot be linear because it has a nonzero dipole moment. Dipole moments can also be used to determine resonance from vibrational-rotational spectra where they are responsible for the interaction of the molecules with radiation in the infrared and microwave regions. The dipole moment has a large effect upon fluid properties as it is part of the intermolecular interactions that give rise to the properties. Such interactions range from small van der Waals forces (which create an attraction between molecules due to electron correlation between them) to dipole-dipole attractions from permanent molecular dipoles, to strong hydrogen-bonding interactions[5,6]. For example, the strong polar nature of water molecules gives rise to the large dipole-dipole interactions that produce hydrogen bonding, giving water a high surface tension and low vapor pressure relative to that which would be expected based on the molecular weight of the molecules.

1.1.2 Methods of Determining Dipole Moments

The existing experimental methods for determining dipole moments of molecules can be divided into two groups. The first group of methods is based on measuring the dielectric constant. It includes the methods proposed by Debye[11] for determining dipole moments in vapors and in dilute solutions of the polar substance in nonpolar solvents and the application of other theories and equations, such as Onsager's formulas. This group of methods will be discussed with dielectric constants in later subsections.

The second group includes methods based on microwave spectroscopy and molecular beams[7,8] and includes such methods as the Stark, molecular beam electric resonance, and non-resonant microwave absorption or dispersion methods. Unfortunately, the Stark method for determining dipole moments is limited by measurement of the effective spacing between electrodes. The electric resonance method has high accuracy, but the complexity of the apparatus and serious experimental difficulties limit the scope of its application. The microwave absorption method is particularly useful for substances with very small dipole moments. DM can be determined by a microwave absorption method with an uncertainty on the order of 2% for fluids with DM values as low as 0.1 D. DM can be measured for even less polar fluids, but with poorer accuracy. On the other hand, this method is confined to the gas phase and uses the three principal moments of inertia of the molecule with respect to the three main axes to calculate DM.

1.1.3 Influencing Factors for Dipole Moments

Because practical determination of dipole moments is based on the existence of an orientation polarization (except for the molecular beam method) of polar molecules in an applied electric field, measurements should be made ideally in the dilute gas phase where intermolecular interactions are minimized and the molecule can freely orient itself in the applied field. Dipole

moments obtained in the gas phase at very low pressures when the distance between the molecules is so large that electrostatic interactions between them are absent are the most theoretically consistent measurements.

Many of the reported dipole moments in the literature have been measured in the liquid phase using a solvent. Measurements are made at high dilution values to disperse the molecules of the test fluid so that they do not interact with each other as they would in the neat fluid. Solvents used are typically benzene, carbon tetrachloride, toluene, or another non-polar fluid, as these are thought to minimize solvent effects. However, the test fluid and solvent molecules do interact in the condensed phase, which can alter the dipole moment. Values in different solvents and in the gas phase can therefore be somewhat different. Higasi[8] and Frank[9] independently came to the same conclusion that the solvent effect depends on the shape of the molecule and the charge distribution in it. As a rule, dipole moments determined by the dilute solution method are somewhat lower than those found in the gas or vapor phase because of the electrostatic interaction with the solvent molecules.

1.2 Dielectric Constant

Dielectric constant (DC) is a fundamental molecular bulk property that can be a useful predictor of the behavior of substances on a macroscopic scale. The static dielectric constant, ε, also called the relative permittivity of the material, is defined as a ratio of the field strength of the external electric field in vacuum to that in the material for the same applied potential charge. Consider two parallel charged plates as shown in Figure 1.1 separated by a distance d with a total positive charge $+Q$ on the left plate and a total negative charge of $-Q$ on the right plate that creates a constant voltage difference V between the plates. The sketch on the left represents the

case where a vacuum is maintained between the plates; the one on the right represents the case of a fluid contained between them.

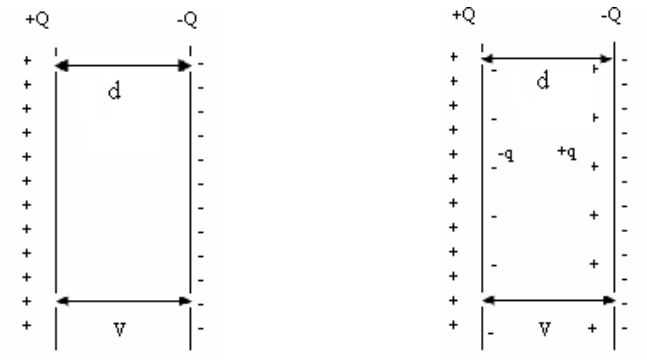

Figure 1.1 The relative permittivity of the material

The capacitance for the case of a vacuum is

$$C_0 = Q/V \,. \tag{1.2}$$

With a polarizable fluid between the two plates, an effective net charge of $-q$ can accumulate at the positive plate and an effective net positive charge of $+q$ can be present at the negative plate. Thus more charge can flow on to the plates for the same voltage drop as a result of the polarization of the dielectric placed between them. The capacitance of the plates is increased by the dielectric under the same voltage drop V to

$$C = (Q+q)/V \,. \tag{1.3}$$

The dielectric constant, or relative permittivity, ε, is defined as the ratio of the capacitance with the fluid to that of a vacuum

$$\varepsilon = C / C_0 = (Q + q) / Q \,. \qquad (1.4)$$

The permittivity of a material will be higher the greater the polarizability of the molecules. It is a measure of the ability of a substance to maintain a charge separation or to orient its molecular dipoles in the presence of an external electric field. Thus, the dielectric constant is an essential piece of information when designing capacitors.

The dielectric constant is particularly important for the interpretation of certain solvent-solute behavior. For example, a polar solvent (high dielectric constant) will dissolve a polar solute and a nonpolar solvent (low dielectric constant) will dissolve a nonpolar solute. So the dielectric constant of a solvent is a relative measure of its polarity which is important for separation designs, sample preparation in analytical chemistry, and chemical reactivity information.

As shown above, insertion of a dielectric between the plates increases the capacitance of the condenser. The cause of this increase is the polarization of the dielectric under the action of the applied electric field. At low and moderate densities, the DC is related to the polarizability of the molecule, α , via,

$$\varepsilon = 1 + 4\pi\rho\alpha \,. \qquad (1.5)$$

where ρ is the number density or number of molecules per unit volume. Because the electric field will cause a displacement of the electrons relative to the nucleus in each atom (electronic polarization), a displacement of the atomic nuclei relative to one another (atomic polarization), and also a displacement from the permanent dipole moment for polar molecules, the polarizability can be written as a sum of three terms:

$$\alpha = \alpha_e + \alpha_a + \alpha_o \tag{1.6}$$

where α is total polarizability of the molecule, and α_e, α_a and α_o are the electronic, atomic, and orientation polarizabilities, respectively. The magnitudes of these polarizations depend on the frequency of the applied alternating field as show in Figure 1.2. If the frequency of the alternating field used in the measurement is sufficiently high, dipolar molecules are unable to orient rapidly enough and the orientation term drops out, i.e., α_o = 0. The reduction of the polarization by high frequency is treated in Smyth, C.P[21].

Eq. (1.5) expresses the connection between the static dielectric constant, the polarizability of the molecule, and the density of the substance. It shows that the magnitude of the static dielectric constant is greater the higher the density of the substance and the greater the polarizability of the molecule.

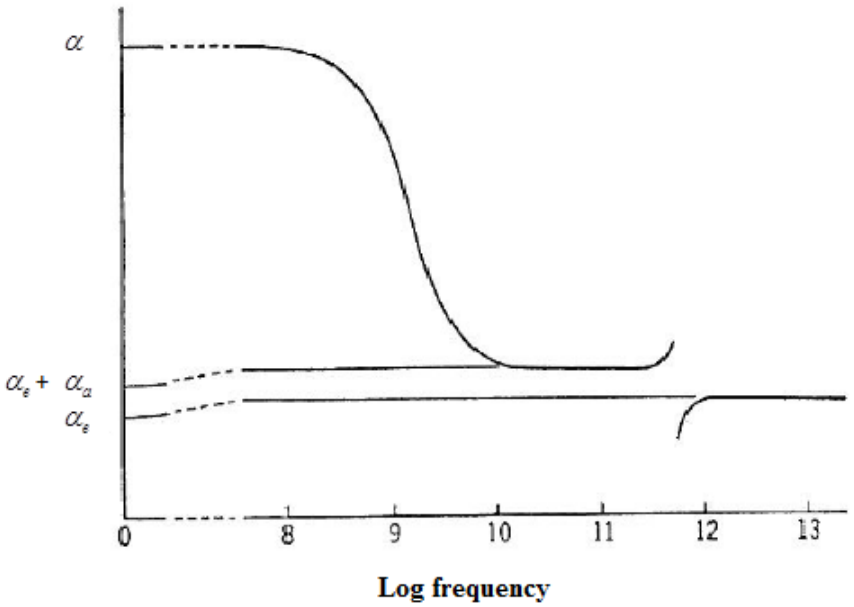

Figure 1.2 Total polarization against log frequency

At higher densities when there are many neighboring molecules, Eq. (1.5) is not strictly correct because it is no longer possible to neglect the action of the electrostatic field of the surrounding molecules. Under the external applied field, the electrostatic field created by the surrounding molecules is distorted, since the molecules are polarized and may in turn influence the neighboring molecules. Short-range interactions between the molecules cannot be neglected at higher densities.

1.2.1. Prediction of Dielectric Constant

While experimentally determined ε values are available for the most commonly used chemicals, there are a large number of industrially important chemicals for which no measured value is available in the literature. This was particularly apparent to the principals involved in the direction and maintenance of the DIPPR® 801 Pure Chemical Database[10] who have financially sponsored this project. A hallmark of the DIPPR database is "completeness," meaning that recommended constant property values or temperature-dependent correlations are provided in the database for all 45 properties of each chemical included in the database. This completeness philosophy requires that recommendations of property values be made from accurate, reliable prediction techniques when experimental data are not available. In the case of the dielectric constant, experimental data are available for only about 30% of the chemicals in the database. Unfortunately, most available prediction methods for ε are rather rudimentary and often fail significantly (with errors of 100% or more) for strongly polar compounds.

1.2.2 Development of Methods for Predicting Dielectric Constant

There is a need for accurate values of pure-component dielectric constants for new and developing processes and materials. Engineers working on such processes and materials depend

upon accurate values of physical properties including the dielectric constant. This need cannot be adequately met with the limited experimental data currently available. Databases such as the DIPPR® 801 Pure Chemical Database are intended to supply recommended values for needed physical properties by including accurately predicted values where experimental data are not available. None of the currently available methods for predicting dielectric constants are of adequate accuracy to be used to populate missing ε values in the DIPPR database for use by practicing engineers. An objective of this study is development of a pure-chemical method for prediction of dielectric constants with an uncertainty of less than 20% for essentially all compounds and less than 10% for the majority of compounds.

Context for the development of the new method is developed in Chapter 2 where the background and theory used in developing the existing prediction methods are discussed. These ideas provide the framework and foundation for development of the method proposed in this study. In Chapter 3, the quality and extent of the experimental DC values available in the DIPPR 801 database are assessed. A Quantitative Structure-Property (QSPR) approach is taken to develop the correlation proposed in this study. In obtaining an empirical correlation in this manner, it is essential that the training set of data be accurate and reliable. The analysis of the experimental data shown in Chapter 3 not only provides the DIPPR database with the best recommended experimental values, but defines a carefully analyzed training set from which an accurate correlation can be developed. The analysis was done by observing family trends, examining consistency in DC values between similar compounds, and obtaining additional literature values not yet in the DIPPR database. In developing the correlation for DC from the resultant training set, theory and practicality have guided the development work in so far as possible. For example, the strategy used was to retain the fewest possible molecular descriptors

in the QSPR correlation to avoid over-fitting the data and to choose descriptors representing the general underlying physics behind the DC to ensure extrapolation capability.

As the dipole moment is a key descriptor in the correlation developed in Chapter 3, broad applicability of the method requires a capability to also predict dipole moments. While this can be done with quantum mechanical methods, the accuracy of the value will depend upon the level of theory and basis set size used. We examine in Chapter 3 the quantum mechanical methods that can be used to predict dipole moments and to identify optimum model chemistry for accurate predictions. The impact of uncertainties in the dipole moment, when these are obtained from *ab initio* or density-functional methods, on the DC value obtained from the new correlation are also examined in Chapter 3.

The paucity of experimental data for the DC and the need for accurate predicted values is compounded when it comes to mixtures because of the infinite number of mixtures and compositions at which data values may be required. Chapter 4 explains the approach taken in this study to accurately predict mixture DC values. The method developed is applicable to mixtures of any number or type of constituent pure components. Building on the capability to predict pure component DC values developed in Chapter 3, the approach taken in Chapter 4 is to define an excess DC quantity, comparable to thermodynamic excess properties. The excess thermodynamic properties of mixture solutions arise from various intermolecular interactions. A local composition model is used for mixture dielectric constants based on the nonrandom two-liquid (NRTL) model commonly used for correlating activity coefficients in vapor-liquid equilibrium data regression. In this manner, mixture DC values can be predicted from the pure-chemical correlation and readily available thermodynamic mixture data without the use of adjustable parameters.

Molecular simulation provides an effective way of relating properties to the underlying interactions between molecules. In Chapter 5, the accurate representation of the dielectric properties of a solvent is a key to the proper description of electrostatic interactions between the solvent and solute molecules. Molecular simulations provide a suitable tool to analyze these properties at the molecular level, providing a direct route from microscopic details to macroscopic properties of experimental interest. A comparison of molecular dynamics and experimental results, both for pure components and mixtures, permits evaluation of the effectiveness of the force fields used to model the intermolecular interactions and a direct probe of the orientational polarization involved in the DC. While the results presented in Chapter 5 do not yet offer an accurate method for prediction of the DC, they do provide a basis for better understanding the molecular contributions to the experimental value and for further development of a predictive method as force-field models are improved.

Chapter 6 provides a summary of the work, insights into its significance, and additional questions that should be addressed in the future.

Chapter 2

Literature Review

2.1 Theory of Dipole Moments and Dielectric Constants

Debye[11] derived a general equation interrelating the dipole moment and dielectric permittivity:

$$\frac{\varepsilon-1}{\varepsilon+2}\frac{M}{\rho_m}=\frac{4\pi N_A}{3}(\alpha_0+\frac{\mu^2}{3k_BT}) \qquad (2.1)$$

where $\frac{\varepsilon-1}{\varepsilon+2}\frac{M}{\rho_m}$ is the molar polarization, ρ_m is the mass density, M is the molecular weight, N_A is Avogadro's number, k_B is Boltzmann's constant, 1.3806×10^{-23} J/K, T is the temperature (K), α_0 is the polarizability by distortion which is expressed as the average of the three polarizabilities along the three axes of the molecule treated as an ellipsoid of polarization, and $\frac{\mu^2}{3k_BT}$ is the polarizability by orientation.

Although the Debye equation holds for a wide variety of gases and vapors at ordinary pressures and has been successfully used to calculate approximate values of the molecular dipole moment from dielectric constants and densities of dilute solutions of polar molecules in nonpolar solvents, it is less accurate for pure liquids and for gases and vapors in which association, dissociation, or strong intermolecular forces occur.

The limitations of the Debye equation in determining dipole moments of liquids from their static dielectric constants led Onsager[12] to reexamine the effect of the internal electric field for polar, spherical molecules. He obtained

$$\frac{(\varepsilon - n^2)(2\varepsilon + n^2)}{\varepsilon(n^2+2)^2} = \frac{4\pi N_A \mu_0^{\,2}}{9k_B TV}, \qquad (2.2)$$

where n is refractive index, by using Maxwell's relation[13] $n^2 = \varepsilon_\infty$, where ε_∞ is the dielectric constant at very high frequencies. For a nonpolar liquid, $n^2 \approx \varepsilon$; whereas for a polar liquid, n^2 is equal to the dielectric constant ε_∞ measured at frequencies so high that the permanent dipoles are unable to contribute. In this equation use has been made of the relationship, $\mu = \frac{(\varepsilon_\infty + 2)(2\varepsilon + 1)}{3(2\varepsilon + \varepsilon_\infty)}\mu_0$, between μ the actual dipole moment and μ_0 the permanent dipole moment of the molecule.

Kirkwood [14,15] generalized the Onsager theory by eliminating the approximation of a uniform dielectric constant identical with the dielectric constant of the medium. The Kirkwood equation represents an advance beyond the Onsager theory because it takes into consideration the hindrance of molecular orientation by molecular interactions through a correlation coefficient parameter, *g*. This correlation coefficient is thought to be a measure of the hindered relative molecular orientation arising from short-range intermolecular interactions; it is expected to have a value close to unity for normal liquids but significantly lower than 1.0 for associated liquids. The Kirkwood equation is

$$\frac{(\varepsilon-1)(2\varepsilon+1)}{3\varepsilon}=\frac{4\pi N_A}{V}(\alpha_0+\frac{g\mu^2}{3k_BT}) \tag{2.3}$$

and a similar equation was used by Frolich[16]

$$\frac{(\varepsilon-1)(2\varepsilon+1)}{3\varepsilon}=\frac{4\pi N_A g\mu^2}{3k_BTV} \tag{2.4}$$

In general, available results indicate that the values of the dipole moment calculated for normal liquids by both the Onsager and the Kirkwood equation are in very good agreement with those obtained from measurement in the vapor phase.[17] Values of the correlation coefficient parameter, however, are neither readily available nor calculable.

The Debye equation can only be used to determine the dipole moment of polar molecules in the vapor phase. However, if the molecules are sufficiently separated from one another by nonpolar solvent molecules that reduce the interaction among the solute's permanent dipole moments, then the condensed system can resemble the dielectric behavior of the gas phase. This approach is used to determine the dipole moment of long molecular chains. Whereas simple molecules have permanent dipole moments that are similar, long molecules are continuously changing spatial conformations, and because the dipole moment associated with each conformation is generally different, the measured dipole moments are average values of the various configurations.

Guggenheim[18,19] and Smith[20] developed an equation for determining dipole moments from dielectric measurements in solution. As a consequence, the Guggeheim and Smith equation

is one of the most reliable methods that can be used to evaluate the dipole moments of isolated molecular chains. Their equation is

$$\frac{4}{3}\pi N_A\left(\alpha_{a2}-\alpha_{a2}^{'}\right)+\frac{\left\langle\mu^2\right\rangle}{3kT}=3M_2V_1\left[\frac{1}{\left(\varepsilon_1+2\right)^2}\frac{\partial\varepsilon}{\partial w_2}-\frac{1}{\left(n_1^2+2\right)^2}\frac{\partial n^2}{\partial w_2}\right] \tag{2.5}$$

$$\alpha_{a2}^{'}=\alpha_{a1}\frac{v_2}{v_1} \tag{2.6}$$

$$v_i=\frac{M_i}{\rho_{m,i}} \tag{2.7}$$

where α_{a2} is the atomic polarizability of the solute. Here, $\alpha_{a2}^{'}$ is the fictitious atomic polarizability, α_{a1} is the atomic polarizability of the solvent, v_2 is the molar volume of component 2 in the solution, v_1 is the molar volume of component 1 in the solution, V_1 is the specific volume of solvent, M_2 is the molecular weight of component 2, ε_1 is the dielectric constant of the solvent with $\varepsilon_1=n_1^2$, and w_2 is the weight fraction of the solute.

Additional theoretical approaches, such as the Clausius-Mosotti[21] equation

$$\frac{\varepsilon-1}{\varepsilon+2}\frac{M}{\rho_m}=\frac{4\pi N}{3}\alpha_0 \tag{2.8}$$

where α_0 is the polarizability per molecule and *N* is the number of molecules, have been based largely on Debye's dielectric theory.[22] The Clausius-Mosotti equation and others of this genre are generally useful only for dilute gases and some liquids of limited polarity. The previously

mentioned Onsager equation[23] and the Kirkwood[24,14] extension of this equation provide improvement for some polar fluids, but again their overall reliability is poor. The poor predictive behavior of these statistical mechanics equations suggests that orientational polarization effects have not been fully accounted for, particularly for fluids where stronger association is possible, as is the case with strongly hydrogen-bonding liquids such as water or alcohols. It is also likely that the inability to correlate the parameter *g* in the Kirkwood theory is due to multiple orientation and distortion polarization effects that are lumped into this parameter because of the difficulty in treating them explicitly. The extension of this concept to mixtures has been limited by the inherent complexities of orientational correlations among various polar species upon mixing.

The objective in this dissertation work is the prediction of the DC from the DM. The reverse is also possible. However, the estimation of dipole moments from experimentally-determined dielectric constants of polar and nonpolar compounds is not common because of the paucity of experimental dielectric constant values. Some methods for estimating DM strictly from structural information have been tried, but without a great deal of accuracy. The most accurate methods for estimating dipole moments require knowledge of the bond angles between atoms. Only a few such methods have been developed, and their complexity makes them unsuitable for inclusion here. Dipole moments of certain molecular structures can be closely estimated without resorting to large-scale *ab initio* computations. Fishtine[10] developed a fairly-easy method for calculating the dipole moment of substituted benzene, naphthalene derivatives, and heterocyclics containing nitrogen, oxygen, and sulfur, such as pyridine, furan, and thiophene. Excluded from this group are substituents that participate in hydrogen bonding, such as phenols

and anilines. Unfortunately, similar methods are not available for aliphatic and acyclic compounds. This method produces errors that are in the 2 - 30% range.

2.2 Available Predictive Methods for Dielectric Constant

The ability to predict dielectric constants theoretically is valuable in the molecular design of new materials. The ability to make fast and reliable predictions over a wide range of diverse chemical structures will substantially increase the ability to screen potential products based on DC values. However, due to the strong sensitivity of the dielectric constant to long-range electrostatic and intermolecular dispersion interactions, the problem of the prediction of the dielectric constant through theoretical calculation is complex.[25] The value of the dielectric constant is strongly related both to the chemical structure of a molecule and to intermolecular interactions. In addition, external conditions (temperature, pressure, etc.) need to be accounted for to obtain an accurate DC value. As indicated above, several theories and methods are available that often give diverse and contrasting results. Tomasi et al.[26] mentioned several computer simulation and molecular dynamics methods, including calculation of the average of the square of the total dipole moment of the system (fluctuation method), the polarization response method, the complete probability distribution of the net dipole moment, integral equations, in particular, the hypernetted chain (HNC) molecular integral equation and the molecular Ornstein-Zernike (OZ) theory.

As previously discussed, theoretical approaches, such as the Clausius-Mosotti equation based on Debye's dielectric theory are generally useful only for dilute gases and some liquids of limited polarity. The Onsager equation and the Kirkwood extension provide improvement for some polar fluids. While the Onsager equation works reasonably well for some small polar

liquids, it does not significantly take into account associations, and it is especially poor with strongly hydrogen-bonding liquids such as water or alcohols.

Several other methods have been proposed for correlating the dielectric constants of liquids with some physical properties. These empirical correlations are discussed by Horvath (1982).[27]

In its Progress Report (PR) 53 (May 2006), the BYU DIPPR-project staff made a comparison of the Thwing method, a group contribution method for estimation of the DC, to the Onsager method which was at the time the priority method accepted by the DIPPR 801 project. The results of that comparison indicated a significant inability to accurately estimate the DC in many cases. The results presented in PR 53 showed average absolute deviations (AAD) of 51.4% and 104% for the Onsager and Thwing methods, respectively, when applied to the 558 compounds for which experimental data were available in the 801 database. While the Onsager method performed adequately for many hydrocarbon families, the results were "disappointing for families containing polar groups, inorganic atoms, and polyfunctional groups, among others." Commonly the AAD for some of these families was 50% or higher. These poor results were particularly disturbing considering that the Onsager equation was specifically extended from the Debye and Claussius-Mossotti equations to account for permanent dipole moments and molecular polarizability. The Kirkwood equation is an extension of the Onsager equation developed to account for intermolecular associations, but has not been of practical use because of its inclusion of the unknown rotational correlation parameter, g.

Correlations have also been developed to relate ε to other measurable properties. The relationship between ε and the refractive index for non-polar molecules and between ε and μ are well-known and arise out of the previously mentioned theories. However, additional empirical

correlations have also been found. For example, there appears to be a strong relationship between surface tension and ε that has been exploited in fairly simple correlations between these two properties by Papazian[28] and Holmes[29]. Paruta and co-workers[30] found a strong correlation between the solubility parameter and ε as did Gorman and Hall.[31]. These correlations were developed for a relatively small numbers of compounds, often specific types of compounds. For example, the Paruta correlation was found to be particularly useful for hydrogen-bonding chemicals. These correlations provide useful but approximate estimations of ε, but they do not constitute accurate predictive equations.

Recently three Quantitative-Structure-Property Relations (QSPR) have been developed to predict the DC. In the past, the only way to obtain DC using just knowledge of the compound's structure was by indirect estimation through approximate relationships to other properties for which QSPR or group estimation methods were available. Such indirect methods include using the properties of surface tension, solubility parameter or dipole moments.

QSPR methods rely on various statistical techniques to find correlations between the investigated property and a predefined set of the theoretical molecular descriptors. Generally there is very little theory involved in development of the correlation between molecular structure and property values. The molecular descriptors themselves are often of a wide variety. Katrizky et al.[32,33] divides molecular descriptors into five main types: (1) constitutional descriptors; (2) topological descriptors; (3) electrostatic descriptors; (4) geometrical descriptors; (5) quantum chemical descriptors. Several common structural molecular descriptors have been used extensively to correlate thermophysical properties and have been widely adopted because of their accuracy and the ease of obtaining the descriptors.

Schweitzer et al.[34] used neural networks to build 70 000 models for a data set of 497 compounds ranging in ε values from 1 to 40. The best 119 models included six to twelve descriptors, but the best correlations still had relative errors larger than 100% for 37 compounds and larger than 50% for 115 compounds. Cocchi et al.[35] used a training set of only 23 compounds to develop a three-parameter QSPR model with a root-mean-squared (RMS) error of 2.26, which then produced a RMS of 4.65 for a training test set consisting of 20 compounds. More recently, Sild et al.[36] developed a QSPR correlation for ε and for the Kirkwood function that uses six molecular descriptors. The average error of their correlation was 23.3% for their training set of 155 compounds ranging in ε values from 1.87 to 46.5. Training sets for these methods were relatively small and extrapolation reliability generally decreases with smaller training sets and larger numbers of parameters.

2.3 Predictive Methods for Dipole Moments

As mentioned in the introduction, *ab initio* calculations are able to provide to some extent accurate calculations for molecular optimal geometries and electron distribution that can then be used to generate dipole moments. But this quantum mechanical approach involves assumptions as to how to model the overall molecular wave function (the level of theory) and the type and number of primitive functions with which to build the molecular wave function (the basis set). Choosing a level of theory and a basis set constitutes the model chemistry or assumptions upon which the results of the quantum chemical calculation rely.

Level of theory refers to representation of the multi-electron wavefunction through combining the single electron molecular orbitals which spread throughout the molecule. The simplest type of *ab initio* electronic structure calculation is the *Hartree-Fock* (HF) method, in which the instantaneous Coulombic electron-electron correlation is not specifically taken into

account, so there is no correlation between the electrons within the molecular system. It uses the Slater determinant (a determinant of molecular spin orbitals) as the model for the wavefunction. Perturbation methods such as the Möller-Plessett method and configurational integral methods can be used in place of HF methods to include electron correlation, but these methods are often time consuming. Density functional methods are much quicker and have been widely used even though they do not explicitly or completely account for electron correlation.

A basis set is a set of functions used to describe the shapes of single-electron molecular orbitals that comprise the molecular wavefunction used in the Schrödinger equation. Usually these basis functions are atomic orbitals, in that they are centered on the atomic nuclei. In order to optimally produce the shape of the single-electron molecular orbitals, linear combinations of different sizes of basis functions which model the single-electron atomic orbitals should be used to represent the molecular orbitals.

Usually, higher levels of theory and larger basis sets provide more flexibility in the shape of the molecular orbitals and produce lower (better) calculated energies at the cost of more integrals and computational time. For dipole moments, the problem is that there is no apparent convergence with basis set size and level of theory. The relationship of the model chemistry to the accuracy of calculated DM values has not been determined yet.

2.4 Summary of Current Predictive Capabilities

Several theoretical models and correlation models have been developed for calculating dielectric constants for some special groups of compounds. But the current state of theoretical and simulation methods does not provide general approaches for calculating dielectric constants for a wide variety of compounds with sufficient engineering accuracy for inclusion in the DIPPR

801 database. Also, none of the QSPR methods developed to date have the accuracy, flexibility, and universality to supply accurate predicted DC values for use in the DIPPR database project.

While *ab initio* calculation of dipole moments is not new, there are still significant difficulties in deciding the "best" model chemistry-the level of theory and basis set size for calculating DM values.

Chapter 3

QSPR Correlation of the Dielectric Constant for Organic Chemicals

The DIPPR® 801 database provides a convenient and powerful tool for QSPR development as over 154 molecular descriptors have been pre-calculated and tabulated in the database in addition to the collection of experimental property data available. In this work, ε data from the DIPPR® 801 database have been used to develop a new QSPR correlation for ε using the available properties and molecular descriptors. In so doing, the guiding philosophy was to use only descriptors with strong independent correlation to ε, minimize the number of descriptors in the correlation, and choose descriptors that rationally relate to the molecular physics presumed to underpin ε.

3.1 Development of the Training Set

Training data for the correlation, obtained from the DIPPR® 801 database, included 686 compounds. In analyzing and assessing the quality of the extant data, 201 new experimental values were obtained from the most recent CRC Chemistry Handbook[37] for missing the DC values in the DIPPR database. These values are given in the Table A.2. While the the DC is a function of temperature, values included in the DIPPR database are all defined at the reference temperature of 298.15 K. Dielectric constant values measured within a few Kelvins of the reference temperature were included in the database as reported; values measured at

temperatures differing from 298.15 K were included in the database with a note specifying the temperature at which they were measured, but their values were not used in the training set.

The dielectric constant was not originally included in the set of properties in the DIPPR 801 database. The DC was added to the DIPPR 801 database in 2005. At that time it was decided to extract from ready sources (handbooks, data compilations, etc.) available experimental values. This extraction process resulted in approximately 550 values that were put into the database. For new compounds entered into the database, after 2005, a full literature search is performed to find experimental DC values, and prediction methods are used for these new compounds when experimental data are not available. Therefore only a relatively small fraction of the compounds in that database have DC values. Because of the decision to rapidly enter the first 550 values as obtained from a single source, these values did not undergo the careful scrutiny for consistency characteristic of the other properties included in the DIPPR 801 project. For example, the family trend for the DC of the *n*-alkane family is shown in Figure 3.1. While all of the values were from the same source and listed as experimental, clearly the value for *n*-decane deviates from the trend for this family and is likely in error.

Assessment of the extant DC values in the database was therefore viewed as an important first step in developing a reliable training set from which to build a correlation for DC. This assessment resulted in 32 modifications to the recommended values in the database. Several of the changes (shown in Table A.3) were required because they were for the incorrect phase at the reference temperature.

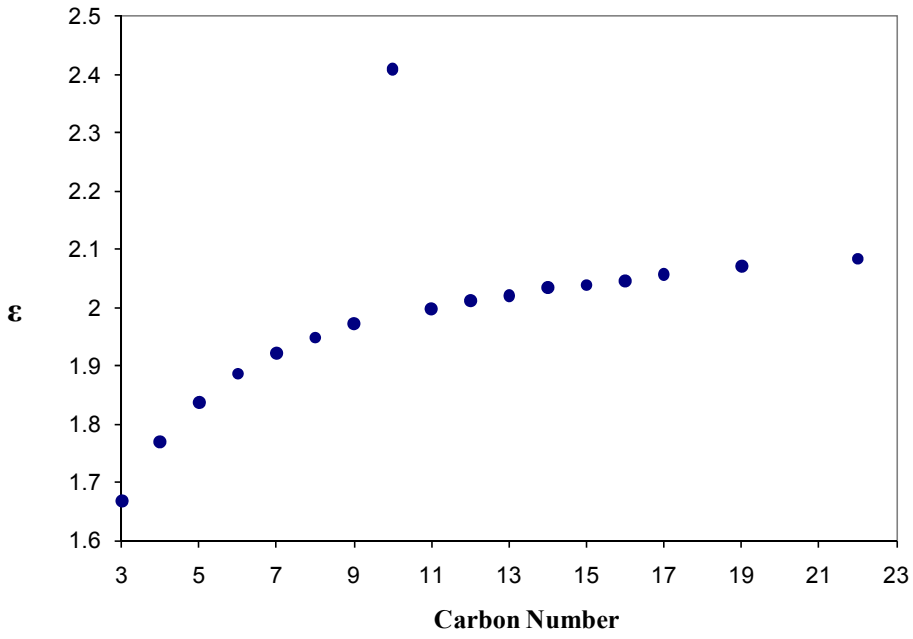

Figure 3.1 DC values for the *n*-alkane family

Only experimental ε values ranging from 1 to 50 were included in the training set. A few experimental values greater than 50 were available, ranging up to 179, but because these were scattered over such a wide DC range with very few representative compounds, they were not included in the training set. Instead, the applicable domain for the correlation was set as $1 \leq \varepsilon \leq 50$.

The training data were divided into two sets: non-polar and polar compounds. For our purposes, non-polar compounds are defined as (1) hydrocarbons, even though they may have a small dipole moment and (2) other organic molecules whose molecular structural symmetry produces no dipole moment. The non-polar training set included 167 chemicals with ε values ranging from 1.76 to 3.35. The polar training set included the remaining 519 chemicals covering a wide range of chemical functionality.

A total of 315 molecular descriptors and physical properties were available either in the DIPPR® 801 database or as directly generated using CODESSA[38] (Comprehensive Descriptors for Structural and Statistical Analysis). In both cases, the descriptors are based on the optimized molecular geometry and electron distributions obtained using Gaussian98[39] HF/6-31G* calculations. Many molecular descriptors are not extremely sensitive to the model chemistry used to generate them, and this is particularly true of the descriptors selected in the final correlation. The available molecular descriptors included structural, topological, electronic, geometric and chemical groups.

A stepwise multiple-linear-regression (MLR) analysis was applied to select the most significant descriptors for a linear QSPR model using Tsar QSAR,[40] a fully integrated analysis package for investigation of Quantitative Structure-Activity Relationships (QSAR). Collinearity and cross-correlation coefficients in Tsar QSAR were used to reduce the original 315-descriptor set to fewer than 20. In so doing, tightly coupled parameters often gave similar correlation coefficients. In this case, the descriptor with the most perceived physical significance and general availability was retained.

The final independent variables were chosen based on (1) sensitivity of ε to the descriptor, (2) a perceived direct relation of the descriptor to the molecular nature of the dielectric constant, and (3) ready availability of the descriptor values to users of the correlation. For example, ε was found to be strongly correlated collinearly to the van der Waals surface area and the Kier-Hall index of order 0, but the former was chosen because of its availability in the main tables of the DIPPR® 801 database. The strongest correlation was found between ε and refractive index (n), dipole moment (μ), solubility parameter (δ), and van der Waals area (ω, $A_{\underline{vdw}}$). Refractive index and dipole moment are of course prominent in the theoretical equations

for dielectric constant and would be expected to be important in its correlation. We can rationalize the other two descriptors as well. The van der Waals area is related to the degree of van der Waals forces among electron correlations. The solubility parameter is related to the energy required to separate molecules from each other.

3.2 Results and Analysis

The final correlation developed contains four molecular descriptors or properties supplemented with nine specific group contribution values for molecules containing oxygen atoms. Chemicals without oxygen atoms were well-correlated with the four descriptors. We speculate that orientation-specific interactions and associations (e.g., hydrogen bonds) that are more prevalent in oxygen-containing molecules may account for the necessity of adding group-specific interactions to the correlation for these compounds.

The general correlation can be written as

$$\ln \varepsilon = C_0 + C_1\left(\frac{\mu}{\mathrm{D}}\right) + C_2\left(\frac{\omega}{\mathrm{m^2 kmol^{-1}}}\right)^{-1} + C_3\left(\frac{\delta}{\mathrm{J^{1/2} m^{3/2}}}\right) + C_4 n^2 + \sum_{i}^{\text{O groups}} \frac{G_i}{k_i} \qquad (3.1)$$

in which G_i are the contributions for the oxygen-containing group i, the values of which are given in Table 3.1, and k_i is the number of instances of group i in the molecule. Obviously, the group contribution term in Eq. (3.1) is to be used only when $k_i > 0$, that is when there is at least one group i present in the molecule.

Values of the correlation coefficients C_i to be used in Eq. (3.1) are given in Table 3.2. Separate regressions were performed on the two training sets yielding different values for the C_i

to be used in predicting ε values for non-polar or polar compounds. Note that $C_2 = 0$ for non-polar/hydrocarbon fluids because the van der Waals force from an induced dipole has less impact for a non-polar fluid so that the correlation for these compounds is only a function of the three descriptors: n, μ and δ, and Eq. (3.1) can be written as

$$\ln \varepsilon = C_0 + C_1\left(\frac{\mu}{\mathrm{D}}\right) + C_3\left(\frac{\delta}{\mathrm{J}^{1/2}\mathrm{m}^{3/2}}\right) + C_4 n^2 \quad \text{(nonpolar and hydrocarbon)} \tag{3.2}$$

Table 3.1 Group contribution values, G_i, for molecules containing oxygen atoms

Group	Example	G_i	Group	Example	G_i
[S,N,P]=O	Thionyl chloride	0.2879	-OH	Alcohol	0.2230
>C=O	Ketones	0.3615	-OH	Phenol	0.0990
>C=O ring	2-pyrrolidone	0.0075	-OH (C<5)*	Ethanol	0.3348
-COO-	Esters	-0.0650	CHO	Aldehydes	0.1617
-COOH	Acids	-0.5900			

*applied in addition to regular –OH group for molecules with fewer than 5 C atoms

Table 3.2 Correlation coefficients for Eq.(3.1)

	C_0	C_1	C_2	C_3	C_4
non-polar	-0.1694	0.1283	0	2.8251×10^{-5}	0.2150
polar	-0.3416	0.5239	4.072×10^{-8}	7.408×10^{-5}	-0.3248

This three-parameter correlation for non-polar and hydrocarbon fluids fits the training set data with the cross-validated R^2 value of 0.9459, an average absolute deviation (AAD) of 0.07, and an average absolute percent deviation (AAPD) of 2.96%. The correlation of calculated and experimental values is shown in Figure 3.2.

The correlation given in Eq. (3.1) represents the 519 compounds in the polar training set well with a few exceptions. The uncertainty in the experimental data is significantly higher for these compounds and our critical examination of the data coupled with the inability of the wide range of possible descriptors to significantly improve the correlation suggests that we are approaching the limit of data accuracy. Figure 3.3 shows the final correlation of calculated and experimental values using Eq. (3.1), which yielded a cross validated R^2 value of 0.8416, an AAD of 2.05, and an AAPD of 17.8%.

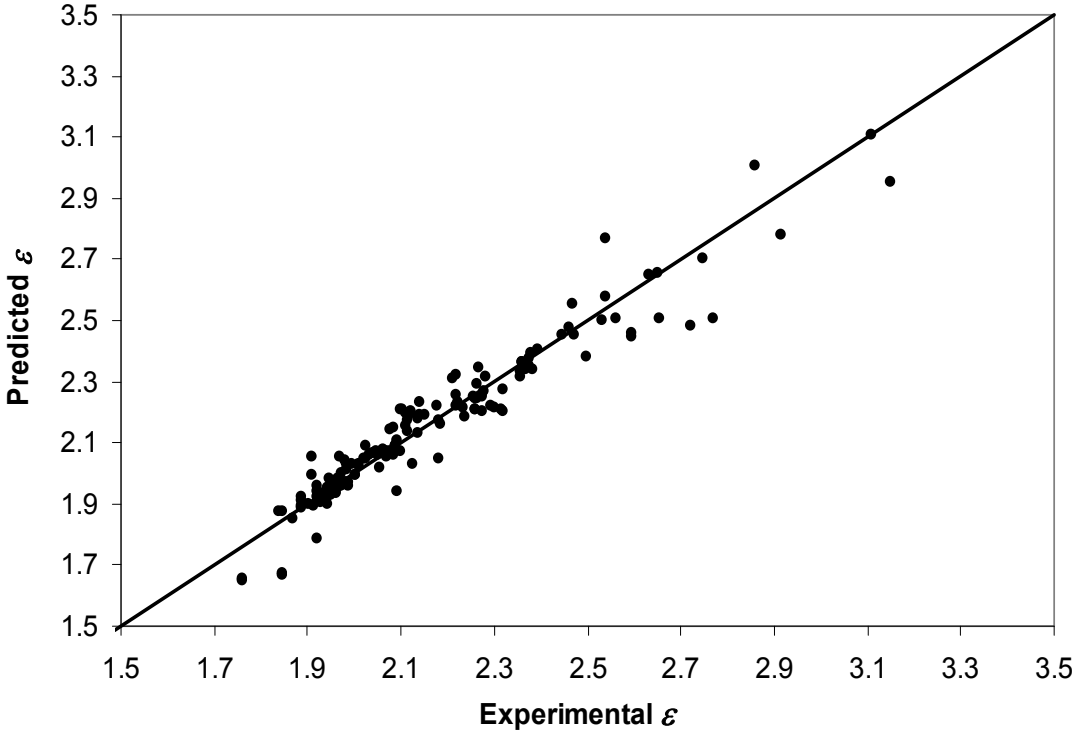

Figure 3.2 Correlated versus experimental values of ε for non-polar training set

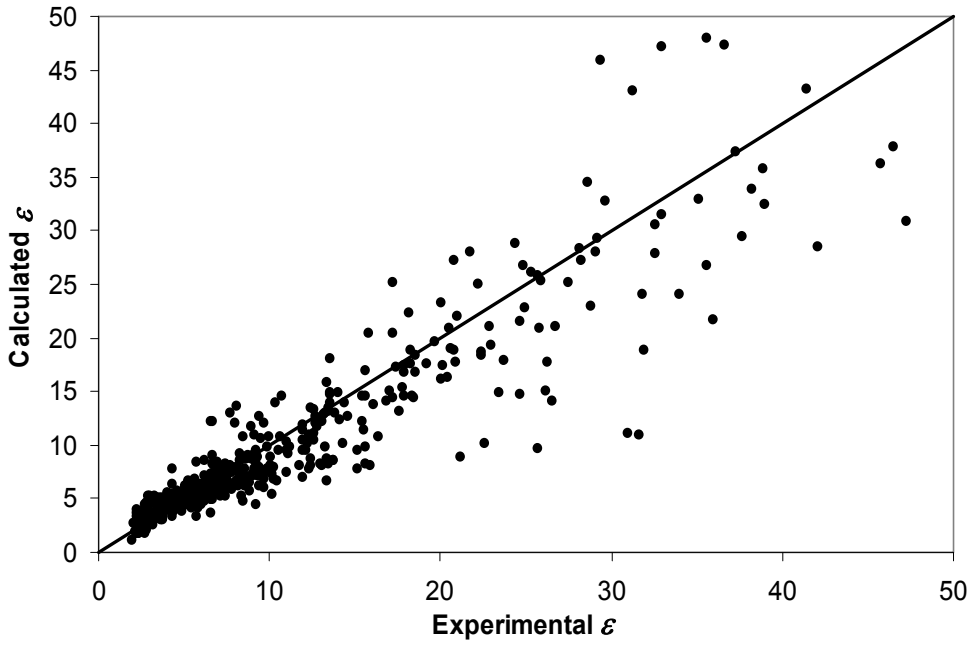

Figure 3.3 Correlated versus experimental values of ε for the polar training set

The correlation represents available experimental values of ε up to 10 extremely well, a range that includes 67.24 % of the training set. Larger deviations are observed for compounds with very high values of ε. There appears to be several outliers around $\varepsilon = 31$. These are for 1, 4-butanediol ($\varepsilon = 31.9$), 3-chloro-1, 2-propanediol ($\varepsilon = 31$), and ethyl cyanoacetate ($\varepsilon = 31.62$). These compounds have multiple polar groups, two –OH groups in the case of the two diol compounds and a cyano and ester groups in the case of ethyl cyanoacetate. Many of the chemicals with high dielectric constant values also have multiple polar groups within them. Unfortunately, the current correlation cannot account for potential internal group-group interactions and other induction effects that are likely to affect the molecular charge distribution and polarizability of the molecule. Available experimental data and their accuracy are currently inadequate to further refine the correlation to include such effects. Likely such a refinement would require a substantial set of group-contribution parameters determined from few

experimental data which decreases the reliability of the use of the correlation to predict unknown ε values.

A breakdown of the correlation results, Figure 3.4, shows that 55% (283 compounds) of the $\boldsymbol{\varepsilon}$ values in the polar training set are within 1.0 of the experimental values and 73% (379 compounds) are within 2.0 of the experimental values. In terms of percentage error, Eq.(4.1) correlates 45% of the compounds within 10% of the experimental values; 81% are correlated within 30% of the experimental values.

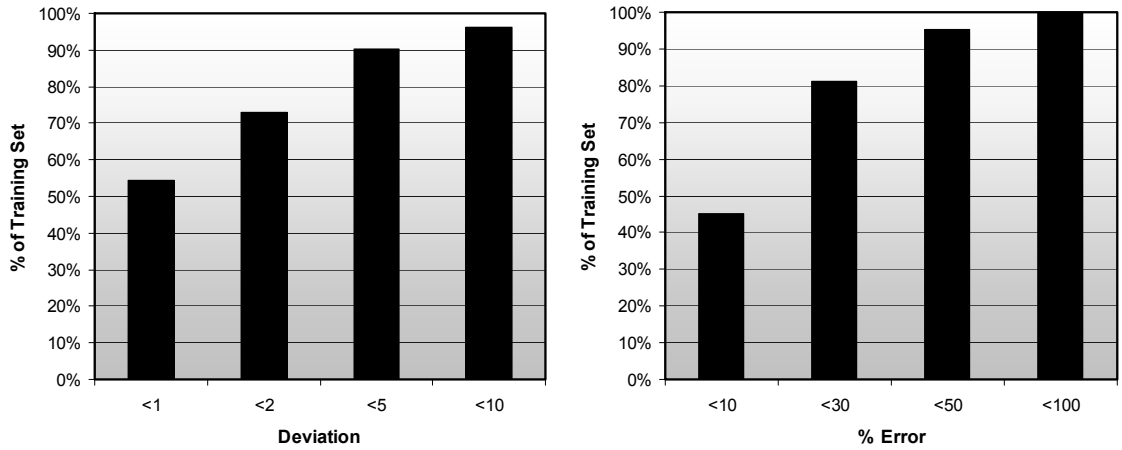

Figure 3.4 Distribution of errors in correlation of $\boldsymbol{\varepsilon}$

3.2.1 Dipole Moments

It should also be mentioned that experimental dipole moments were not available in the DIPPR® 801 database for 74 of the chemicals in the test set.

Experimental dipole moments in the DIPPR database and in a NIST[41] on-line repository of *ab initio* results (The NIST sites contains computational results generated by numerous researchers using various levels of theory and basis set sizes) have been used to identify the "best" model chemistry for quantum mechanical determination of DMs.

Table 3.3 Comparison of *ab initio* and experimental DM values (average % error)

semi-empirical	**AM1**	42.107
	MNDod	36.042
	PM3	40.985
	MM3	60.515

		STO-3G	3-21G	3-21G*	6-31G	6-31G*	6-31G**	6-31+G**	6-311G*
Hartree Fock	HF	36.92	44.25	32.30	50.94	24.06	23.56	24.22	23.45
density functional	BLYP	47.90	27.81	19.39	26.87	17.06	15.21	14.75	15.50
	B3LYP	43.83	27.53	16.77	29.78	16.16	15.45	14.83	14.61
	B3PW91	43.14	27.59	17.09	30.32	17.37	15.46	14.46	14.42
	mPW1PW91	42.27	27.89	17.47	31.50	15.51	15.34	14.52	14.52
	PBEPBE	47.72	27.91	19.02	27.78	16.09	15.91	14.17	15.36
Möller-Plesset	MP2FC		33.40	21.75	46.60	16.84	16.08	16.10	19.71

		6-311G**	6-31G(2df,p)	cc-pVDZ	cc-pVTZ	aug-cc-pVDZ	6-311+G(3df,2p)	6-311+G(3df,2pd)
Hartree Fock	HF	21.98	18.33	20.36	16.02	18.68	17.99	
density functional	BLYP	14.11	15.10	14.99	9.05	10.27		
	B3LYP	12.96	13.87	15.30	8.65	13.05	8.08	
	B3PW91	13.47	14.10	13.80	9.89	10.13		
	mPW1PW91	13.35	13.94	13.53	9.39	10.12		
	PBEPBE	14.69	10.69	15.85	11.11	10.97		
Möller-Plesset	MP2FC		31.82	16.40	11.77	16.26		

		CEP-31G	CEP-31G*	CEP-121G	CEP-121G*	LANL2DZ	SDD
Hartree Fock	HF	59.14	26.56	54.10	22.09	54.17	53.82
density functional	B3LYP	42.03	17.94	35.24	10.63	36.27	35.56
Möller-Plesset perturbation	MP2FC	44.08	20.41	39.15	16.32	47.75	50.18

The basis sets and theories are explained in Appendix A which adapted from: K. K. Irikura In "Computational Thermochemistry: Prediction and Estimation of Molecular Thermodynamics" (ACS Symposium Series 677); Irikura, K. K., Frurip, D. J. Eds.; American Chemical Society: Washington, DC 1998.

In this work, I have compared quantum-mechanically obtained values, tabulated in the NIST databook site with experimental values for the DM for 191 compounds. The results of this test are shown in Table 3.3.

A comparison of the results for 191 compounds shows that B3LYP/6-311+G(3df,2p) calculations are the most reliable of the commonly used *ab initio* and DFT methods for calculating μ. This model chemistry gave an average error of 8.08%.

In the correlation, values of μ were calculated with density functional theory in Gaussian03 using B3LYP/6-311+G(3df,2p).

Table 3.4 Prediction of ε from calculated μ using B3LYP/6-311+G(3df,2p)

AAPD in calculated μ (191 compounds)	8.08%
AAPD in calculated μ (44 compound test set)	7.25%
AAPD in predicted ε with *experimental* μ (44 compounds)	9.78%
AAPD in predicted ε with *calculated* μ (44 compounds)	9.21%

Table 3.4 shows an AAPD of 7.25% between experimental μ values and those calculated using B3LYP/6-311+G(3df,2p). A 44-compound subset of the dielectric constant training set was also used to test the sensitivity of ε values calculated from Eq.(3.1) to predicted values of μ calculated with B3LYP/6-311+G(3df,2p). This test produced an AAPD of 9.8% for the dielectric constant when calculated values of μ were used in Eq.(3.1) versus 9.2% when experimental values were used.

3.2.2 Predictive Capability of the Correlation

To test the predictive capability of the correlation, a test set of 42 polar compounds was developed from the data used by Sild and Karelson[35]. None of these compounds were in the DIPPR® 801 database nor used in development of the correlation. These compounds included a variety of chemical functional groups with ε values over nearly the entire domain of the correlation from 1 to 50. Table 3.5 lists the test set compounds, the values of the independent descriptors, and the predicted and experimental ε values. Values for δ were calculated from the definition of the solubility parameter,

$$\delta = \left(\frac{\Delta H_{vap} - RT}{V} \right)^{0.5} \Bigg|_{T=298.15\text{K}} \tag{3.3}$$

using the gas constant, R, and available literature values for the heat of vaporization, ΔH_{vap}, and liquid molar volume, V, at 298.15 K. Values of n were readily available in the literature, but values for A_{vdw} were calculated from Bondi group contributions,[41] consistent with the method by which the DIPPR® 801 values are obtained.

Table 3.5 also shows the values and reference for the values of μ used. Experimental μ values were available for four[42,43] of the 42 compounds; all of the remaining μ values were calculated using B3LYP/6-311+G(3df,2p).

Table 3.5 Test set compounds and their descriptor and ε values

Compound	μ /D	V_{vdw}/ $10^8 m^2 kmol^{-1}$	δ/ $10^3 J^{1/2} m^{3/2}$	n	ε_{calc}	ε_{exp}	% diff.
ethyl methyl carbonate	0.6356	8.39	17.55	1.378	2.99	2.985	0.13
1-chlorohexane	2.4547	10.69	15.46	1.4199	6.14	6.104	0.66
butyl phenyl ether	1.6366	10.75	15.67	1.497	3.77	3.734	1.04
N,N-dibutylformamide	4.2496	12.01	15.78	1.443	17.77	18.4	-3.40
propyl chlorocarbonate	3.3628	8.84	17.36	1.411	11.65	11.2	4.01
2-methyl-2-butanethiol	1.7606	7.71	15.42	1.441	4.84	5.087	-4.88
methyl heptanoate	1.7035	9.14	15.27	1.41237	4.12	4.355	-5.49
ethyl hexanoate	1.7912	10.49	15.21	1.406	4.07	4.45	-8.44
ethyl 4-pyridinecarboxylate	2.8681	9.67	17.74	1.501	8.16	8.95	-8.83
N,N-dibutylacetamide	3.9905	13.36	15.00	1.447	17.23	19.1	-9.80
4-ethylpyridine	2.8518	7.47	17.78	1.498	9.83	10.98	-10.43
cyclohexyl butanoate	1.9079	7.02	15.43	1.445	5.14	4.58	12.27
2,2-dimethylpropanal	2.8616	8.73	16.46	1.3794	10.88	9.051	20.22
tribromoacetaldehyde	1.6619	8.64	19.79	1.621	5.90	7.6	-22.38
octanenitrile	4.5214	13.52	16.47	1.42	18.06	13.9	29.91
ethyl 2-bromopropanoate	2.4502	9.88	17.10	1.446	6.53	9.4	-30.53
1-fluorooctane	2.2446	12.72	15.12	1.389	5.20	3.89	33.57
cyclohexyl propanoate	2.0142	5.67	15.85	1.4425	6.45	4.82	33.90
2-ethylpyridine	1.8004	7.47	17.33	1.496	5.49	8.33	-34.07
dibenzylamine	0.6908	11.65	16.39	1.5745	2.18	3.446	-36.76
1-nitrooctane	4.3559	10.42	15.57	1.433	16.73	11.46	46.01
2,2,2-trifluoroethanol	3.4195	6.26	21.32	1.281	40.64	27.68	46.81
tributyl phosphate	3.07*	16.86	13.36	1.424	8.39	8.34	0.62
2-methylpropanenitrile	4.191	6.55	18.41	1.379	25.06	24.42	2.63
1-chloroheptane	2.4471	12.04	15.10	1.425	5.68	5.521	2.96

Table 3.5 con't

Compound	μ /D	V_{vdw}/ $10^8 m^2 kmol^{-1}$	δ/ $10^3 J^{1/2} m^{3/2}$	n	ε_{calc}	ε_{exp}	% diff.
tribromofluoromethane	0.4432	7.42	18.37	1.524	2.85	3	-5.14
butyl nitrate	3.6364	9.17	17.10	1.412	13.83	13.1	5.58
1-iodopentane	1.88†	7.52	16.48	1.495	5.36	5.78	-7.19
ethyl isothiocyanate	3.5992	4.77	18.85	1.511	21.17	19.6	8.02
tetrahydropyran	1.5202	7.35	17.25	1.419	5.12	5.66	-9.61
methyl pentanoate	1.7185	9.14	15.84	1.396	4.39	4.992	-12.02
1-bromooctane	2.5931	13.66	15.07	1.4518	5.74	5.096	12.54
benzoyl fluoride	4.0657	8.08	18.26	1.496	26.57	22.7	17.03
2,4-dimethylpyridine	2.383	7.24	17.69	1.501	7.75	9.6	-19.25
N,N-diethylformamide	4.1677	9.31	18.34	1.434	22.92	29.6	-22.58
trichloronitromethane	1.935	11.06	18.82	1.503	5.48	7.319	-25.17
ethyl nitrate	3.4269	9.67	18.91	1.388	14.15	19.7	-28.17
1-fluoropentane	1.85†	8.67	15.17	1.36	5.05	3.931	28.58
N,N-diethylacetamide	3.9253	10.66	17.35	1.44	21.54	32.1	-32.91
2-bromo-2-methylpropane	2.5419	8.45	15.79	1.4279	7.24	10.98	-34.08
isobutyl vinyl ether	1.2†	5.41	14.85	1.398	4.50	3.34	34.85
methyl nitrate	3.198	8.32	20.31	1.368	15.17	23.9	-36.51
AAPD							17.83

*Experimental value from reference 44 †Experimental value from reference 41

Values of ε predicted from the correlation for these 42 polar compounds produced an AAPD of 17.83%, indicating no real degradation in results when Eq. (3.1) is used to predict, as opposed to correlate, ε. To our knowledge, the most accurate and generally applicable correlation for dielectric constant previously available in the literature is that by Sild and

Karelson. As mentioned earlier, the correlations by Schweitzer et al. with six to twelve descriptors had errors of over 100% for 7% of the 497 compounds in the training set and errors of over 50% for 23% of the compounds. While other correlations have been developed for the dielectric constant of specific families of chemicals, we compare here only correlations generally applicable to all organic compounds. Table 3.6 shows a comparison between the Sild and Karelson correlation and the one developed in this work. The correlation developed in this work is based on a much larger training set, but the test set is slightly smaller. The accuracy of the newly developed correlation is comparable to that obtained in tuning it to the training set data and is notably less than that reported for the Sild and Karelson correlation.

Table 3.6 Comparison of available methods

	Sild & Karelson[36]	This work
No. of descriptors	6	4 + 9 O group contributions
Training set	155	519
Test set	46	42
AAPD for training set	23.34%	17.78%
AAPD for test set	39.33%	17.83%
Combined AAPD	27.00%	17.78%

3.2.3 Predictions Using the Correlation for DIPPR Database

There are 301 compounds for which no DC value is currently in the database which could be upgraded to a predicted value using the correlations what we have developed internally. Our testing shows the correlation (Eq. (3.1)) for DCs to be the most accurate prediction method available for this property. Table A.4 lists these 301 compounds. The DIPPR project has now incorporated these predicted values into the database.

3.3 Summary of Pure-Chemical Correlation for DC

A new QSPR correlation for the DC has been developed using dipole moments, van der Waals area, solubility parameter, and refractive index, descriptors readily available in the DIPPR® 801 database. Different coefficients are to be used with non-polar and hydrocarbon fluids than with polar fluids. Dielectric constants were accurately correlated for a test set of 167 non-polar chemicals with an average absolute error of 0.07 or an average absolute percent deviation of 2.96%. The correlation's coefficients for polar fluids were obtained by correlating values for 519 polar chemicals which gave an average absolute error of 2.05 or an average absolute percent deviation of 17.78%. The polar correlation was tested in prediction mode on a set of 42 chemicals not included in the training set with ε values ranging from 1 to 50. The test results showed little degradation from the correlating effectiveness with an average absolute percent deviation of 17.83%. Although more extensive testing is desirable, the availability of more experimental data is required to do so.

The accuracy of the correlation is believed to be limited by the accuracy of the currently available experimental data. Further refinement of the correlation would likely require not only additional data but a limitation on the training set data to that of the highest accuracy. This has not been done because of our objective to keep the correlation generally applicable to all organic compounds and the requisite need for an extensive database of 500 compounds or more to satisfy that objective. Nevertheless, these results suggest that the correlation can be used to predict ε values with an average uncertainty of about 18% for polar compounds and of about 3% for non-polar and hydrocarbon compounds. The correlation is not intended for compounds where the predicted value is greater than 50. It has also been demonstrated that dipole moments obtained

from B3LYP/6-311+G(3df,2p) calculations can be used in the correlation for ε, when experimental μ values are not available, with little decrease in accuracy of the predicted ε values.

Chapter 4

A Local-Composition Model for the Prediction of Mixture DC

4.1 Liquid Structure and DC

The thermodynamic nonidealities of liquid mixtures, usually expressed in terms of excess properties, arise from the fundamental intermolecular interactions within the condensed phase. Permanent and induced charge separation within the molecules contributes significantly to these intermolecular interactions along with the dispersion and repulsion forces. The static dielectric constant, ε, a measure of the fluid's ability to reduce the electric force between separated charges, has implications about these intermolecular interactions. Relative values of ε suggest a propensity for molecular polarization within the liquid by molecular alignment of permanent charge distribution moments (dipole, quadrupole, etc.), which we have called orientational polarization, and by distortion of the electron distribution within the molecule in response to the local electrostatic field, which we called distortional polarization. It seems logical therefore that mixture thermodynamic excess properties and dielectric constant are related at the level of their molecular underpinnings.

Relating local fluid structure to ε is not a new idea. As reviewed in Chapter 2, a popular early method for predicting values of ε is the Clausius-Mosotti equation (Eq. 2.8) based on Debye's dielectric theory. The Onsager equation and the Kirkwood extension provide improvement for some polar fluids, but their overall reliability in predicting ε is poor and not

applicable in their original forms to mixtures. While the Onsager theory predicts the dielectric constants for so-called "unassociated" or "normal" liquids such as ethyl bromide or chloroform from molecular dipole moments, it fails to adequately predict values for fluids such as water, alcohol, etc. The Kirkwood theory includes a correlation parameter, *g*, intended to be a measure of the rotational hindering effect that the local environment has on a polar molecule because of the local intermolecular interactions that impact the orientational polarization. Extension of this concept to mixtures has been limited by the inherent complexities of orientational correlations among various polar species upon mixing.

Oster[45] assumed that the Kirkwood correlation parameter for each pure component remains unchanged upon mixing at constant temperature and pressure, and this model has been the starting point of most mixture models that have been developed.[46,47,48,49] The Oster model also assumes no volume change upon mixing, and significant errors can occur when applied to mixtures with large excess volumes. Mixing rules employed in later models generally contain an adjustable parameter to accommodate the thermodynamic mixing nonidealities associated with the complexity of the intermolecular interactions. As such these models are correlational (as opposed to predictive) in nature and require mixture data to obtain the adjustable parameter in the mixing rule. Because the adjustable parameter has no physical interpretation, it is difficult to identify ways in which this parameter could be calculated so as to make these models entirely predictive. This is particularly true for multicomponent mixtures in which it is unclear whether the parameters from binary mixture data are relevant for the multicomponent mixture, and the extant experimental data on ternary and higher mixtures are too minimal to evaluate the efficacy of empirical parameters.

In an attempt to relate the common molecular underpinnings of thermodynamic excess properties and the mixture dielectric constant, a mixture ε prediction method is proposed here based on the concept of local compositions which has proven effective in development of excess thermodynamic properties. Effective local compositions obtained from readily-available binary mixture excess properties are used to provide the specific molecular interaction information from which the mixture ε is predicted. Use of thermodynamic local compositions is expected to primarily account for orientational polarization, although because they are empirically obtained from VLE data, some effects of distortion polarization may be included.

4.2 Theoretical Background

The Kirkwood equation relates the dielectric constant of a pure fluid to the molar polarization p per unit volume

$$p = \frac{(\varepsilon - 1)(2\varepsilon + 1)}{9\varepsilon}. \tag{4.1}$$

The relationship of p to charge distribution within the molecule is usually given in terms of the Onsager equation written in slightly rearranged form from Eq. (2.3) as

$$p = \rho \frac{4\pi N_A}{3}\left(\alpha + \frac{\mu^2}{3k_B T}\right), \tag{4.2}$$

where N_A is Avogadro's number, T is temperature, k_B is Boltzmann's constant, ρ is molar density, α is the electronic polarizability, and μ is the dipole moment. In the Osager theory, distortion and orientation polarization are explicit in the two terms of Eq. (4.2). Orientational

polarization is accounted for by the propensity of the permanent dipole to align with the field and distortion polarization, in which the electron distribution within the molecule adjusts to the electrostatic field, is accounted for through the α term.

The Onsager equation is derived under the assumption of a random molecular environment and does not account for molecular interactions that induce order in the neighboring molecules as would occur with highly polar molecules that can associate or have orientationally specific interactions. Kirkwood introduced a correlation factor g to account for short-range intermolecular forces that would hinder rotation to obtain

$$\frac{(\varepsilon-1)(2\varepsilon+1)}{9\varepsilon}=\rho\frac{4\pi N_A}{3}\left(\alpha+\frac{\mu^2 g}{3k_BT}\right). \tag{4.3}$$

There has been little success in calculating g from first principles, and so it is usually treated as an adjustable parameter when correlating experimental data. The Kirkwood correlation factor is usually defined as

$$g=1+Z\langle\cos\gamma\rangle\ , \tag{4.4}$$

where Z is the number of nearest neighbors and $<\cos\gamma>$ is the mean cosine of the angles between the dipole moments of the neighboring molecules. Experimental ε values have been used to obtain molecular structure information through regression of g.[50] For example, values of g close to 1 suggest little hindrance to molecular rotation, hence a random arrangement of the molecular-level dipoles since $<\cos\gamma> = 0$. Values of $g < 1$ or $g > 1$ respectively indicate antiparallel and parallel statistical alignments.

For mixtures, the local structure effects due to different intermolecular interactions are expected to have a large effect on *g*, hence the dielectric constant. These effects can be conveniently represented in terms of excess quantities or deviations from the ideal mixture value. Generally, deviations from ideality have been defined with respect to the molar polarization per unit volume rather than the dielectric constant. The molar polarizations per unit volume are additive for the "ideal mixture"

$$p^{id} = \sum_{i=1}^{n} \phi_i p_i \,, \tag{4.5}$$

where n is the number of components and ϕ_i is the volume fraction of component i. This equation by Oster[45] assumes no volume change upon mixing the components. An excess molar polarization per unit volume can be defined as the deviation of the mixture p from the p^{id},

$$p^{E} = p - p^{id} = p - \sum_{i=1}^{n} \phi_i p_i \,. \tag{4.6}$$

The dielectric constant is then obtained from the mixture polarization by inverting Eq. (4.1). This can be conveniently written as

$$\varepsilon = \frac{1}{4}\left(1 + 9p + 3\sqrt{9p^2 + 2p + 1}\right). \tag{4.7}$$

Equation **(4.5)**, generally known as Oster's rule, was suggested by Oster as a rough approximation for estimation of mixture ε values. Harvey and Prausnitz[45] determined that a linear volume-fraction mixing rule like Eq. (4.5) did not reflect the increased or decreased degree of correlation between neighboring molecules in the mixture and proposed a quadratic mixing rule of the form

$$p = \sum_{i=1}^{n}\sum_{j=1}^{n} \varphi_i^{\dagger}\varphi_j^{\dagger} p_{ij}^{\dagger} \quad \text{with} \quad p_{ij}^{\dagger} = \frac{1}{2}\left(p_i^{\dagger} + p_j^{\dagger}\right)\left(1 + k_{ij}\right), \tag{4.8}$$

where k_{ij} is a binary parameter, close to zero, regressed from dielectric constant data for the *i-j* binary system, and the superscript † signifies that the property is evaluated at a density corresponding to the reduced density of the mixture (using a mole fraction average of the critical volumes as the reducing factor). However, if all the $k_{ij} = 0$, then Eq. (4.8) reduces to a linear mixing rule. Wang and Anderko[48] suggested a similar quadratic mixing rule

$$p = \sum_{i=1}^{n}\sum_{j=1}^{n} x_i x_j (vp)_{ij} \quad \text{with} \quad (vp)_{ij} = \frac{1}{2}\left(v_i p_i + v_j p_j\right)\left(1 + k_{ij}\right), \tag{4.9}$$

where v_i is the molar volume of component *i*. Again the mixing rule reduces to a linear form when all of the $k_{ij} = 0$. For many mixtures these mixing rules require that the k_{ij} be regressed from experimental binary data for accurate prediction of multicomponent ε values.

4.3 Local Composition Model for ε

Like ε, excess thermodynamic properties are strongly related to the local structuring that occurs due to intermolecular interactions. The concept of local compositions has been widely used to obtain correlations for the composition dependence of excess properties. Here we develop a correlation for the excess molar polarization in terms of nonrandom local compositions which are themselves obtained from other excess properties, specifically from the excess Gibbs energy or the mixture activity coefficients.

Analogous to the Nonrandom-Two-Liquid (NRTL) model for the Gibbs energy developed by Renon and Prausnitz[51], we consider a mixture p as an ideal mixture of n hypothetical fluids having polarizations per unit volume of $p^{(i)}$

$$p = \sum_{i=1}^{n} \varphi_i p^{(i)} \quad \text{where} \quad p^{(i)} = \sum_{j=1}^{n} \varphi_{ji} p_{ji}\,, \tag{4.10}$$

where p_{ji} are yet unidentified parameters characteristic of j-i polarization interactions and ϕ_{ji} are local volume fractions of molecule type i around a central molecule of type j. The local volume fractions add to one, and they are related to the local mole fractions x_{ij} by

$$\sum_{j=1}^{n} \varphi_{ji} = 1 \qquad \text{and} \qquad \varphi_{ji} = \frac{x_{ji} v_j}{\sum_{k=1}^{n} x_{ki} v_k}\,. \tag{4.11}$$

Here v_k is the molar volume of component k at the mixture temperature and pressure. In the NRTL model, the local mole fractions deviate from bulk mole fractions, x_i, because of the difference in interaction energies, u_{ji}, between the unlike ($i \neq j$) and like ($i = j$) molecules within the hypothetical pure fluids. This relationship can be written as

$$\frac{x_{ji}}{x_{ii}} = \frac{x_j}{x_i} \exp\left[-\alpha \frac{\left(u_{ji} - u_{ii}\right)}{RT} \right] = \frac{x_j}{x_i} G_{ji}\,, \tag{4.12}$$

where,

$$G_{ji} = \exp\left[-\alpha \frac{\left(u_{ji} - u_{ii}\right)}{RT} \right] = \exp\left[-\alpha \frac{A_{ji}}{RT} \right]. \tag{4.13}$$

Here R is the gas constant and A_{ji} are interaction parameters that are regressed from experimental data, generally vapor-liquid (VLE) or liquid-liquid equilibrium (LLE) data. The non-

randomness parameter α times the interaction parameter A_{ji} is a measure of the local structuring caused by the interactions. When $\alpha = 0$, $G_{ji} = 1$ and the local and overall compositions are equal. The local volume fractions defined in Eq. (4.11) have the same relationship to the overall volume fractions seen in Eq. (4.12), or

$$\frac{\phi_{ji}}{\phi_{ii}} = \frac{\phi_j}{\phi_i} G_{ji}. \tag{4.14}$$

Using the conservation of the volume fractions expressed in Eq. (4.11), one can write the individual local volume fractions that appear in Eq. (4.10) as

$$\phi_{ji} = \frac{\phi_j G_{ji}}{\sum_{k=1}^{n} \phi_k G_{ki}} \qquad \phi_{ii} = \frac{\phi_i}{\sum_{k=1}^{n} \phi_k G_{ki}}. \tag{4.15}$$

Substitution of Eq. (4.15) into Eq. (4.10) yields

$$p = \sum_{i=1}^{n} \varphi_i \left[\sum_{j=1}^{n} p_{ji} \phi_j G_{ji} / \left(\sum_{k=1}^{n} \phi_k G_{kj} \right) \right]. \tag{4.16}$$

Equation (4.16) can be used as a general equation to correlate the polarizability of an *n*-component mixture by treating p_{ji} (with $p_{ji} = p_{ij}$) as one adjustable parameter for each constituent binary mixture. Use of the equation as a correlation requires at least one experimental value for each constituent binary mixture.

In order to obtain a nonparametric or predictive model, the p_{ji} interaction terms must be identified. It is clear that $p_{ii} = p_i$, the pure-component *i* polarization pure unit volume, because all volume fractions except ϕ_i are zero in the pure-component limit. There is, however, no rigorous relationship for the cross interaction p_{ji} ($j \neq i$). We follow, however, the assumption previously

made in developing NRTL models for thermal conductivity[52] and viscosity[53] to obtain a non-parametric value for p_{ji} in mixtures of nonpolar fluids. We write Eq. **(4.16)** for a binary mixture of components 1 and 2 and set the mixture p equal to p_{21} at the specific composition where $x_{21} = x_{12}$. The rationale for this assignment is that there are equivalent numbers of 1-2 and 2-1 interactions at the composition where $x_{21} = x_{12}$. Likewise there must be the same number of 1-1 and 2-2 interactions at this composition. This mixing rule allows direct evaluation of p_{21} from the pure component polarizations and the mixture thermodynamics contained in the G_{21} and G_{12} values. The volume fraction of component 1 at this composition, denoted with an asterisk, can be obtained from Eqs. (4.11) and (4.12) as

$$\phi_1^* = \frac{V_1\sqrt{G_{21}}}{V_1\sqrt{G_{21}} + V_2\sqrt{G_{12}}}. \tag{4.17}$$

Setting $p = p_{21}$ at this composition yields for the binary mixture of components 1 and 2,

$$p_{21} = p_{12} = \frac{\sqrt{G_{21}}V_1 p_1 + \sqrt{G_{12}}V_2 p_2}{\sqrt{G_{21}}V_1 + \sqrt{G_{12}}V_2}. \tag{4.18}$$

Eq. **(4.18)** can be used generally for all of the binary pair interactions in a multicomponent mixture. Finally, Eq. (4.16) can be written as a predictive equation in the form

$$p = \sum_{i=1}^{n}\phi_i p_i + \sum_{i=1}^{n}\phi_i\left[\sum_{j=1}^{n}\phi_j G_{ji}\left(p_{ji} - p_j\right)/\left(\sum_{k=1}^{n}\phi_k G_{kj}\right)\right], \tag{4.19}$$

where the binary cross interaction p_{ji} are obtained from Eq. (4.18) and the G_{ji} are obtained from available binary mixture thermodynamic data. The second term on the right-hand-side of this equation is the excess polarization per unit volume, p^E, shown in Eq. (4.6). The expression is

general in form for any number of components and includes a temperature dependence through the G_{ji} terms, as seen in Eq. (4.13), in addition to the temperature dependence of the pure polarization terms. The structural information included in the local composition model is intended to reflect the restriction on random orientation of the molecules in a polarizing field due to the interactions between the molecules much like Kirkwood's *g* factor in Eq. (4.3).

The procedure for computing the mixture ε at a given temperature and composition consists of six steps:

1. Use Eq. (4.1) to calculate p_i for each component from its ε_i value.
2. Obtain NRTL parameters, α, A_{12} and A_{21} for all constituent binary mixtures.
3. Compute G_{12} and G_{21} and for each binary system at the desired mixture temperature.
4. Compute the p_{ij} for each binary *i-j* pair from Eq. (4.18).
5. Compute the mixture *p* from Eq. (4.19) at the desired compositions.
6. Use Eq. (4.7) to compute the mixture ε value.

4.4 Discussion

There is a shortage of experimental mixture ε values available in the literature against which to test the predictive capabilities of the method. Sixteen binary systems and six ternary systems are shown in Table 4.1 for which there are reliable mixture experimental ε values and NRTL parameters. The NRTL parameters were obtained from equilibrium VLE data[54] at 298 K except as noted below; the ε values were measured at 1 atm and various temperatures and compositions as reported in the references cited in Table 4.1. Pure molar volumes were obtained from the recommended correlations in the DIPPR® 801 database.[9] While most of the mixture data are available at only a single temperature, there are a few mixtures shown in the table for

which data were available over a significant temperature range. For these systems, the NRTL model includes a temperature-dependent excess term in addition to that arising out of the temperature dependence of the pure-component ε values. Table 4.1 shows the average absolute percent deviation (AAD %) of predicted mixture ε values by the NRTL model in comparison to the predicted values from Eq. (4.5). The results are in all cases improved, often substantially, over Oster's mixing rule. Also shown in Table 4.1 are the results obtained if the p_{ij} in the NRTL model are fitted to binary experimental data. The results of using the NRTL model as a correlation are compared to the results reported in the literature for Eqs. (4.8) and (4.9) with k_{ij} fitted to the extant binary experimental data. The NRTL model correlates the binary data as well or better than Eqs. (4.8) and (4.9) and significantly improves upon the correlation of the ternary data. In several cases, the overall *predicted* results by the NRTL model are as good, or nearly so, as the correlated values using one adjustable parameter with Eq. (4.8) or (4.9). The NRTL predictive model does have problems with several of the 1-propanol-containing systems, though it still performs better than the other predictive methods. These same systems can be correlated well with the NRTL model suggesting that the mixing rule defined in Eq. (4.18) may be inadequate for all mixtures.

Because Oster's rule assumes that volumes are additive, there is little difference between the values predicted by it and the NRTL model for mixtures with small excess volumes as illustrated in Figure 4.1 for methanol + acetone mixtures.Mixture dielectric constants predicted by Oster's rule tend to deviate more for mixtures with larger excess volumes such as the alcohol + water systems illustrated in Figure 4.2 and the 1-propanol + water systems shown at 80 ºC in Figure 4.3. In the latter case the AAD of the predicted values are 6.72 % and 2.82 % for Oster's rule and for the NRTL method, respectively. The local compositions in the NRTL method

provide a reasonable estimation of ε^E although the minimum is shifted toward the water-rich compositions compared to the experimental values.

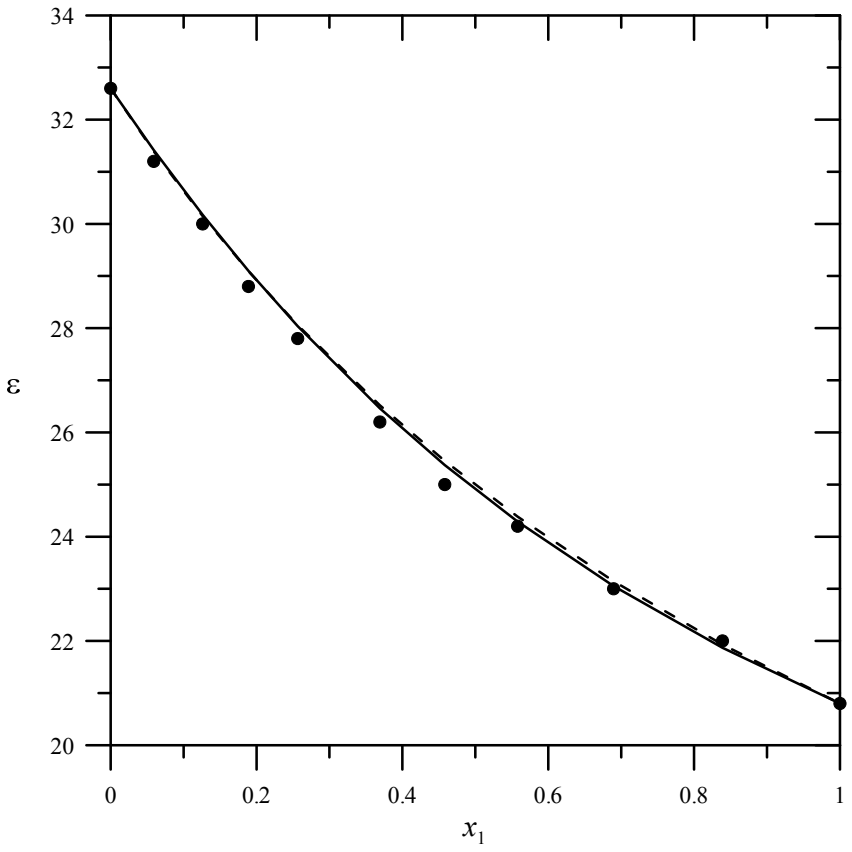

Figure 4.1 Comparison of experimental[55] (●) ε values to those predicted using the NRTL model (——) and Oster's rule (- - - - -) for mixtures of methanol(1) + acetone(2) at 25 ºC.

Table 4.1 Absolute average deviation (AAD) for prediction and correlation of binary and ternary mixtures using the NRTL model in comparison to other available methods

			Predicted AAD (%)		Correlation AAD (%)		
System	# pts.	T (◦C)	Eqs. (4.18)-(4.19)	Eq. (4.5)	Eq. (4.19)	Eq. (4.8)	Eq. (4.8)
Methanol-Acetone[55]	11	25	0.62	0.71	0.43	0.4	0.4
Methanol-Carbon disulfide[55]	8	25	3.27	3.73	3.21	NA	3.6
Water-1-Propanol[56]	55	20–80	2.93	6.1	1.74	3.9	1.7
Water-Methanol[56]	45	5–60	2.31	3.4	0.69	0.6	1.4
Water-Ethanol[56]	55	20–80	1.40	1.6	0.83	1.3	1.6
Water-2-Propanol[56]	55	20–80	3.68	5.8	1.55	4.4	2.5
Water-Acetone[56]	55	20–50	2.92	3.5	0.87	1.2	2.1
Water-Ethylene Glycol[56]	50	20–100	2.14	3.0	0.29	1.0	1.1
Water-Dioxane[57,58]	11	25	2.46	24.6	0.95	7.9	3.2
Methanol-Carbon tetrachloride[58]	10	35	4.01	10.1	3.85	12.7	6.5
Acetone-Carbon disulfide[55]	11	25	3.85	5.08	1.15	3.2	2.3
2-Propanol- Nitromethane[58]	12	35	3.90[b]	5.55	1.67[b]	2.1	1.4
1-Propanol- Nitromethane [58]	10	35	2.91	5.2	0.29	0.3	0.3
1-Propanol-Benzene[58]	10	35	14.34	18.87	2.78	NA	4.0
1-Propanol- Carbon tetrachloride [58]	10	25	9.76	22.6	2.01	NA	3.6
Dimethyl sulfoxide – Carbon tetrachloride[59]	19	25	1.90[b]	6.59	1.26[b]	NA	NA
1-Propanol- Nitromethane-Water[58]	10	35	0.94	6.21	0.20[a]	1.1	1.4[a]
1-Propanol- Carbon tetrachloride -water[58]	8	35	11.76[b]	38.64	1.0[a]	NA	9.0[a]
2-Propanol-Nitromethane -Water[58]	10	35	2.66[b]	3.42	0.23[a]	0.8	1.3[a]
Acetone-methanol- Carbon disulfide[55]	11	25	7.26	14.6	2.23	14.2	11.7
Methanol-Carbon tetrachloride -water[58]	8	35	6.75[b]	7.78	0.83[a]	5.0	4.5[a]
1-Propanol- benzene-water[58]	8	35	10.35[a]	28.80	0.61[a]	NA	4.2[a]

[a] One of the three binary k_{ij} was determined from ternary mixture data
[b] NRTL parameters obtained from activity coefficients predicted using UNIFAC[62] rather than experimental VLE data

The difference in the efficacy of the two predictive methods is largest for the water-dioxane system. This is likely due to the local molecular structuring that occurs due to association even though dioxane has no dipole moment. Viscosity studies of water-dioxane mixtures suggest that dioxane forms a four- or five-water-molecule hydrate which also modifies the highly coordinated structure of bulk water.[60] Recent dielectric spectroscopy studies[61] suggest that microheterogeneous clustering occurs as localized water-water hydrogen bonding is

strengthened in water-rich clusters surrounded by dioxane-rich regions. This local structuring, too complex from which to formulate a Kirkwood *g* value, gives rise to the rather large ε^E values shown Figures 4.5 and 4.6.

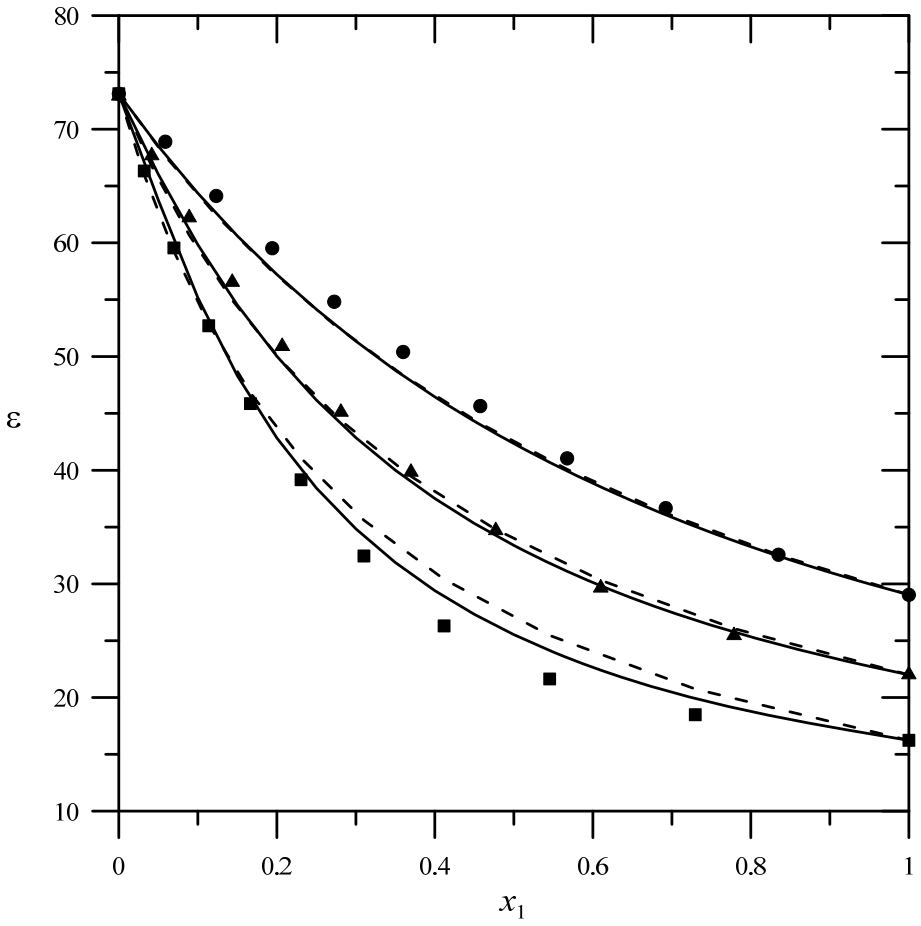

Figure 4.2 Experimental[56] (points) dielectric constants at 40 ºC for methanol(1) + water(2) (●), ethanol(2) + water(2) (▲) and 2-propanol(1) + water(2) (■) mixtures compared to predicted values using the NRTL model (——) and Oster's rule (- - - - -).

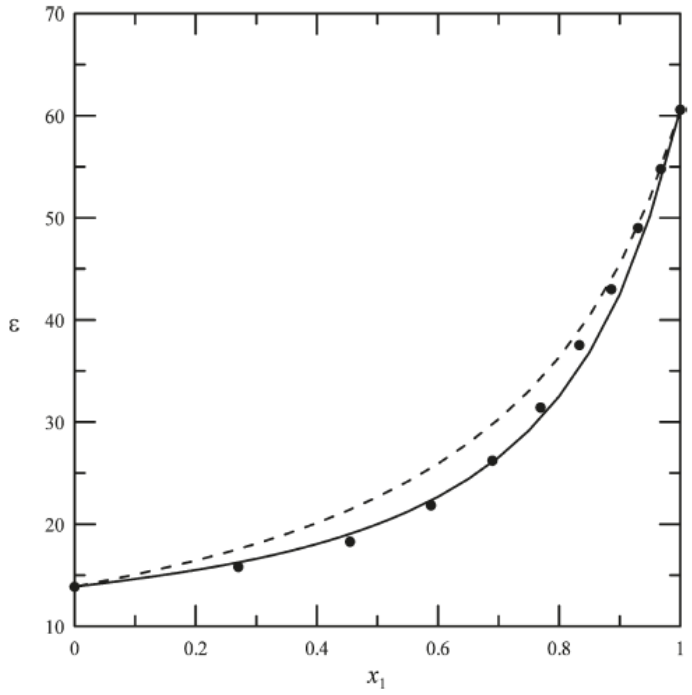

Figure 4.3 Comparison of experimental[56] (●) ε values to those predicted using the NRTL model (——) and Oster's rule (- - - - -) for mixtures of water(1) + 1-propanol(2) at 80 ºC.

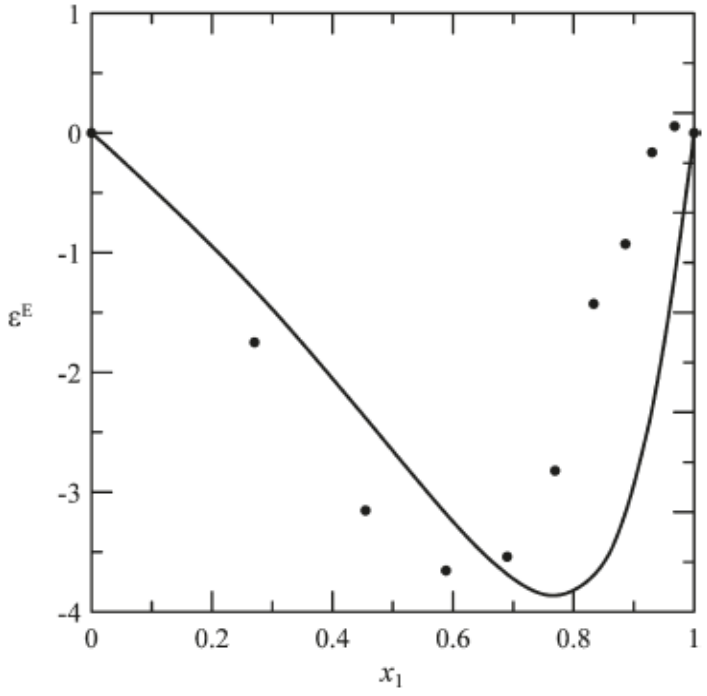

Figure 4.4 Experimental[56] (●) excess dielectric constant values compared to those predicted using the NRTL model (——) for mixtures of water(1) + 1-propanol(2) at 80 ºC.

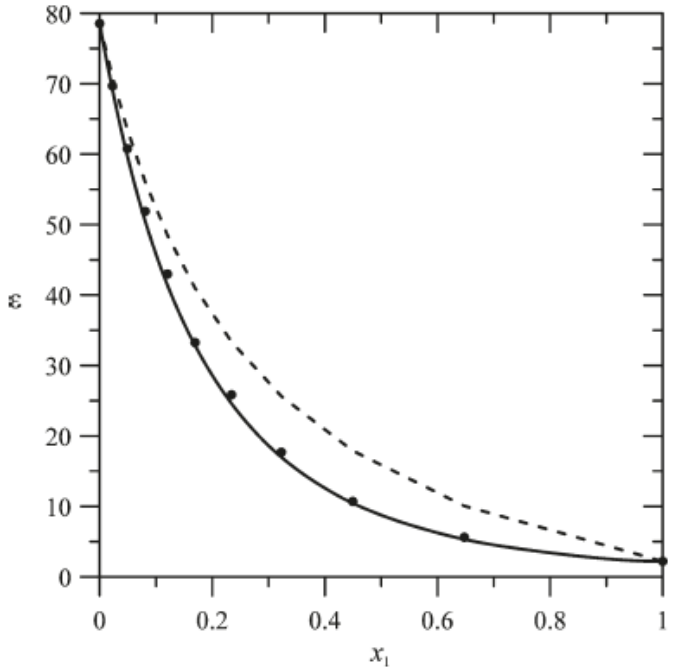

Figure 4.5 Comparison of experimental[60] (●) ε values to those predicted using the NRTL model (——) and Oster's rule (- - - - -) for mixtures of dioxane(1) + water(2) at 25 ºC.

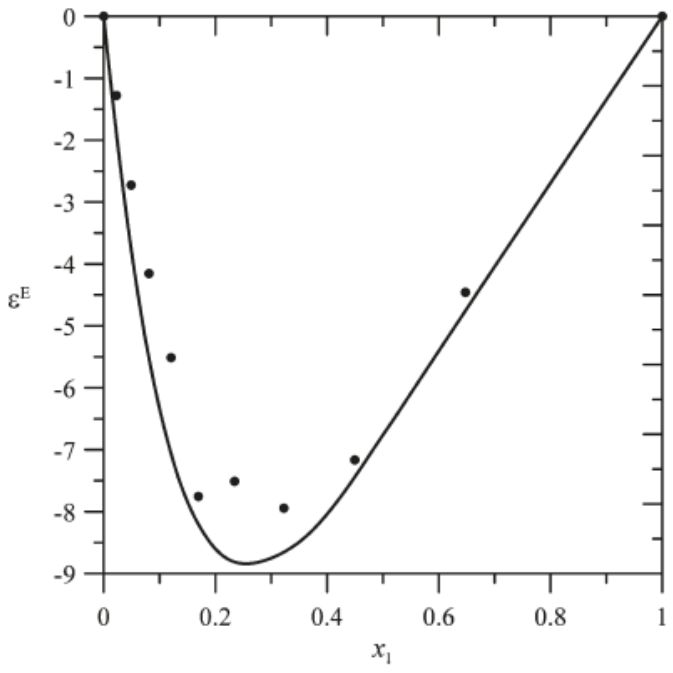

Figure 4.6 Experimental[60] (●) excess dielectric constants and values predicted using the NRTL model (——) for mixtures of dioxane(1) + water(2) at 25 ºC.

Electron polarization of nonpolar molecules by strongly polar molecules produces local structure and changes in ε that are difficult to model. Figure 4.7 shows that ε in nonpolar-polar mixtures typically show more nonpolar character than would be expected by either ideal behavior or the NRTL mixing rule developed here, especially at compositions rich in the nonpolar component. Interestingly, the mixing rule does produce the correct S-shape behavior with composition even though the magnitude of ε^E is underestimated by the NRTL model as shown in Figure 4.8.

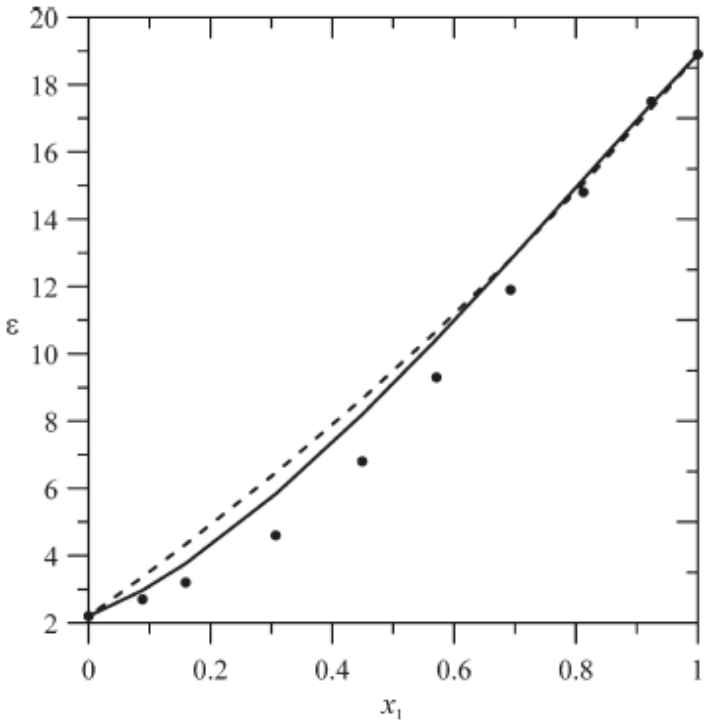

Figure 4.7 Comparison of experimental[56] (●) ε values to those predicted using Oster's rule (- - - -) and the NRTL model (——) for mixtures of 1-propanol(1) + benzene(2) at 35 ºC.

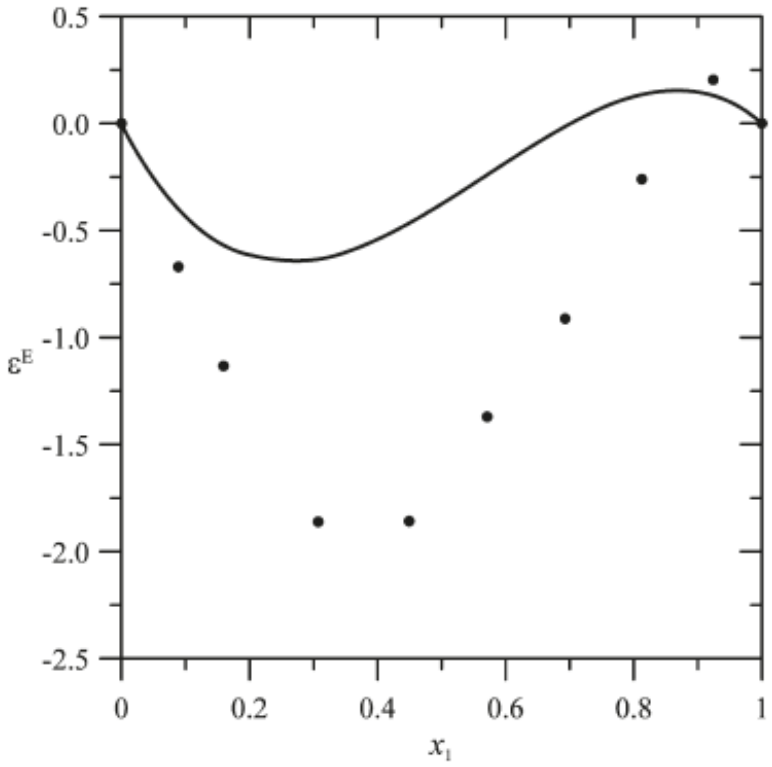

Figure 4.8 Excess dielectric constant from measurements[56] (●) compared to those predicted using NRTL model (——) for mixtures of 1-propanol(1) + benzene(2) at 35 ºC.

Because the NRTL method requires the binary NRTL parameters α, A_{12} and A_{21} to model the local molecular structure, a limitation in use of the method may be the availability of these parameters. While extensive compilations of VLE data are available, it would be naïve to assume that parameters would have been regressed for all desired binary mixtures. UNIFAC[62] is a prediction method for activity coefficients and excess Gibbs energy that, like the NRTL model, is based on local compositions. Because UNIFAC utilizes tabulated group contributions regressed from experimental VLE data to obtain the effective molecular interaction parameters, it can currently be applied to a wide variety of compounds although the accuracy and reliability of the predicted activity coefficients will obviously be less than activity coefficients correlated directly from experimental data. For cases where NRTL parameters are not available, we have

taken the approach of using UNIFAC to predict activity coefficients as a function of composition at the desired temperature from which the NRTL parameters are regressed to use to calculate ε. With this procedure, the NRTL method can be applied to a wide range of compounds for which VLE data have not been measured. Table 4.1 results for dimethyl sulfoxide + carbon tetrachloride, water + carbon tetrachloride, and nitromethane + isopropanol mixtures were determined in this manner.

The temperature dependence in the NRTL excess properties is known to be only approximate. Normally the temperature dependence of A_{12} and A_{21} is assumed to be either linear or inverse when VLE data are regressed over a range of temperatures. Alternatively, different values for A_{12} and A_{21} can be used at different temperatures. Similarly, one should used NRTL parameters that have been regressed from experimental VLE data at temperatures closest to the desired temperature for the most accurate predictions of ε. This can be seen in Figure 4.9 where NRTL values at 20 ºC were used to predict ε^E values at 20 ºC, 60 ºC, and 80 ºC for mixtures of ethylene glycol + water. Although the predicted and experimental values are in very good agreement at the temperature at which the NRTL parameters were obtained, these same parameters incorrectly predict almost no ε^E at higher temperatures where the model reduces to Oster's rule.

The NRTL model exhibits the largest deviation from the experimental data for those ternary systems in Table 4.1 that have a partially miscible constituent binary system. LLE requires a large positive excess Gibbs energy and it is known that NRTL parameters regressed from VLE data generally do not predict the LLE tie lines accurately. While this may explain the larger deviations, there is not enough experimental data on similar systems and at compositions approaching the two-phase coexistence curves to adequately test this hypothesis. On the other

hand, the local-composition model predicts the available data for completely miscible ternary mixtures, shown in Table 4.1, quite well. An example is shown in Figure 4.10 where contour lines from the NRTL-predicted ε surface are shown in comparison to the extant experimental data[58].

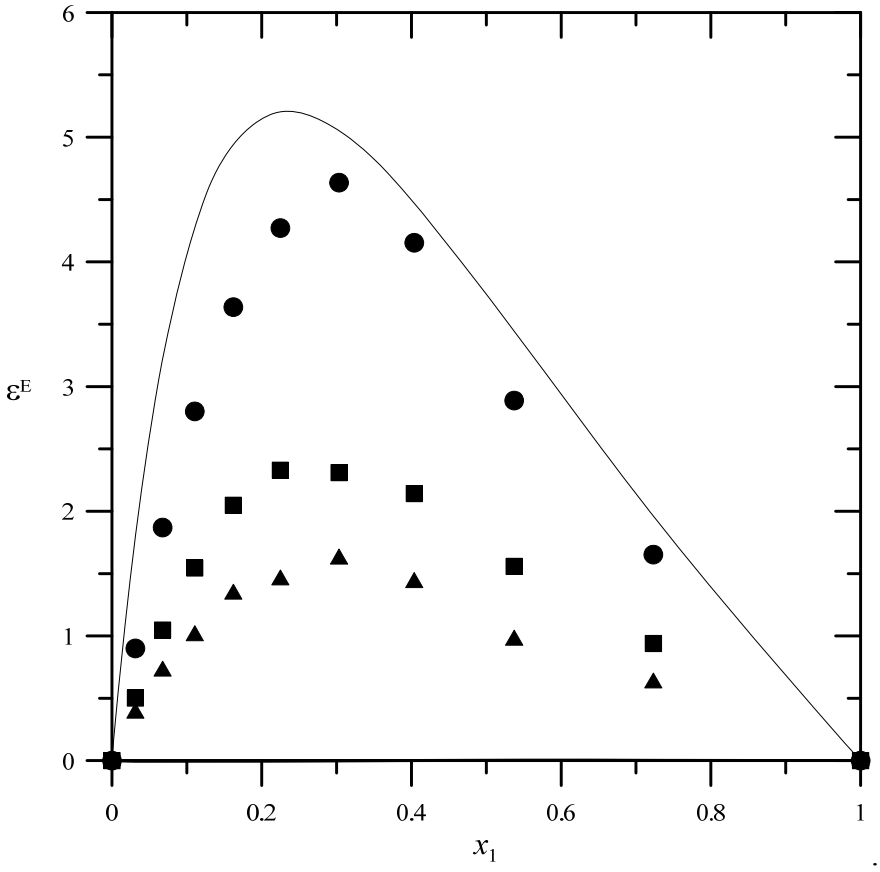

Figure 4.9 Comparison of experimental[56] (points) ε^E values to those predicted using the NRTL (lines) model for mixtures of ethylene glycol(1) + water(2) at 20 ºC (●), 60 ºC (■), and 80 ºC (▲). NRTL values at 60 and 80 ºC are shown but indistinguishable from the *x* axis.

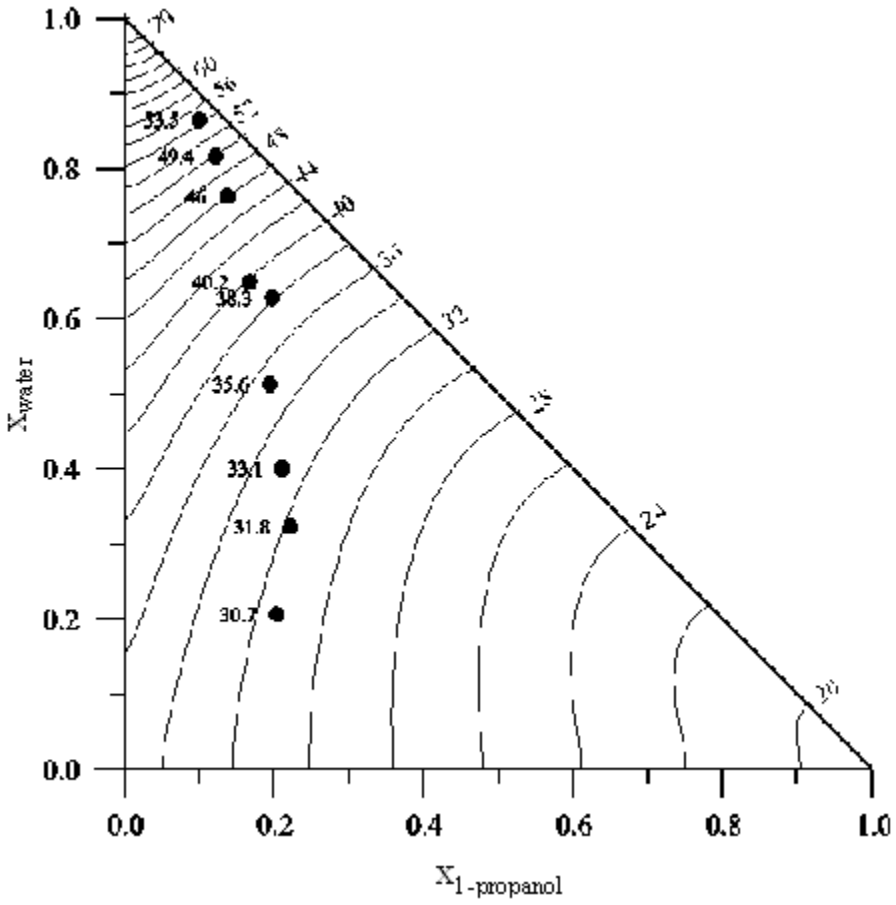

Figure 4.10 Contour plot of ε values predicted from the NRTL model for ternary mixtures of 1-propanol(1) + water(2) + nitrobenzene at 35 ºC compared to available experimental data[58] (●, value labeled on plot. Contours are for increments of 2 in ε with labels shown along the 45º line.

4.4 Conclusion

A method for prediction of liquid mixture static dielectric constant has been developed. The method requires values for the pure-component dielectric constant and information and binary NRTL model parameters available from VLE data compilations or predicted from UNIFAC. A comparison of available experimental mixture ε values for 16 binary systems

showed a maximum AAD of 5% for the NRTL predicted values. For the six ternary mixtures with available experimental data, the maximum AAD was 12%. The agreement with experiment is better than currently available predictive methods and is on par with correlative methods that contain one adjustable parameter in the mixing rule.

Chapter 5

Molecular Simulation of Dielectric Constant

5.1 Introduction

Molecular simulation provides a fundamental probe of the molecular nature of properties. Specifically, it links the fundamental interaction energies and forces between the molecules to observed macroscopic properties. For example, simulations can be used to understand the effects of the solvent on the DC value of the solute in condensed phases. It can also be used to isolate and understand the separate contributions from orientational and distortional polarizations. It can be used to obtain information about either pure fluids or mixtures and is suitable to examine the temperature, pressure and composition dependence of the DC. Results of the simulation are only as good as the force-field model used to describe the molecular interactions. Therefore, comparison of simulated and experimental data for the relative permittivity of the liquid or for a solute in a specific solvent represents an important test for the accuracy of the model.

In a pure (homogeneous) liquid simulation, the static dielectric permittivity ε is related to the fluctuations in the total dipole moment of the sample.[63,64] The exact dynamics of molecules, electrons is a complex calculation which depends on the specific functional form of long-range electrostatic interactions and on the boundary conditions applied to the liquid sample. However, the equations which connect the fluctuations to the dipole moments are well established and can be added without too much difficulty to standard molecular dynamics codes.[65,66,67,68,69]

Computation of the dielectric constant of fluids can then be done by monitoring dipole moment fluctuations in MD simulations. The rate of convergence of these fluctuations during a MD simulation is, however, determined by the relaxation of the time correlation function of the dipole moments. This may require long simulations to overcome the slow relaxation time. Moreover, statistically accurate calculations of the relative bulk properties will also require long simulations since only one value of a given collective property such as the DC is obtained at each time step. In the case of water, this simulation time is relatively long, and simulation times on the order of nanoseconds are required to accurately determine the static permittivity.

5.2 Theoretical Framework

The relative static dielectric permittivity of a liquid can be computed from the fluctuation in the dipole moment of a liquid sample. Barker[70] and Tironi[71] developed the following equation through reaction-field correction to calculate ε in the simulation for rectangular periodic boundary conditions:

$$\varepsilon = \frac{3(2\varepsilon_{RF}+1)\beta^{-1}V + 8\pi\varepsilon_{RF}\left[\left\langle M^2\right\rangle - \left\langle M\right\rangle^2\right]}{3(2\varepsilon_{RF}+1)\beta^{-1}V - 4\pi\left[\left\langle M^2\right\rangle - \left\langle M\right\rangle^2\right]} \tag{5.1}$$

where $\beta = \left(k_B T\right)^{-1}$, V is volume of the simulation box, ε_{RF} is the dielectric constant of the medium outside the cutoff sphere (used for the reaction-field correction) and M is the system's total dipole moment. M can be calculated at any time t during the simulation as a sum over the dipoles in the simulation cell

$$M(t) = M\left(r(t)\right) = \left(4\pi\varepsilon_0\right)^{-1/2} \sum_{i=1}^{N} q_i r_i(t) \tag{5.2}$$

where ε_0 is the vacuum permittivity, N is the total number of molecule in the box, q_i is the point charge located at vector position r_i, and r is the $3N$-dimensional vector defining the coordinates of all molecules in the box. The implicit assumption in this equation is that the fluid model includes fixed point charges to represent the permanent dipole moment of the molecule. Polarizable models in which q_i can change with the instantaneous molecular environment have been developed in recent years, but in this work only the effects of the orientational polarization for permanent dipoles are considered.

From Eq. (5.1) and Eq. (5.2), the ensemble average of total dipole moment $\langle M \rangle$ can be calculated by averaging over the configurations generated during the molecular dynamics simulation. So,

$$\langle M \rangle^2 = \left[\frac{1}{N_s} \sum_{i=1}^{N_s} M(t_i) \right]^2 \tag{5.3}$$

and

$$\langle M^2 \rangle = \frac{1}{N_s} \sum_{i=1}^{N_s} M^2(t_i) \tag{5.4}$$

where t_i is the time at simulation step i and N_s is the total number of simulation steps. As previously mentioned, the convergence of Eq. (5.3) and Eq. (5.4) is rather slow, typically requiring perhaps a nanosecond of simulation time.

Eq.(5.1) can be simplified to

$$\frac{1}{\varepsilon - 1} = \frac{1}{3yg(\varepsilon)} - \frac{1}{2\varepsilon_{RF} + 1} \tag{5.5}$$

where

$$g(\varepsilon) = \frac{\langle M^2 \rangle - \langle M \rangle^2}{N\mu^2} \tag{5.6}$$

and

$$y = \frac{4\pi\rho\mu^2}{9k_B T\varepsilon_0} \tag{5.7}$$

where $\rho = N/V$ is, as before, the molecular number density of the system. A Barker and Watts[69] reaction-field correction was included with a relative dielectric permittivity value for different media outside the cutoff sphere. If $\varepsilon_{RF} \to \infty$, Eq. (5.5) changes to

$$\varepsilon = 1 + \frac{4}{3}\frac{\pi\rho}{Nk_B T\varepsilon_0}\left[\langle M^2 \rangle - \langle M \rangle^2\right] \tag{5.8}$$

If the Ewald summation technique is used to handle the long-range Coulombic interactions and conducting walls boundary conditions as assumed, ε and the total dipole moment are related by[72]

$$\varepsilon = 1 + \frac{\left\langle \left|\vec{M}(0)\right|^2 \right\rangle}{3Vk_B T\varepsilon_0}\left[1 + it\phi(t)\right] \tag{5.9}$$

where $\phi(t)$ is the Fourier transform of the M autocorrelation function:

$$\phi(t) = \frac{\langle M(t) \cdot M(0) \rangle}{\langle |M(0)|^2 \rangle}. \tag{5.10}$$

Finally, the static dielectric constant is given by

$$\varepsilon = 1 + \frac{\rho \mu^2}{3 k_B T \varepsilon_0} G_k \tag{5.11}$$

where G_k is the finite system Kirkwood correlation factor

$$G_k = \frac{\langle |M(0)|^2 \rangle}{N \mu^2}. \tag{5.12}$$

G_k accounts for the correlation of the total dipole moment. It can be expressed as

$$G_k = \frac{\langle |M(0)|^2 \rangle}{N \mu^2} = 1 + \frac{N-1}{\mu^2} \langle \mu_i \cdot \mu_j \rangle \tag{5.13}$$

where the average of the dot product of the dipole moments $\mu_i \cdot \mu_j$ is performed for different molecules ($i \neq j$). G_k as defined in Eq. (5.13) is therefore a normalized molecular orientational correlation function and corresponds to the Kirkwood g factor shown in previous chapters. It is defined such that it has a value of unity for perfect orientational correlation between molecules and zero if the dipole moments are uncorrelated or orthogonal.

In this study, standard NVT molecular dynamics simulations are performed, and the auto time correlation function for M is calculated using Eq. (5.13) to obtain the Kirkwook factor G_k. This is used in conjunction with Eq. (5.11) to obtain ε.

5.3 Computer Simulation Details

5.3.1 Water

Because of the central importance of water in nearly all fields of study and its rather unique properties, water has been the focus of many computer simulation studies. It has proven difficult to develop a force field model for water that will accurately produce the unique properties of water. A large number of water models have been published, from very simple to very detailed. Attempts to improve the water force-field model include the addition of off-nuclear interaction sites, the incorporation of dipoles, the treatment of explicit polarizability, and the use of smeared charges.[73,74] In general, but not always, the more detailed the model, the larger extent to which more properties can be reproduced and the more accuracy obtained for targeted properties. Prediction of the dielectric constant is problematic for some of these models because of the direct relationship between the DC, the solvent dynamics, and the solvent-mediated electrostatic interactions.

Here we have chosen to use the simple-point-charge (SPC)[75] model, the extended simple-point-charge model (SPC/E),[76] and the flexible SPC model[77] to study the possible effects of internal vibrational and angle bending modes on the dielectric constant. In this case, we are not so much interested in the model's ability to quantitatively predict the correct DC value for water, but rather the contribution that polarization by means of bond and angle distortion makes to the value of DC in the condensed phase. To explore the effects of various internal modes on the DC value of water, simulations were performed using several variations of the SPC model. As shown in Figure 5.1, all of the SPC models use three Coulombic interaction sites centered on the atomic nuclei. In the standard SPC model, the intermolecular degrees of freedom are frozen so that the bond lengths and bond angles have constant fixed values. We label this model as SPC_{RR},

indicating rigid bonds (first index) and rigid angles (second index). Flexibility in the model can be introduced piecewise. The label SPC_{RF} then indicates the SPC model with rigid bonds and a flexible angle. Likewise, SPC_{FR} and SCP_{FF} designate variations of the SPC model with flexible bonds and a rigid H-O-H angle and full flexibility in the bonds and angles, respectively.

The intermolecular interactions in the SPC models also include a Lennard-Jones potential located only on the oxygen atoms to model dispersion and repulsion due to electron cloud overlap. The Coulombic interactions are modeled with fixed partial point charges located on all three sites. The SPC/E model is a widely used SPC model with rigid bonds and angle fixed at the same values as $SPC_{RR,}$ but with a reparameterization of the point charges on the nuclei from the original SPC model.

Flexibility is added to the basic SPC model by including simple harmonic stretching of the O-H bond and scissoring motion of the H-O-H angle; both are controlled with harmonic spring potentials. The molecular geometry in these models can be defined by the three internal degrees of freedom shown in Figure 5.1: two O-H bond lengths (r_{OH_1} and r_{OH_2}) and the H-O-H bond angle ($\theta_{\angle HOH}$). The general potentials for the various SPC models can be written as

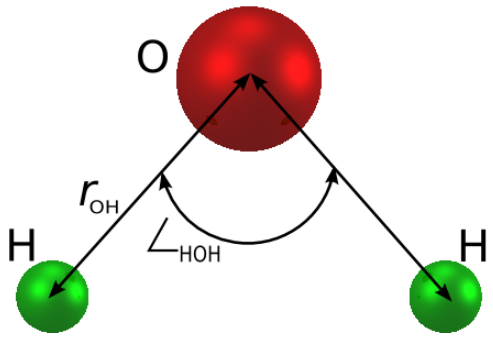

Figure 5.1Three-site water model (from http://www.sklogwiki.org/SklogWiki/index.php)

$$U_{\text{intra}} = \frac{k_b}{2}\left[\left(r_{OH_1} - r_{OH}^0\right)^2 + \left(r_{OH_2} - r_{OH}^0\right)^2\right] + \frac{k_a}{2}\left(\theta_{\angle HOH} - \theta_{\angle HOH}^0\right)^2 \tag{5.14}$$

$$U_{\text{inter}} = \sum_i \sum_{j<i} \left\{ 4\varepsilon_{ij}\left[\left(\frac{\sigma_{ij}}{r_{ij}}\right)^{12} - \left(\frac{\sigma_{ij}}{r_{ij}}\right)^{6}\right] + \frac{q_i q_j}{r_{ij}} \right\} \tag{5.15}$$

where U_{intra} and U_{inter} are the intra- and intermolecular interactions, k_b and k_a are the harmonic spring constants for bond vibrations and angle bending, respectively, r_{OH}^o and $\theta_{\angle HOH}^o$ are the equilibrium bond lengths and angle, r_{ij} is the distance between atoms i and j, ε_{ij} and σ_{ij} are the Lennard-Jones parameters for the i-j atom pair, and q_{i} is the partial charge on atom i, Geometrical and intra-molecular model parameters for the variations of the SPC water model that we have mentioned are listed in Table 5.1; Lennard-Jones site interaction parameters are given in Table 5.2.

Table 5.1 Parameters for the three-site SPC water models

Model	k_b (kcal·mol^{-1}Å^{-2})	r_{OH}^0 (Å)	k_a (kcal·mol^{-1}rad^{-2})	$\theta_{\angle HOH}^0$ (degrees)	q_O	q_H
SPC_{RR}	∞	1.0	∞	109.47	-0.82	0.41
SPC/E	∞	1.0	∞	109.47	-0.8476	0.4238
SPC_{RF}	∞	1.012	75.90	113.24	-0.82	0.41
SPC_{FR}	1059.162	1.012	75.90	113.24	-0.82	0.41
SPC_{FF}	1059.162	1.012	75.90	113.24	-0.82	0.41

Table 5.2 Lennard-Jones site parameters for water

Site	Atomic mass (gm/mol)	ε_{ij}/k_B (K)	σ (Å)
O	15.999	78.197	3.166
H	1.008	0.000	0.000

The corresponding vibration or angle-bending pieces of Eq. (5.14) are not used for the frozen internal modes in SPC_{FR}, SPC_{RF}, and SPC_{RR}. Rather, the MD simulations use Gaussian mechanics to move the system forward in time subject to the appropriate bond length and/or bond angle constraints. This method, popularized by Evans and coworkers[78,79] and used extensively in the research group at BYU, is well documented in the literature (see for example references 80 and 81). In this method, the bond length can be fixed at its equilibrium value r_{OH}^{o} and/or the bond angle can be fixed at its equilibrium value $\theta_{\angle HOH}^{o}$ by constraining the O-H distances in the first case and the H-H distance (to a fixed value as given by the law of cosines) in the latter case. These holonomic constraints are incorporated into the Gaussian equations of motion as derivative constraints, so a proportional feed-back controller is also used to compensate for numerical drift during the course of the simulation.

Molecular dynamics simulations of liquid water were performed at room temperature (T = 298.15K) and the experimental density at atmospheric pressure (ρ_m = 0.997 g/cm^3). The number of molecules in the central box was N = 125. Lennard-Jones interactions were truncated using the standard method of a spherical cutoff (cutoff radius = 9 Å) with long-range corrections for both the energy and pressure.[82] The equations of motion were integrated using a fourth-order Gear predictor-corrector method[83] with a time step of 1 fs for rigid and flexible models. The

Ewald sum with conducting boundary conditions[84] was used for the longer-range Coulombic interactions.

Figure 5.2 shows the convergence of the cumulative average of the static dielectric constant as obtained from Eqs. (5.11) and (5.13). As shown in this figure, typically the system was equilibrated from a cold start (initial configuration of molecules on a regular grid) for approximately 5 ns. A minimum of 3 - 4 ns beyond equilibration was generally required to provide adequate statistical averaging to obtain values of DC with an uncertainty within about 5%.

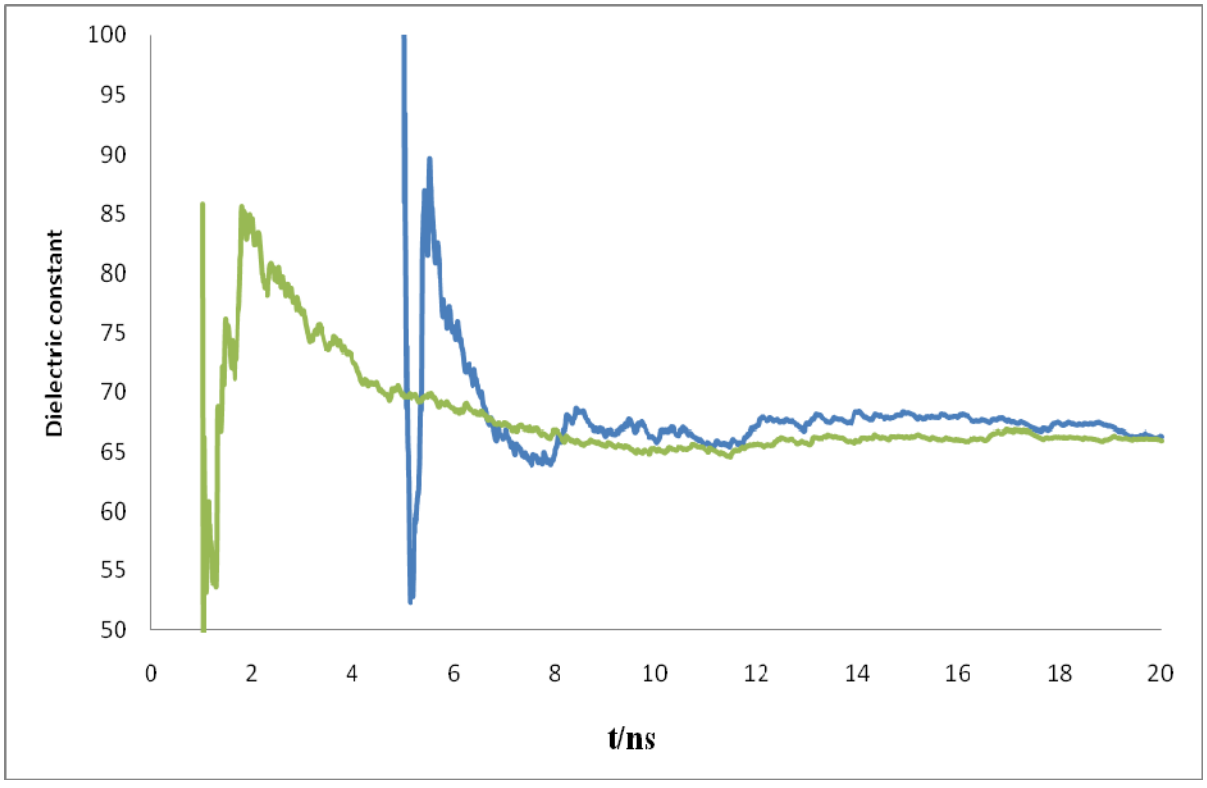

Figure 5.2 Cumulative average of the dielectric constant for SPC water as a function of the simulation length from a cold start configuration (green line) and from an equilibrated configuration (blue line)

DC values obtained for the different variations of the SPC water model are shown in Table 5.3. The experimental value for water at 298.15 K is 78.48. The reparameterization of the charges in the SPC/E model was done in order to better model the dipole moment of the liquid phase, so it is not surprising that the SPC/E model also predicts a better value for DC than the standard SPC model, since the DM and DC are so closely related. Unfreezing the scissoring angle mode without changing the point charges also produced a significant change in the simulated DC; the effect is considerably larger than that found by unfreezing the bond vibrational modes. This is likely because angle compression in the liquid phase increases the instantaneous dipole moment, corresponding to what we have termed the distortion polarizability, while the bond vibrations do not directly increase charge separation in the direction of the dipole vector. Interestingly, these internal mode contributions to the simulated value of water DC are approximately summative. That is, the vibrational degrees of freedom increased the DC value by about 5.5, the angle-bending mode increased the DC value by about 11, and the combination of both increased the model DC by about 15.

Table 5.3 Simulated DC values for variations on the SPC water model at 298.15 K

SPC_{RR}	SPC/E	SPC_{RF}	SPC_{FR}	SPC_{FF}
67.12 ± 1.38	75.58 ± 1.35	78.38 ± 2.33	72.6 ± 1.5	82.02 ± 1.08

5.3.2 Pure Organic Compounds

The most commonly used force-field models for organic compounds are united atom (UA), meaning interaction sites are only assigned to the heavy (non-hydrogen) nuclear centers. That is, hydrogen atoms are subsumed into the carbon atoms to which they are attached. The UA approach, or grouping of H atoms with their attached carbon atom, is only applied to C-H bonds; hydrogen atoms attached to strongly electronegative atoms that would impart a different chemical functionality to the hydrogen atom are still explicitly treated as separate interaction sites. Such is the case for the hydroxyl H in organic alcohols for example.

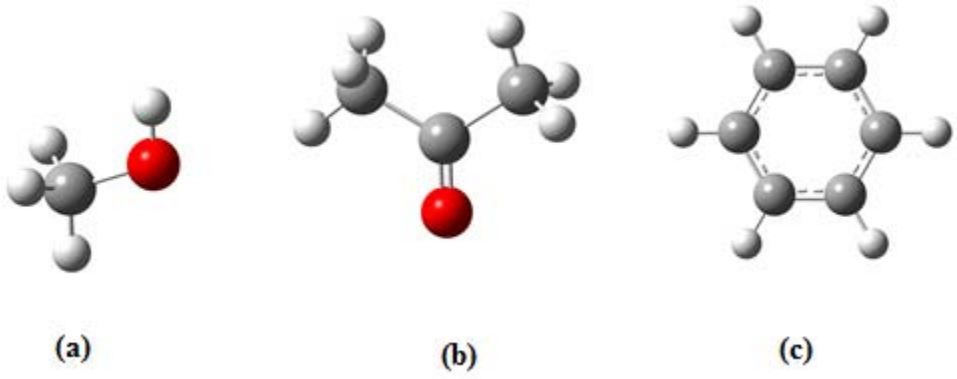

Figure 5.3 Model geometries use for (a) methanol, (b) acetone, and (c) benzene.

We have performed pure-component MD simulations on rigid models for methanol, acetone and benzene. The geometries of these models are shown in Figure 5.3 with the bond lengths and angles specified in Table 5.4. Bond lengths and bond angles were taken from the literature optimized geometries, and all internal vibrational modes were frozen using neighbor and next-neighbor distance constraints in conjunction with Gaussian mechanics.

Table 5.4 Geometry parameters for methanol[85], acetone[85] and benzene[86]

Molecule	Bond	r_o (Å)	Angle	θ (degrees)
Methanol	H_3C–O	1.425	H_3C–O–H	108.5
	O–H	0.945		
Acetone	H_3C–C	1.518	H_3C–C=O	121.7
	C=O	1.212	H_3C–C–CH_3	116.6
Benzene	H–C	1.082	C–C–C	120
	C–C	1.390	C–C–H	120

Table 5.5 Simulation parameters for methanol[85], acetone[85] and benzene[86]

Molecule	Site	Mass (gm/mol)	ε_{ii}/k_B (K)	σ_{ii}(Å)	q
Methanol	CH3	15.0347	105.200	3.7400	0.265
	O	15.9994	86.500	3.0300	-0.700
	H	1.008	0.000	0.000	0.435
Acetone	O(=C)	15.9994	68.0	2.97	-0.51
	CH3	15.035	85.0	3.81	0.03
	CH3	15.035	85.0	3.81	0.03
	C	12.011	50.0	3.60	0.45
Benzene	C	12.011	35.743	3.6316	-0.153
	C	12.011	35.743	3.6316	-0.153
	C	12.011	35.743	3.6316	-0.153
	C	12.011	35.743	3.6316	-0.153
	C	12.011	35.743	3.6316	-0.153
	C	12.011	35.743	3.6316	-0.153
	H	1.008	15.950	2.3291	0.153
	H	1.008	15.950	2.3291	0.153
	H	1.008	15.950	2.3291	0.153
	H	1.008	15.950	2.3291	0.153
	H	1.008	15.950	2.3291	0.153
	H	1.008	15.950	2.3291	0.153

Lennard-Jones potentials and point charges were used to model all of the site-site interactions in accordance with Eq. (5.15). Values for the LJ parameters and the site point partial charges, all obtained from the literature, are provided in Table 5.5. The LJ ε_{ii} and σ_{ii} values shown in the table are for the "like" interactions, interactions between the same two kinds of sites. All of the "cross" interactions between dissimilar sites were calculated using the Lorentz-Berthelot combining rules

$$\varepsilon_{ij} = \sqrt{\varepsilon_{ii}\varepsilon_{jj}} \quad \sigma_{ij} = \frac{\sigma_{ii} + \sigma_{jj}}{2} \tag{5.16}$$

in accordance with the manner in which the original parameters were regressed.

Table 5.6 Experimental and model values for DM and experimental and simulated values for DC for organic liquids

	Methanol	Acetone	Benzene
Model DM	2.22 D	0.32 D	0 D
Experimental DM	1.70 D	2.88 D	0 D
Simulated DC model	21.56	9.06	1.05
Experimental DC	32.66	20.8	2.3

Simulated DC values for these three fluids are shown in Table 5.6 along with the experimental values for the real fluids. Unlike the SPC/E model for water, these models from the literature were not optimized to reproduce the condensed-phase dipole moment and so the simulated values of DC are substantially in error. The reliability of the DC value obtained from the simulation depends critically on the quality of the model, especially upon the way in which

the partial charges are chosen and arranged. In the case of the water study, it was evident that polarization through small changes in the bond distances and angle impact the simulated value of the DC. This is likely the case with methanol where the model dipole is actually higher than the gas-phase experimental dipole moment, but the simulated DC value is 34% below the experimental value. However, for acetone, the model's charge assignment gives a DM value substantially too low, which is likely the dominant reason for a simulated DC that is less than half the experimental value. This discrepancy in the DM value has been noted by others[87,88] and there is indirect evidence that omission of polarizability also impacts the DM value. The model for benzene produces a value of DC very close to 1.0, which is to be expected for non-polar fluids. The experimental DC is significantly larger than this, likely due to the out-of-plane electron density in the pi-cloud electrons that are not included in the force-field model. It is evident from these three examples that inaccuracies in the force-field model's charge distribution, and therefore its permanent dipole moment, has a large impact on the quantitative accuracy of the simulated static dielectric constant.

5.3.3 Mixture Simulations

As discussed above, not all of the commonly used force-field models have been tuned to provide the correct DM value and therefore they may not produce accurate values of DC in condensed-phase simulations of the pure fluid. It is nevertheless of interest to perform simulations on model mixtures for at least two reasons. First, dipole moments are often measured in nonpolar solvents. The permanent dipole moment of the isolated molecule is generally the value reported in databases, and it is thought that measuring the DM for a chemical in a dilute mixture provides a good value for the DM of the isolated molecule if the solvent is

nonpolar. However, even nonpolar molecules interacting in the condensed phase can have impact on the dipole moment and therefore the value of DC. Therefore, observation of the effect of a nonpolar solvent on the solute DM and DC through MD simulations can provide insight into the accuracy of values obtained in solution. Second, the magnitude and composition dependence of the excess DC, as defined in Eqs. (4.6) and (4.7), is determined by the local structuring in the fluid. The excess DC, ε^E, depends upon the relative interactions between the like and unlike molecules. Although the simulations may not quantitatively predict the DC for the pure fluids, the shape and magnitude of ε^E as a function of composition may be obtainable from simulations somewhat independent of the accuracy of the pure fluid simulated DC value. The manner in which a change in the compositional environment impacts the orientational polarization of the molecule can be examined with the current force fields using molecular dynamics.

Simulations were performed at varying compositions for both polar-polar and polar-nonpolar binary mixtures. Polar-polar mixtures included water + methanol, water + acetone, and methanol + acetone; polar-nonpolar mixtures included water + benzene, methanol + benzene, and acetone + benzene mixtures. Benzene is often the non-polar solvent that experimentalists use in making DM measurements for liquid polar solutes. The geometries and force-field models used for the mixtures are the same as those previously specified for the pure fluids. The SPC_{RF} water model was used for all of the aqueous mixtures. As with the pure fluid simulations, 125 total molecules were used in the simulation cell, but the fraction of molecules of each component was varied in accordance with the desired mole fraction of the mixture.

Simulated values of ε at 298.15 K for mixtures of methanol+water are shown in Figure 5.4 along with the experimental ε values obtained by Åkerlöf.[56] The compositional trend is a monotonic decrease in the value of the mixture dielectric constant with increasing concentration

of methanol, the less polar of the two components. Also shown in the figure are the curves obtained from Oster's rule and from the NRTL predictive model developed in Chapter 4. Both of these models under predict the mixture DC values compared with the experimental data. Interestingly, the MD results are in good agreement with the experimental values for methanol mole percents less than 25% in spite of the fact that the pure methanol model DC value is only two thirds that of the experimental value. This suggests that the strongly polar compound dominates the local structure and electrostatic field within the fluid. Deviations of the MD simulated values from the experimental data increase at the methanol-rich compositions where the inaccuracy of the model for the less polar molecule now becomes increasingly influential in the localized field felt by neighboring molecules and the orientational polarizations are significantly diminished relative to what happens in the real fluid.

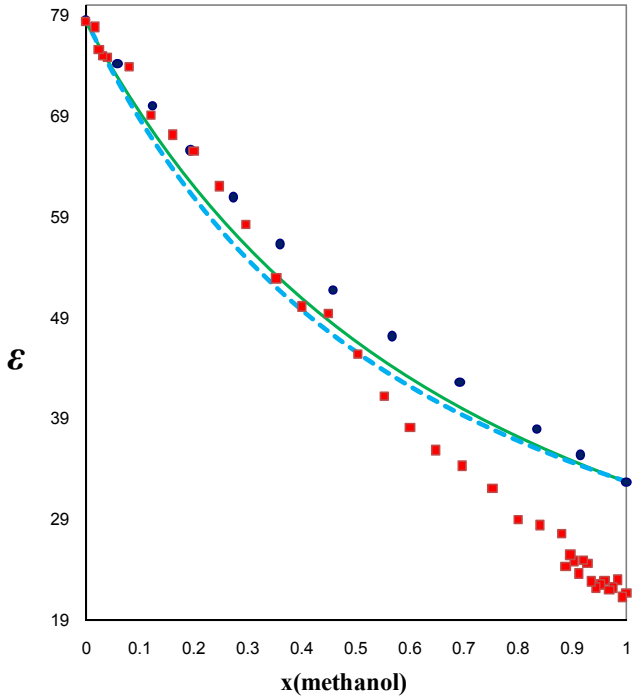

Figure 5.4 Comparison of experimental ε values (●) to those obtained from MD simulations (■), NRTL model (——) and Oster's rule (- - - - -) at 298.15 K for methanol + water mixture

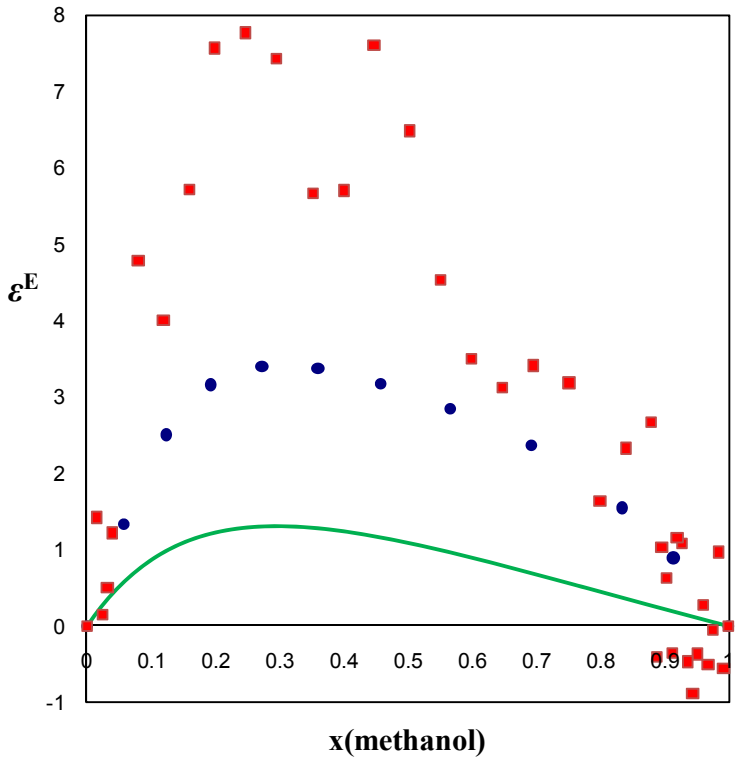

Figure 5.5 Experimental ε^E values (●) compared to those predicted by simulation (■) and by the NRTL model (——) for methanol + water mixtures at 298.15 K

Because the pure ε value for methanol is in error, it is of interest to compare the simulated excess dielectric constant as calculated from Eq. 4.6 for this system with that obtained from the experimental data as this eliminates the offset due to the pure component error. These results are shown in Figure 5.5. The experimental values are used for the pure-component values in the NRTL and Oster's rule calculations to focus strictly on the excess DC values. The shapes of all three curves in Figure 5.5 are similar with the asymmetric maximum in the excess DC in the water-rich region. The uncertainty in the simulated values is reflected in the scatter of points and is on the order of 2 DC units. Although the simulated ε^E values are larger than the experimental values, the shape and location of the maximum are in good agreement with the experimental data. The methanol-rich region from 50% to 100% methanol is modeled quite

well. The system deviates from ideality most in the water-rich region from 10 – 50 mol% methanol. Easteal[89] and Schneider[90] report larger excess volumes in this composition region which is known to produce deviations from Oster's rule. This effect is mimicked by the model fluids in the MD simulation.

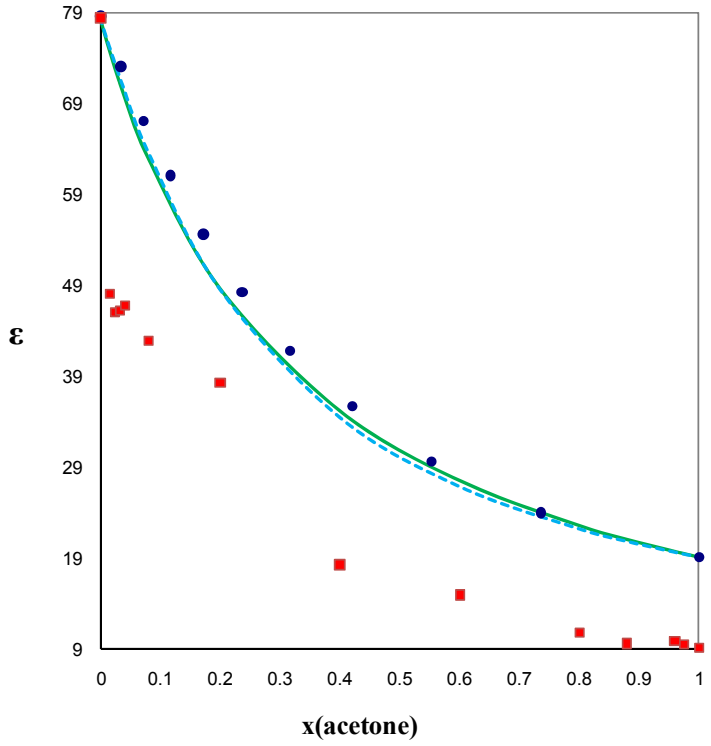

Figure 5.6 Comparison of experimental ε values (●) to those obtained from MD simulations (■), NRTL model (——) and Oster's rule (- - - - -) for acetone + water mixtures at 298.15 K

Figures 5.6 and 5.7 show ε and ε^E for acetone + water mixtures. Tolosa[91] found that the solvent-solvent energy in acetone-water solutions was weaker than that of both pure solvents and this was attributed to a predominance of the hydrophilic group interactions over those of the hydrophobic groups in acetone. This is expected to weaken mutual interactions and decrease the DC values especially for the acetone-rich compositions, and Tolosa's model predicts a negative ε^E for this system.

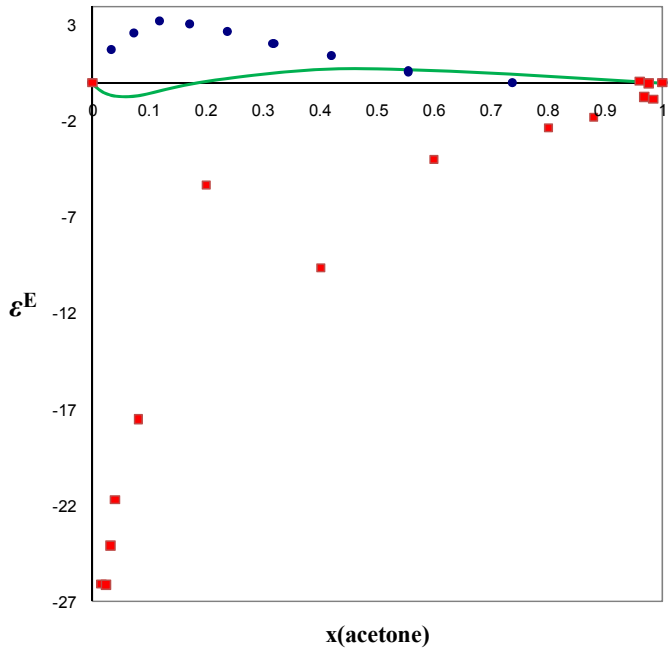

Figure 5.7 Experimental ε^E values (●) compared to those predicted by simulation (■) and by the NRTL model (——) for acetone + water mixtures at 298.15 K

It will be remembered that the pure acetone DC value is severely under predicted by the force-field model, which is again emphasized in Table 5.7. The simulated value is only 20% of the actual experimental value. It is very interesting that the introduction of a very small amount of acetone into water drops precipitously the simulated DC value as seen in Figure 5.6. Table 5.7 shows that even two acetone molecules added to water drops the $\langle M^2 \rangle$ value by 16%. Because the acetone model is so under-polarized (only 11% of the actual dipole moment), insertion of even 1.6 mol% significantly breaks up the local orientational structuring that occurs in pure water due to the strong hydrogen-bond network, lowering the DC value to 48.04. Interestingly, Tolosa[92] used the $MCY_{EX\text{-}DIS\text{-}ES}$ model[93] estimated a value of 41.65 for ε in very dilute solutions of acetone in water. As can be seen in Figure 5.7, this structure breaking corresponds to a very large negative ε^E. On the other hand, the experimental data show positive

values for ε^E in the water-rich region and essentially no excess DC in the acetone-rich region. The presence of water molecules does not greatly impact the orientational polarizability of the acetone molecules, but the presence of (real) acetone molecules does increase the orientational structure of water due to its large dipole moment.

Table 5.7 Dielectric properties of simulated acetone-water mixtures

System	$\langle M^2 \rangle$	ε	DM (D)	DM (D) exp
Pure water	2870.8	78.38	2.274	1.850
Pure acetone	1590.5	9.06	0.32	2.881
2 molecules of acetone (with 123 water molecules)	2401.3	48.04		

Figures 5.8 and 5.9 show the simulation results for acetone + methanol mixtures at 298.15 K. The results for this system are similar to those obtained for the acetone-water system. Again the addition of a small amount of model acetone with its artificially low DM value significantly disrupts the orientational alignment of the more strongly polar molecules, in this case methanol. The result is a strongly negative excess DC value, again significantly biased at compositions rich in the strongly polar compound.

The results of the MD simulations for the polar-polar mixtures suggest three important inferences. First, in order for the simulations to be quantitatively correct, the models for the pure components must be parameterized to give the correct dipole moment. This is certainly not surprising. Second, mixtures of molecules of disparate DM values exhibit a great deal of asymmetry in the excess DC. That is, ε of a strongly polar fluid is significantly more impacted

(reduced) by the addition of a lower-ε impurity or fluid than the reverse case of the addition of a strongly polar fluid impurity into a weakly polar fluid. A small amount of the highly polar molecule does not produce strong orientational polarization in the weakly polar fluid, but the weakly polar molecule can significantly disrupt the orientational alignment of a more polar fluid. And third, it appears possible to make mixture MD simulations of ε quantitative if the pure fluid charges are parameterized appropriately to produce correct DMs. That is to say, the charge distribution in the molecule dominates the prediction of ε and the dispersion interactions are less important. Treating the cross interaction terms with the simple Lorentz-Berthelot combining rule is probably sufficient. The ability to use MD simulations to quantitatively obtain multicomponent DC values is particularly appealing and likely realizable if the pure fluid models are appropriately parameterized.

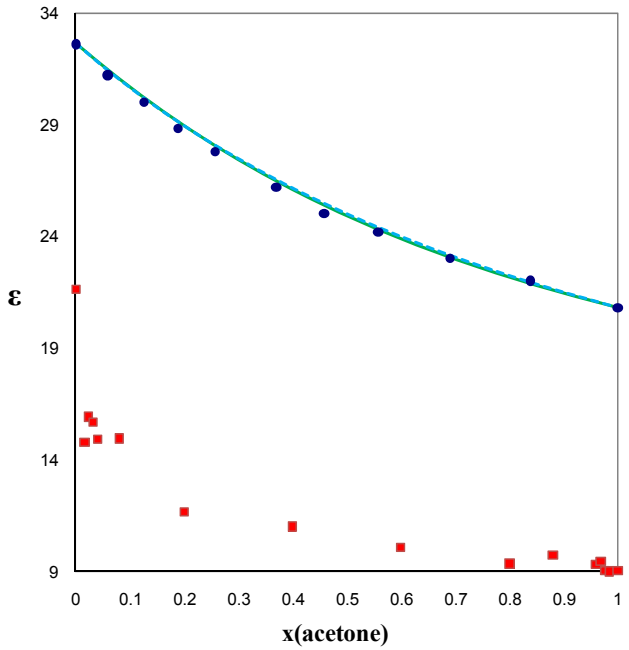

Figure 5.8 Comparison of experimental ε values (●) to those obtained from MD simulations (■), NRTL model (——) and Oster's rule (- - - - -) for acetone + methanol mixtures at 298.15 K

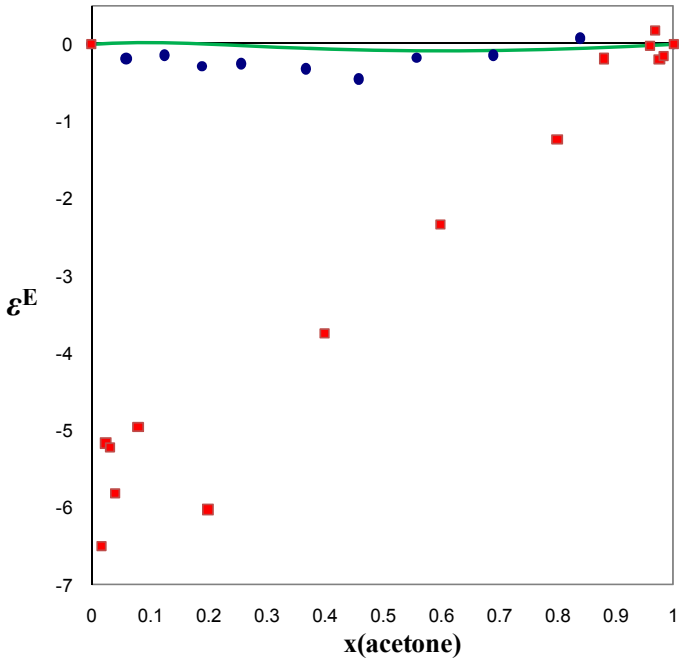

Figure 5.9 Experimental ε^E values (●) compared to those predicted by simulation (■) and by the NRTL model (——) for acetone + methanol mixtures at 298.15 K

The simulation results for the polar-nonpolar mixtures are next examined. Figures 5.10 and 5.11 show ε and ε^E for benzene + water mixtures at 298.15 K. The literature force-field model for benzene produces a value of ε close to 1, roughly half that of the experimental value. This is most likely due to neglecting the quadrupole moment of benzene in the model. Table 5.8 shows that even one benzene molecule added to water drops the $\langle M^2 \rangle$ value by 15.4%, which is comparable to the effect seen with the addition of two acetone molecules to water. Because benzene is nonpolar, actual mixtures with water are only partially miscible. The results shown are for the hypothetical homogeneous mixtures. The addition of benzene molecules is expected to disrupt the hydrogen bonding network within the water. Meng et al. [94] stated that the water-solute interaction sacrifices about one solvent-solvent hydrogen bond. They suggested that one to

two water molecules donate hydrogen bonds to the aromatic system. In our MD simulations the addition of only 1% benzene decreases the DC value to 49.12 for the mixture.

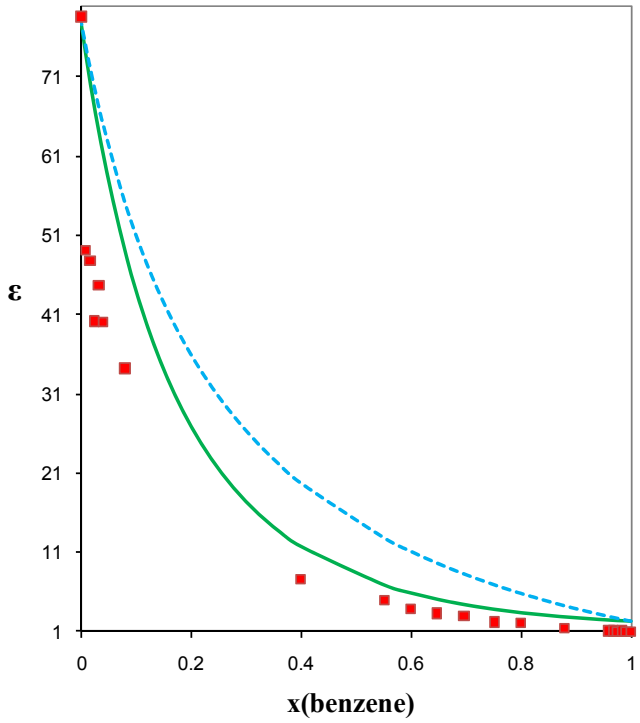

Figure 5.10 Comparison of ε values from MD simulations (■), NRTL model (——) and Oster's rule (- - - -) for benzene + water mixtures at 298.15 K

Figure 5.10 also shows that in the benzene-rich region, the values from the MD simulations are very close to the NRTL predicted values. In this region and the DC values are close to unity because of the propensity for the water to form all possible hydrogen bonds around the benzene "ring" and restrict the rotational degrees of freedom. Figure 5.11 shows that the excess DC value is quite well predicted by the simulations in the benzene-rich region.

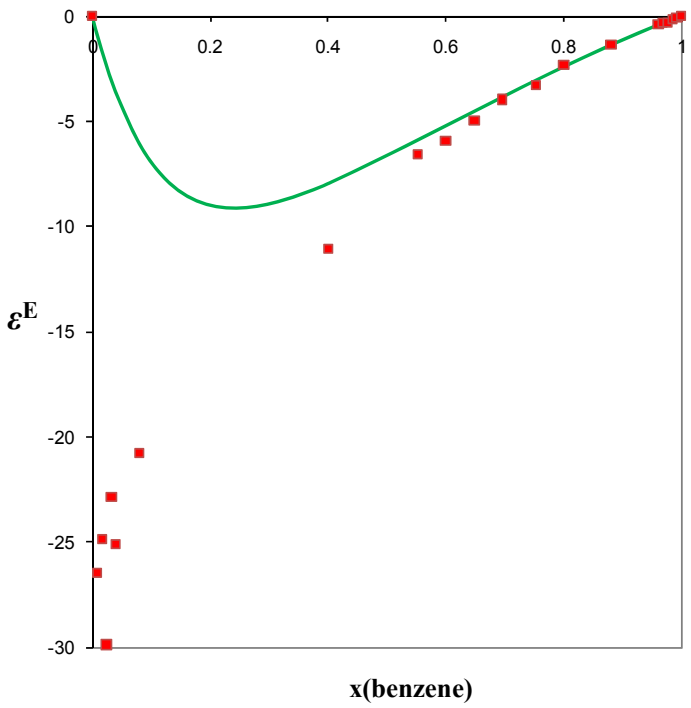

Figure 5.11 Comparison of ε^E values obtained from MD simulations (■) and from the NRTL model(——) for benzene + water mixtures at 298.15 K

Table 5.8 Dielectric properties of benzene-water solution

System	$\langle M^2 \rangle$	ε
Pure water	2870.8	78.38
Pure benzene	0	1.05
1 molecule of acetone in the mixture	2429.7	49.12

Figure 5.12 to Figure 5.14 show the simulation results for benzene + methanol and benzene + acetone mixtures at 298.15 K. The results for these two binary systems are similar to those obtained for the benzene-water system. Because of the inadequacies of the pure-fluid

models, the excess DC values have the largest value when small amounts of nonpolar molecules are added to the mixture.

There are no experimental values to which the NRTL and MD values can be compared for these three nonpolar + polar systems. But the shapes for the excess DC are very close to those predicted by the NRTL model, Oster's rule and MD simulation. For the benzene + acetone mixtures, the DC values are almost linear between the pure values with very small excess DC values.

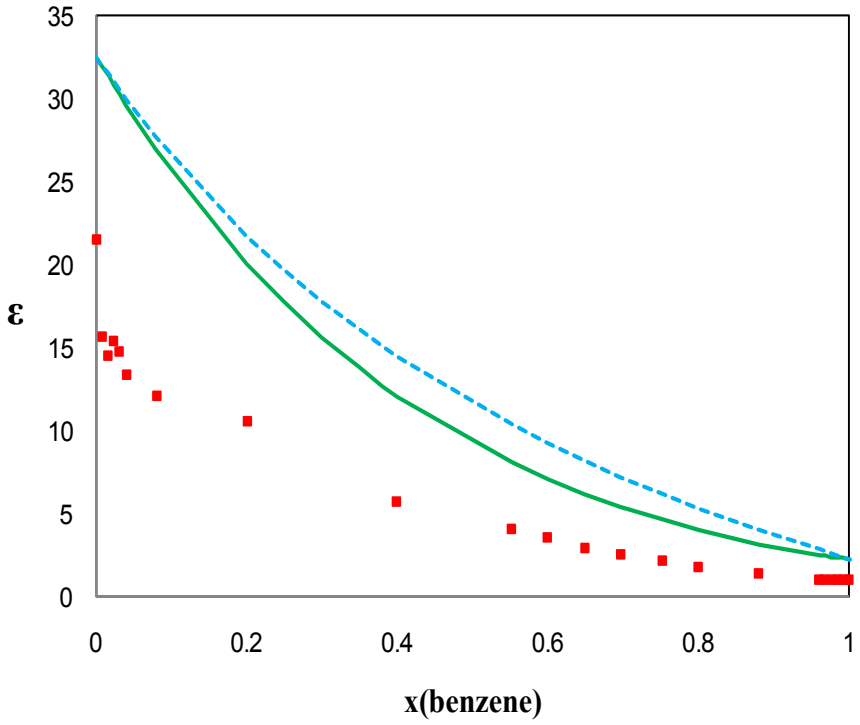

Figure 5.12 Comparison of ε values from MD simulations (■), NRTL model (——) and Oster's rule (- - - - -) for benzene + methanol mixtures at 298.15 K

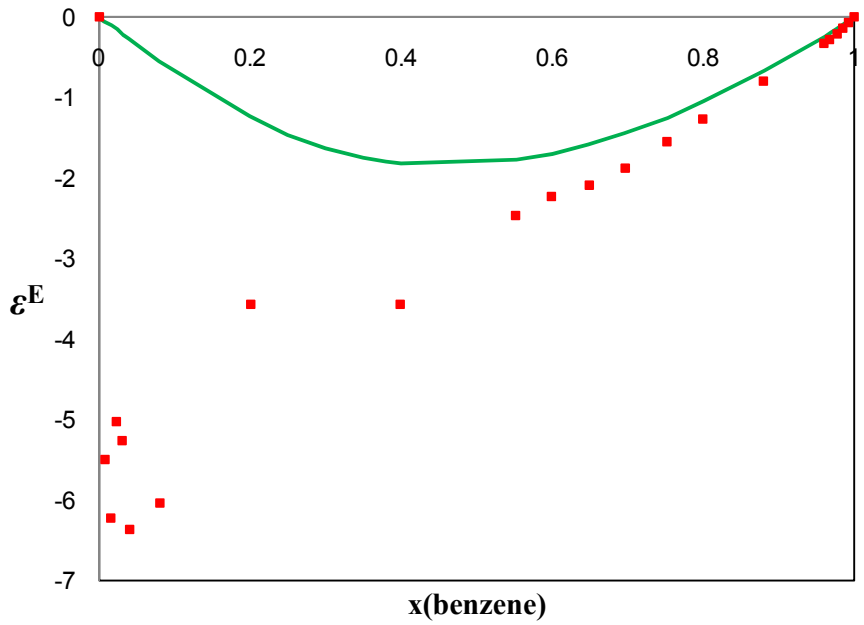

Figure 5.13 Comparison of ε^E values obtained from MD simulations (■) and from the NRTL model(——) for benzene + methanol mixtures at 298.15 K

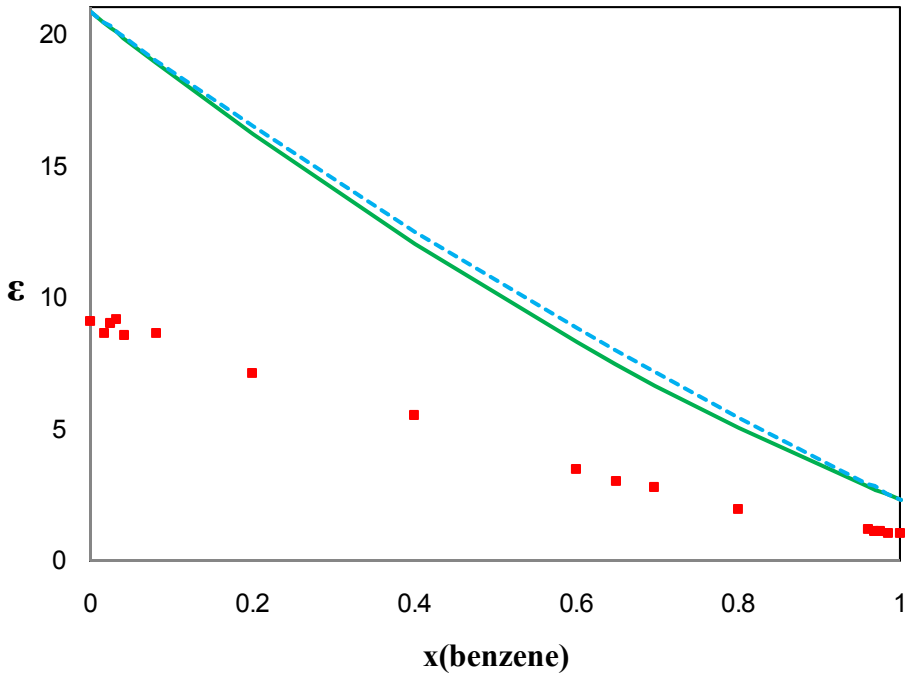

Figure 5.14 Comparison of ε values from MD simulations (■), NRTL model (——) and Oster's rule (- - - - -) for benzene + acetone mixtures at 298.15 K

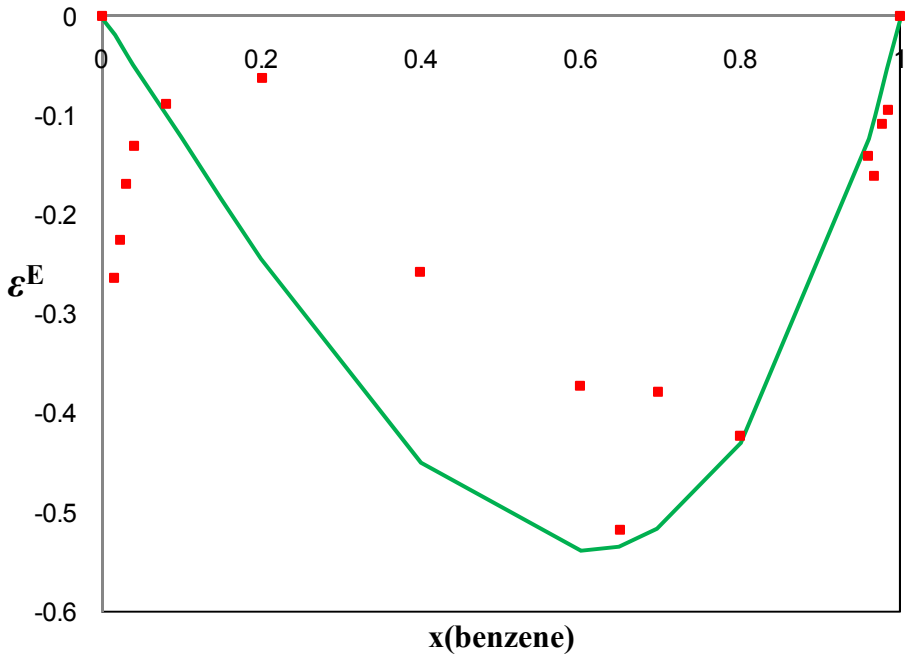

Figure 5.15 Comparison of ε^E values obtained from MD simulations (■) and from the NRTL model (——) for benzene + acetone mixtures at 298.15 K

5.4 Conclusion

In this chapter, DC values for the SCP water model and variations of that model with additional internal flexibility were obtained from MD simulations. Starting from the rigid standard SPC model, flexibility was introduced by adding harmonic O-H bond and H-O-H angle potentials. It was found that SPC/E model predicted a better DC value than the standard SPC model, since it is a reparameterization of the SPC charges to give a more correct dipole moment. The angle flexibilty affects the DC value more than flexibility in the bonds as the angle tends to have a more direct effect on the distortional polarization of the molecule, but the two effects appear to be nearly summative.

We have also performed pure-component MD simulations on rigid models for methanol, acetone and benzene to investigate the orientational polarization of these organic molecules. The

force-field models for these fluids are also from the literature, but unlike the water SPC models, the parameters were not optimized to reproduce the condensed-phase dipole moment. Simulated ε values were in error directly related to the error in the DM of the model. The reliability of the DC values obtained from simulation depends critically on the quality of the model, particularly the charge distribution within the model.

Mixture simulations and analysis of resultant excess dielectric constants suggest that mixture ε values can be quantitatively obtained if pure-component models have been appropriately parameterized to reproduce the experimental dipole moment. The results also reveal interesting asymmetries in the mixture ε values when the constituent components of the mixture differ significantly in dipole moment. In general, the impact on DC value is substantially larger when a low-ε impurity is introduced into high-ε pure fluid than the converse situation. Low-ε fluids disrupt the orientational polarizability more effectively than enhancement of ε by the addition of a high-ε impurity. The discrepancy between model prediction and experimental data indicates the limitation of the force-field model, specifically the assignment of charge distribution within the molecule. The results suggest that quantitative prediction of multicomponent mixture DC values is likely possible if models for the pure fluids have been properly parameterized to yield values of DM and DC consistent with experimental values.

Chapter 6

Conclusions and Recommendations

6.1 Conclusions

The DIPPR 801 pure chemical database provides values for all 45 physical properties of each chemical. This means that accurately predicted values must be used when experimental data are not available. Unfortunately, none of the currently available methods for predicting dielectric constants are of adequate accuracy and sufficient reliably to be used to predict DC values for inclusion in the DIPPR database and for use by practicing engineers. The first objective of this work was development of a universal, accurate, prediction method for the dielectric constant of pure fluids with an uncertainty of less than 20% for essentially all compounds and less than 10% for the majority of compounds. A second objective has been the development of an accurate predictive method for mixture dielectric constants, given that the pure-component values can be accurately obtained. The NRTL and simulation methods were developed in fulfillment of this objective. A third objective has been to gain a better understanding of the role orientational and distortional polarization plays in the observed value of DC and how fluid structure in mixtures impacts these values. Again, both the NRTL theory and the MD simulations have aided in accomplishing this objective.

Analysis of available DC data in the literature has led to both improvement of values previously available in the DIPPR database and in the addition of new quality experimental data

not previously included. The literature data, analyzed for accuracy, was used as a training set for development of the pure-chemical prediction method developed in this work. A new Quantitative Structure-Property (QSPR) method was developed using dipole moment, van de Waals area, solubility parameter, and refractive index as the molecular descriptors. Values of these descriptors are readily available in the DIPPR 801 database. Development was based on the strategy of retaining the fewest possible molecular descriptors to avoiding over-fitting the data, and choosing descriptors representing the general underlying physics behind DC to ensure extrapolation capability. On the basis of the regression analysis and tests of the correlation in prediction mode, different coefficients are to be used with non-polar and hydrocarbon fluids than with polar fluids. The average absolute percent error is 2.96% or average absolute error of 0.07 for a test set of 167 hydrocarbons and non-polar compounds. Oxygen group-specific interactions are added for polar fluids. The correlation developed for polar fluids used a training set of 519 polar chemicals. It gave an average absolute error of 2.05 or an average absolute percent deviation of 17.78%. The test results showed little degradation from the correlating effectiveness with an average absolute percent deviation of 17.83% for a test set of 42 compounds not included in the training set with ε values ranging from 1 to 50.

The accuracy of the correlation is currently limited by the extent and accuracy of the available experimental data. Further refinement of the correlation would likely require not only additional data but a limitation on the training set data to include data of only the highest accuracy. This has not been done because of our objective to keep the correlation generally applicable to all organic compounds and the requisite need for an extensive database of 500 compounds or more to satisfy that objective. Nevertheless, these results suggest that the correlation can be used to predict ε values with an average uncertainty of about 18% for polar

compounds and of about 3% for non-polar compounds. The correlation is not intended for compounds where the predicted value is greater than 50.

The impact of uncertainties in the dipole moment was tested through quantum mechanical methods that can be used to predict dipole moment and to indentify optimum model chemistry (basis set size and level of theory in *ab initio*) for accurate predictions. Comparing 191 compounds shows that B3LYP/6-311+G(3df,2p) gave an average error of 8.08%. This was determined (based on results compiled in the NIST database) to be the most reliable of the commonly used *ab initio* and DFT methods for calculating μ, when experimental μ values are not available.

A local composition model was developed for mixture dielectric constants based on the nonrandom two-liquid (NRTL) model commonly used for correlating activity coefficients in vapor-liquid equilibrium (VLE) data regression. In this model the NRTL local compositions, which represent an effective local molecular structure, are the counterpart of the Kirkwood factor *g*, which in dielectric constant theory characterizes local molecular orientations and their effect on the static dielectric constant. The resultant model requires values for the pure-component dielectric constant and binary NRTL model parameters available from VLE data compilations or predicted from the universal functional activity coefficient model (UNIFAC). It is predictive in that no mixture dielectric constant data are used and there are no adjustable parameters. Predictions made on 16 binary mixtures yielded a maximum AAD of 5%, and predictions on six ternary systems produced a maximum AAD of 12% over a variety of compositions and temperatures. Predicted results with no adjustable parameters compare favorably with extant correlations that require experimental values to fit an adjustable parameter in the mixing rule and

are significantly improved over values predicted by Oster's equation that similarly has no adjustable parameters.

The opportunity to predict mixture DC values from molecular simulation was also investigated. As in the case with the NRTL model, mixture results depend upon good pure-component DC values. However, in the case of MD simulations, the pure component values are obtained directly from simulation as opposed to using values from experiment or from the pure-component correlation developed in this work. Different variations of the SPC water model were tested to obtain a preliminary understanding of the relative importance of that portion of distortion polarization that occurs by angle and bond compression or expansion. Angle distortion had a larger impact than bond distortion on DC, but the two effects were nearly summative. A rigid model appropriately parameterized to yield a DM value consistent with experiment yields good results for predicted DC of the pure fluid. The reliability of the DC value obtained from the simulation depends critically on the quality of the model, particularly the charge distribution.

Mixture simulations and analysis of excess dielectric constants showed that quantitative mixture ε values are likely obtainable if the simulated DC values of the constituent pure components agree with experimental values. The shapes of the excess DC are generally consistent with experimental data as a function of composition if the pure component DC values are reasonably good. Mixture simulations also show that the orientational polarization of high dielectric fluids is changed significantly by small amounts of low dielectric fluids. The reverse is not the case; small amounts of high dielectric fluid does not significantly enhance the DC value of a low dielectric fluid.

6.2 Recommendations

The accuracy of the new QSPR correlation for pure DC values for polar and nonpolar fluids is limited by the quality and quantity of currently available experimental data. Further improvement of the correlation would require additional accurate experimental not only in training set but also in a more extensive test set. A comprehensive measurement program for fluid DC values would be a substantial boon to both the DIPPR database and the refinement of the correlation developed in this study.

The dielectric constant is not independent of temperature though it is treated as a constant property in the DIPPR database. This is possible because the DIPPR project defines the property as the value at 298.15 K and 1 bar. Most measurements have been made at this temperature, but there are cases where the DC value for a pure liquid is available only at a single temperature and pressure, but not necessarily at 298.15 K and 1 bar. In these cases, the variation of the dielectric constant with changing temperature and pressure needs to be predicted. Additionally, the NRTL model for mixtures also need pure fluids DC values at different temperatures. In future work it would be important to extend our method to the calculation of pure fluid DC values at different temperatures and pressures. Again, the ability to do so would be strongly dependent upon the available experimental data. The requirement for such data again prompts a call for more experimental studies to be performed.

The MD simulation results suggest the model for pure fluids should be parameterized to be quantitative correct. Future studies in this area should look at re-parameterizing existing force-field models for the pure components to give the correct condensed-phase dipole moments. The application of these models to mixture simulations will then better define the capability of

MD simulations to generate accurate mixture DC values. In particular, the opportunity to use MD simulations for prediction of DC in multi-component mixtures is particularly appealing.

It is also important to develop the force-field model to deal with charge distribution and polarizability which impacts the dipole moments in future studies. In this work we have not used polarizable potentials in the sense of the charges within the molecule adjusting to the local environment. The effect of this portion of the distortion polarization should be examined in more complete studies of the relationship between the force field model and the resultant DC value.

Nomenclature

Symbol

AAD	average absolute deviation
AAPD	Average Absolute Percent Deviation
A_{ji}	NRTL energy parameter
$A_{\underline{\text{vdw}}}$	van der Waals area
C	capacitance of a material
C_0	capacitance of a vacuum
C_i	correlation coefficients
CODESSA	comprehensive descriptors for structural and statistical analysis
D	Debye – dipole unit
DC	static dielectric constant
DIPPR	Design Institute for Physical Properties
DM	dipole moment
e_i	partial charge on site i
g	rotational correlation parameter
G_i	group contribution for an oxygen containing group i in Eq. (3.1)
G_{ji}	NRTL parameter in Eq. (4.13)
G_k	finite-system Kirkwood correlation factor
HF	Hartree-Fock method
k_a	harmonic spring constant for angle bending
k_b	harmonic spring constant for bond vibration
k_B	Boltzmann's constant, 1.3806×10^{-23} J/K
k_i	the number of instances of group i in the molecule in Eq.(3.1)
k_{ij}	binary parameter in Eq. (4.9)
M	molecular weight
$\langle M \rangle$	ensemble average of total dipole moment
MLR	Multiple Linear Regression
n	refractive index
N_A	Avogadro's number
NRTL	nonrandom-two-liquid
N_s	total number of simulation steps
p	molar polarization per unit volume
p^E	excess molar polarization per unit volume for mixture
p_i	molar polarization per unit volume for pure component i
$p^{(i)}$	polarizations per unit volume for hypothetical fluid i

p^{id}	molar polarization per unit volume for ideal mixture
p_{ji}	parameters characteristic of *j*-*i* polarization interactions in Eq. (4.10)
$-Q$	negative charge
$+Q$	positive charge
QSAR	Quantitative Structure-Activity Relation
QSPR	Quantitative Structure-propertyProperty Relation
R	gas constant
r_i	position vector of molecule *i*
r_{OH_1}	O-H bond lengths in water molecule
RMS	root-mean-squared error
SPC	simple-point-charge water model
SPC/E	extended simple-point-charge water model
SPC_{FF}	flexible bond and flexible angle SPC model
SPC_{FR}	flexible bond and rigid angle SPC model
SPC_{RF}	rigid bond and flexible angle SPC model
SPC_{RR}	rigid bond and rigid angle SPC model
superscript †	density corresponding to the reduced density of the fluids
T	temperature (K)
UA	United atom (model)
u_{ji}	interaction energy parameter in Eq. (4.12)
U_{inter}	intermolecular potential energy
U_{intra}	intramolecular potential energy
UNIFAC	the UNIversal Functional Activity Coefficient method
V	voltage difference
V_i	specific volume of component *i*
w_i	weight fraction of component *i*
x_{ij}	local mole fraction of *i* around *j* in hypothetical fluid *j*
Z	number of nearest neighbor
$\Delta H_{\varpi\alpha\pi}$	heat of vaporization
α	polarizability of a molecule
α_a	atomic polarizability
α_{a2}	atomic polarizability of the solute
α'_{a2}	fictitious atomic polarizability
α_{a1}	atomic polarizability of the solvent
α_e	electronic polarizability
α_o	orientation polarizability
γ	angle between the dipole moment of the neighbor molecule
δ	solubility parameter
ε	static dielectric constant
ε^E	excess dielectric constant
ε_{ij}	Lennard-Jones potential well-depth parameter
ε_{RF}	the dielectric constant of the medium outside the cutoff sphere

ε_{∞}	static dielectric constant at optical frequencies
$\theta_{\angle HOH}$	H-O-H bond angle in water molecule
μ	dipole moment
ν_i	molar volume of component *i* in solution
ρ	number density - number of molecules per unit volume
ρ_m	mass density
σ_{ij}	Lennard-Jones potential size parameter
ϕ_i	volume fraction of component *i*
$\phi_{i,j}$	local volume fraction of molecule *i* around a central molecule *j*
$\phi(t)$	Fourier transform of the dipole moment autocorrelation function

Appendix

Table A.1 The basis sets and theories

Set and theories	Explanation
3-21G	A VDZ basis set.
3-21G*	The asterisk indicates that a set of polarizing d-functions (6D) is included to supplement the 3-21G basis, but only on second-row and heavier atoms (beyond neon).
5D	Indicates that five functions are used in each d-set.
6D	Indicates that six (cartesian) functions are used in each d-set. This includes the s-like combination $(x^2 + y^2 + z^2)$.
6-31G	The "6" indicates that each core basis function is built using six primitives. The "3" indicates that the inner valence basis functions are each built using three primitives. The "1" indicates that the outer valence basis functions are each built using a single uncontracted primitive. The "G" stands for "Gaussian", indicating the type of primitive function.
6-311G*	The asterisk indicates that a set of polarization d-functions (5D) has been added to heavy atoms to supplement the 6-311G basis; also denoted 6-311G(d).
6-311G**	The second asterisk indicates that a set of polarization p-functions has been added to hydrogen; also denoted 6-311G(d,p).
6-311+G(3df,2p)	In addition to the 6-311G basis, the "+" indicates that diffuse s- and p-functions are added to heavy atoms, the "3df" indicates that three sets of polarization d-functions and one set of polarization f-functions are added to heavy atoms, and the "2p" indicates that two sets of polarization p-functions are added to hydrogen.
6-31G*	The single asterisk indicates that a set of polarizing d-functions (6D) is included on "heavy" atoms (beyond helium). Also denoted 6-31G(d).
6-31G**	A set of polarizing d-functions (6D) is included on "heavy" atoms and a set of p-functions on hydrogen. Also denoted 6-31G(d,p).
6-31+G*	Augmented 6-31G* basis; the single "+" indicates that a set of diffuse s-functions and a set of diffuse p-functions has been added to each heavy atom. Also denoted 6-31+G(d).
6-31++G*	Augmented 6-31+G* basis; the second "+" indicates that a set of diffuse s-functions has been added to each hydrogen atom. Also denoted 6-31++G(d).
AM1	Austin model 1. One of the most popular semi-empirical MO theories.
aug-cc-pVDZ	Augmented cc-pVDZ basis (diffuse functions added).
B3LYP	DFT using Becke exchange functional and Lee-Yang-Parr correlation functional, as well as Hartree-Fock exchange. A hybrid method; the parameters were optimized for thermochemistry, but using a different functional and numerical (basis set-free) code
BLYP	DFT using the Becke exchange functional and the Lee-Yang-Parr correlation functional.
CBS	Complete basis set. Indicates that some method of basis set extrapolation was applied in an attempt to determine the result that would have been obtained using an infinitely large basis set. The two major extrapolation methods are (1) repeating the calculation with increasingly large basis sets and making an empirical extrapolation, and (2) using analytical formulas that are correct to second-order.

Table A.1 Con't

Set and theories	Explanation
cc-pVDZ	Correlation-consistent polarized valence double-zeta basis set. The smallest in a series of correlation consistent basis sets developed by Dunning and coworkers for high-level calculations.
cc-pVTZ	Correlation-consistent polarized valence triple-zeta basis set.
CEPA	Coupled electron pair approximation. An approximate coupled-cluster-type method. Pretty high level.
DFT	Density-functional theory. *Ab initio* method not based upon a wavefunction. Instead, the energy is computed as a functional of the electron density.
ECP	Effective core potential. The core electrons have been replaced by an effective potential. Saves computational expense. May sacrifice some accuracy, but can include some relativistic effects for heavy elements. It has basis set of CEP-31G, CEP-31G*, CEP-121G, CEP-121G*, LANL2DZ and SDD, et.
Hartree-Fock	Simplest and least expensive *ab initio* wavefunction. Involves only a single Slater determinant (a single electron configuration). Orbitals that contain electrons are "occupied," those that are vacant are called "virtual."
MBS	Minimal basis set. Only enough basis functions are supplied to put all the electrons somewhere; the number of basis functions is equal to the number of orbitals. The most common of these is "STO-3G". Qualitative results at best.
MM	molecular mechanics
MNDO	A semi-empirical method ("minimal neglect of differential overlap").
MO	Molecular orbital.
MP2	Second-order Møller-Plesset perturbation theory. Standard Rayleigh-Schrödinger perturbation theory taken to second order
Mulliken population	A procedure for assigning net atomic charges within a molecule. It includes an arbitrary choice involving overlap populations, and more seriously is very sensitive (values varying by more than 100%) to the choice of basis set.
PM3	A semi-empirical method.
semi-empirical	An approximate version of Hartree-Fock theory in which the more computationally expensive integrals are replaced by adjustable parameters, which are determined by fitting experimental atomic and molecular data. Different choices of parameterization lead to different specific theories (e.g., MNDO, AM1, PM3). Semiempirical calculations are much faster than *ab initio* calculations.
STO	Slater-type orbital. Basis function with an exponential radial function, i.e., exp(- zeta r). Also used to denote a fit to such a function using other functions, such as gaussians..
STO-3G	The most popular MBS.
VDZ	Valence double-zeta. A minimal basis is used to describe core electrons, but the valence electrons have twice the minimum number of functions (see "DZ").
VTZ	Valence triple-zeta. A minimal basis is used to describe core electrons, but the valence electrons have three times the minimum number of functions (see "DZ").

Table A.2 New experimental DC values

ChemID	Compound	Phase	New value	Recom. Value
204	1-BUTENE	G	2.2195	1.00
205	cis-2-BUTENE	G	1.96	1.00
301	PROPADIENE	G	2.025	1.00
303	1,3-BUTADIENE	G	2.05	1.00
402	METHYLACETYLENE	G	3.218	1.00
904	NITROGEN TRIOXIDE	G	31.13	1.00
917	FLUORINE	G	1.4913	1.00
918	CHLORINE	G	2.147	1.00
926	ARSINE	G	2.4	1.00
1601	DICHLORODIFLUOROMETHANE	G	3.5	1.00
1602	TRICHLOROFLUOROMETHANE	G	3	1.00
1606	CHLOROTRIFLUOROMETHANE	G	3.01	1.00
1609	1,2-DICHLOROTETRAFLUOROETHANE	G	2.4842	1.00
1614	DIFLUOROMETHANE	G	53.74	1.00
1701	METHYLAMINE	G	16.7	1.00
1704	ETHYLAMINE	G	8.7	1.00
1893	CARBONYL SULFIDE	G	4.47	1.00
1905	HYDROGEN FLUORIDE	G	83.6	1.00
1983	DIBORANE	G	1.8725	1.00
1986	NITROSYL CHLORIDE	G	18.2	1.00
1987	PERCHLORYL FLUORIDE	G	2.194	1.00
2651	HEXAFLUOROACETONE	G	2.104	1.00
2686	BROMOCHLORODIFLUOROMETHANE	G	3.92	1.00
2687	BROMOTRIFLUOROMETHANE	G	3.73	1.00
2688	DIBROMODIFLUOROMETHANE	G	2.939	1.00
2694	VINYL BROMIDE	G	5.63	1.00
55	SQUALANE	L	1.9106	1.9106
91	2-METHYLOCTANE	L	1.967	1.967
209	1-PENTENE	L	2.011	2.011
216	1-HEXENE	L	2.077	2.077
218	trans-2-HEXENE	L	1.978	1.978
234	1-HEPTENE	L	2.092	2.092
250	1-OCTENE	L	2.113	2.113
259	1-NONENE	L	2.18	2.18
260	1-DECENE	L	2.136	2.136
261	1-UNDECENE	L	2.137	2.137
262	1-DODECENE	L	2.152	2.152
263	1-TRIDECENE	L	2.139	2.139
314	trans,trans-2,4-HEXADIENE	L	2.123	2.123
331	1,3-CYCLOHEXADIENE	L	2.68	2.68
516	MESITYLENE	L	2.279	2.279
532	1,2,4,5-TETRAMETHYLBENZENE	L	2.223	2.223
541	PENTAMETHYLBENZENE	L	2.358	2.358
547	HEXAMETHYLBENZENE	L	2.172	2.172
549	n-HEPTYLBENZENE	L	2.26	2.26
558	BIPHENYL	L	2.53	2.53

Table A.2 Con't

ChemID	Compound	Phase	New value	Recom. Value
564	1,2-DIPHENYLETHANE	L	2.47	2.47
565	TRIPHENYLMETHANE	L	2.46	2.46
613	alpha-METHYLSTYRENE	L	2.28	2.28
701	NAPHTHALENE	L	2.54	2.54
703	2-METHYLNAPHTHALENE	L	2.747	2.747
804	ANTHRACENE	L	2.649	2.649
805	PHENANTHRENE	L	2.72	2.72
1065	MESITYL OXIDE	L	15.6	15.6
1068	DIISOBUTYL KETONE	L	9.91	9.91
1092	gamma-BUTYROLACTONE	L	39	39
1113	2,2-DIMETHYL-1-PROPANOL	L	8.35	8.35
1137	1-UNDECANOL	L	5.98	5.98
1141	1-TRIDECANOL	L	4.02	4.02
1142	1-TETRADECANOL	L	4.42	4.42
1143	1-PENTADECANOL	L	3.7	3.7
1144	1-HEXADECANOL	L	3.69	3.69
1145	1-HEPTADECANOL	L	3.41	3.41
1146	1-OCTADECANOL	L	3.38	3.38
1147	2-ETHYL-1-BUTANOL	L	6.19	6.19
1148	1-EICOSANOL	L	3.13	3.13
1166	TETRAHYDROFURFURYL ALCOHOL	L	13.48	13.48
1168	2-PHENYL-2-PROPANOL	L	5.61	5.61
1169	2-BUTYL-OCTAN-1-OL	L	3.28	3.28
1170	2,3-XYLENOL	L	4.81	4.81
1174	2,5-XYLENOL	L	5.36	5.36
1176	2,6-XYLENOL	L	4.9	4.9
1177	3,4-XYLENOL	L	9.02	9.02
1178	3,5-XYLENOL	L	9.06	9.06
1242	1,5-PENTANEDIOL	L	26.2	26.2
1244	1,2-BENZENEDIOL	L	17.57	17.57
1245	1,3-BENZENEDIOL	L	13.55	13.55
1250	SORBITOL	L	35.5	35.5
1256	n-BUTYRIC ACID	L	2.98	2.98
1272	n-HEXADECANOIC ACID	L	2.417	2.417
1298	MALEIC ANHYDRIDE	L	52.75	52.75
1306	n-PENTYL FORMATE	L	5.7	5.7
1324	n-PROPYL PROPIONATE	L	5.249	5.249
1327	n-PROPYL n-BUTYRATE	L	4.3	4.3
1332	METHYL n-BUTYRATE	L	5.48	5.48
1361	ISOPENTYL ISOVALERATE	L	4.39	4.39
1363	n-HEXYL ACETATE	L	4.42	4.42
1364	BENZYL BENZOATE	L	5.26	5.26
1365	n-BUTYL BENZOATE	L	5.52	5.52
1367	n-HEPTYL ACETATE	L	4.2	4.2
1373	METHYL SALICYLATE	L	8.8	8.8

Table A.2 Con't

ChemID	Compound	Phase	New value	Recom. Value
1383	n-BUTYL STEARATE	L	3.12	3.12
1385	n-BUTYL n-BUTYRATE	L	4.39	4.39
1422	TRIOXANE	L	15.55	15.55
1432	ACETAL	L	3.8	3.8
1458	DIETHYLENE GLYCOL DIETHYL ETHER	L	5.7	5.7
1465	DIPHENYL ETHER	L	3.726	3.726
1478	FURAN	L	2.94	2.94
1480	DIBENZOFURAN	L	3	3
1501	CARBON TETRACHLORIDE	L	2.2379	2.2379
1524	1,1,2-TRICHLOROETHANE	L	7.1937	7.1937
1527	1,1,1-TRICHLOROETHANE	L	7.243	7.243
1528	1,1,1,2-TETRACHLOROETHANE	L	9.22	9.22
1529	1,1,2,2-TETRACHLOROETHANE	L	8.5	8.5
1541	TRICHLOROETHYLENE	L	3.39	3.39
1574	p-DICHLOROBENZENE	L	2.3943	2.3943
1576	BENZOTRICHLORIDE	L	6.9	6.9
1580	cis-1,2-DICHLOROETHYLENE	L	9.2	9.2
1581	trans-1,2-DICHLOROETHYLENE	L	2.14	2.14
1590	PENTACHLOROETHANE	L	3.716	3.716
1591	1,1-DICHLOROETHYLENE	L	4.6	4.6
1649	1,1,2,2-TETRABROMOETHANE	L	6.72	6.72
1655	1-BROMOBUTANE	L	7.315	7.315
1698	TRIBROMOMETHANE	L	4.404	4.404
1714	ISOBUTYLAMINE	L	4.43	4.43
1720	n-TETRADECYLAMINE	L	2.9	2.9
1725	TRIETHANOLAMINE	L	29.36	29.36
1727	tert-BUTYLAMINE	L	58.5	58.5
1738	p-TOLUIDINE	L	5.058	5.058
1755	PYRAZINE	L	2.8	2.8
1756	DIPHENYLAMINE	L	3.73	3.73
1772	ACETONITRILE	L	36.64	36.64
1779	p-NITROTOLUENE	L	22.2	22.2
1787	ISOBUTYRONITRILE	L	24.42	24.42
1805	ISOBUTYL MERCAPTAN	L	4.961	4.961
1845	SULFOLANE	L	43.26	43.26
1849	DI-n-BUTYL SULFONE	L	25.72	25.72
1852	CHLOROACETIC ACID	L	12.35	12.35
1859	o-CHLOROANILINE	L	13.4	13.4
1866	DI(2-CHLOROETHYL)ETHER	L	21.2	21.2
1876	N,N-DIMETHYLFORMAMIDE	L	38.25	38.25
1923	SULFUR	L	3.4991	3.4991
1924	PHOSPHORUS (WHITE)	L	4.096	4.096
1925	PHOSPHORUS TRICHLORIDE	L	3.498	3.498
1926	PHOSPHORUS PENTACHLORIDE	L	2.85	2.85
1927	PHOSPHORUS THIOCHLORIDE	L	4.94	4.94
1931	VANADIUM TETRACHLORIDE	L	3.05	3.05

Table A.2 Con't

ChemID	Compound	Phase	New value	Recom. Value
1934	ANTIMONY TRICHLORIDE	L	3.222	3.222
1937	TETRACHLOROSILANE	L	2.248	2.248
1965	HEXAMETHYLDISILOXANE	L	2.179	2.179
1966	HEXAMETHYLCYCLOTRISILOXANE	L	2.139	2.139
1998	IODINE	L	11.08	11.08
2081	n-TRIACONTANE	L	1.9112	1.9112
2115	2-PHENYLETHANOL	L	12.31	12.31
2118	1-PHENYL-1-PROPANOL	L	6.68	6.68
2219	2,4-PENTANEDIOL	L	24.69	24.69
2279	2-ETHYL BUTYRIC ACID	L	2.72	2.72
2376	DI-n-BUTYL PHTHALATE	L	6.58	6.58
2527	1,3-DICHLOROPROPANE	L	10.27	10.27
2637	DIBROMOMETHANE	L	7.77	7.77
2655	1,1,2-TRICHLOROTRIFLUOROETHANE	L	2.41	2.41
2656	1,1,2,2-TETRACHLORODIFLUOROETHANE	L	2.52	2.52
2661	p-BROMOTOLUENE	L	5.503	5.503
2685	n-BUTYL IODIDE	L	6.27	6.27
2707	n-HEPTYLAMINE	L	3.81	3.81
2708	n-OCTYLAMINE	L	3.58	3.58
2710	n-DECYLAMINE	L	3.31	3.31
2740	m-DINITROBENZENE	L	22.9	22.9
2779	NITROGLYCERINE	L	19.25	19.25
2780	o-NITROANILINE	L	47.3	47.3
2781	p-NITROANILINE	L	78.5	78.5
2782	m-NITROANILINE	L	35.6	35.6
2790	NICOTINONITRILE	L	20.54	20.54
2853	ACETAMIDE	L	67.6	67.6
2859	p-METHOXYPHENOL	L	11.05	11.05
2862	2-BUTOXYETHANOL	L	9.3	9.3
2882	m-CHLORONITROBENZENE	L	20.9	20.9
2886	ACETYLSALICYLIC ACID	L	6.55	6.55
2894	p-CHLOROPHENOL	L	11.18	11.18
2965	TITANIUM TETRACHLORIDE	L	2.843	2.843
3107	THYMOL	L	4.259	4.259
3717	2-BUTOXIME	L	3.4	3.4
3925	TIN(IV) CHLORIDE	L	3.014	3.014
3988	TRIMETHYLCHLOROSILANE	L	10.21	10.21
4858	m-CHLOROANILINE	L	13.3	13.3
4865	TRICHLOROACETALDEHYDE	L	6.8	6.8
4866	TRICHLOROACETIC ACID	L	4.34	4.34
4873	ETHYL CHLOROFORMATE	L	9.736	9.736
4882	o-CHLORONITROBENZENE	L	37.7	37.7
4883	p-CHLORONITROBENZENE	L	8.09	8.09
4887	CYCLOHEXANONE OXIME	L	3.04	3.04
5884	2-ETHOXYETHYL ACETATE	L	7.567	7.567
5889	ETHYL CYANOACETATE	L	31.62	31.62

Table A.2 Con't

ChemID	Compound	Phase	New value	Recom. Value
5898	1-CHLORO-2-PROPANOL	L	59	59
6855	THIODIGLYCOL	L	28.61	28.61
7856	1-CHLORO-3-PROPANOL	L	36	36
7865	METHYL para-TOLUATE	L	4.3	4.3
7895	IRON PENTACARBONYL	L	2.602	2.602
21113	2,2-DIMETHYL-1-PROPANOL_2003Review	L	8.35	8.35
21137	1-UNDECANOL_2002Review	L	5.98	5.98
21141	1-TRIDECANOL_2002Review	L	4.02	4.02
21142	1-TETRADECANOL_2002Review	L	4.42	4.42
21143	1-PENTADECANOL_2002Review	L	3.7	3.7
21144	1-HEXADECANOL_2002Review	L	3.69	3.69
21145	1-HEPTADECANOL_2002Review	L	3.41	3.41
21146	1-OCTADECANOL_2002Review	L	3.38	3.38
21147	2-ETHYL-1-BUTANOL_2003Review	L	6.19	6.19
21148	1-EICOSANOL_2002Review	L	3.13	3.13
21256	n-BUTYRIC ACID_2002Review	L	2.98	2.98
21272	n-HEXADECANOIC ACID_2002Review	L	2.417	2.417
21655	1-BROMOBUTANE_2005Review	L	7.315	7.315

Table A.3 Recommended changes to experimental DC values

Chem ID	Compound	Phase	Current value	New value	Recom. value	Uncertainty
3	PROPANE	G	1.6678	1.002	1.002	<0.2%
4	ISOBUTANE	G	1.7518	1.0026	1.0026	<0.2%
5	n-BUTANE	G	1.7697	1.00258	1.00258	<0.2%
202	PROPYLENE	G	2.1365	1.00228	1.00228	<0.2%
901	OXYGEN	G	1.0004947	1.00049	1.00049	<0.2%
902	HYDROGEN	G	1.0002538	1.00025	1.00025	<0.2%
905	NITROGEN	G	1.000548	1.00025	1.00055	<0.2%
908	CARBON MONOXIDE	G	1.00065	1.00262	1.00262	<0.2%
909	CARBON DIOXIDE	G	1.4492	1.000922	1.000922	<0.2%
910	SULFUR DIOXIDE	G	16.3	1.00825	1.00825	<0.2%
913	HELIUM-4	G	1.000065	1.00007	1.00007	<0.2%
914	ARGON	G	1.0005172	1.00052	1.00052	<0.2%
1401	DIMETHYL ETHER	G	6.18	1.0062	1.0062	<0.2%
1502	METHYL CHLORIDE	G	10	1.0108	1.0108	<0.2%
1503	ETHYL CHLORIDE	G	9.45	1.01325	1.01325	<0.2%
1616	CARBON TETRAFLUORIDE	G	1.00121	1.00126	1.00126	<0.2%
1911	AMMONIA	G	16.61	1.00622	1.00622	<0.2%
3964	CHLORINE TRIFLUORIDE	G	1.7876	4.394	1	<0.2%
21502	METHYL CHLORIDE_2005Review	G	10	1	1.0108	<0.2%
21503	ETHYL CHLORIDE_2005Review	G	9.45	1.01325	1.01325	<0.2%
21616	CARBON TETRAFLUORIDE_2004Review	G	1.00121	1.00126	1.00126	<0.2%
56	n-DECANE	L	2.41	1.9853	1.9853	<1%
1222	HEXYLENE GLYCOL	L	25.86	23.4	23.4	<10%
1354	DIOCTYL PHTHALATE	L	5.22	5.3	5.3	<3%
1366	ETHYLENE CARBONATE	L	89.78	90.5	90.5	<1%
1549	CHLOROCYCLOHEXANE	L	8.056	7.9505	7.9505	<1%
1681	METHYL IODIDE	L	1.00914	6.97	6.97	<3%
2260	2-ETHYL HEXANOIC ACID	L	2.5	2.64	2.64	<3%
3715	8-METHYLQUINOLINE	L	2.3231	6.58	6.58	<10%
3929	TETRAETHOXYSILANE	L	4.1	2.5	2.5	<10%
3932	EICOSAMETHYLNONASILOXANE	L	2.149	2.645	2.645	<5%
22685	n-BUTYL IODIDE_2005Review	L	6.12	6.27	6.27	<5%

Table A.4 New predicted DC values based on Eq. (4.1)

ChemID	Compound	Phase	Recommended	Unc
29	3-METHYLHEPTANE	L	1.9604	<1%
30	4-METHYLHEPTANE	L	1.9579	<1%
33	2,3-DIMETHYLHEXANE	L	1.9589	<1%
34	2,4-DIMETHYLHEXANE	L	1.9352	<1%
38	2-METHYL-3-ETHYLPENTANE	L	1.9683	<1%
44	2,2,3,3-TETRAMETHYLBUTANE	L	1.9979	<10%
47	2,2,5-TRIMETHYLHEXANE	L	1.9324	<1%
48	3,3,5-TRIMETHYLHEPTANE	L	1.9857	<3%
49	2,4,4-TRIMETHYLHEXANE	L	1.9535	<1%
50	3,3-DIETHYLPENTANE	L	2.0001	<1%
51	2,2,3,3-TETRAMETHYLPENTANE	L	1.9993	<1%
52	2,2,3,4-TETRAMETHYLPENTANE	L	1.9712	<1%
53	2,2,4,4-TETRAMETHYLPENTANE	L	1.9361	<1%
54	2,3,3,4-TETRAMETHYLPENTANE	L	1.9988	<1%
57	2,2,3,3-TETRAMETHYLHEXANE	L	2.0035	<3%
58	2,2,5,5-TETRAMETHYLHEXANE	L	1.9382	<3%
61	iso-BUTYLCYCLOHEXANE	L	2.1064	<10%
62	tert-BUTYLCYCLOHEXANE	L	2.0797	<10%
70	n-OCTADECANE	L	2.0665	<1%
72	2,2-DIMETHYLOCTANE	L	1.9655	<3%
73	n-EICOSANE	L	2.0687	<1%
74	n-HENEICOSANE	L	2.0707	<1%
76	n-TRICOSANE	L	2.0721	<1%
77	n-TETRACOSANE	L	2.0735	<1%
78	n-PENTACOSANE	L	2.0727	<3%
79	n-HEXACOSANE	L	2.0744	<3%
80	n-HEPTACOSANE	L	2.0785	<3%
81	n-OCTACOSANE	L	2.0745	<3%
82	n-NONACOSANE	L	2.0715	<3%
85	3-METHYLNONANE	L	1.9957	<1%
86	2-METHYLNONANE	L	1.9874	<1%
87	4-METHYLNONANE	L	1.9954	<1%
88	5-METHYLNONANE	L	1.9940	<1%
90	2,2,4,4,6,8,8-HEPTAMETHYLNONANE	L	2.0082	<5%
92	3-METHYLOCTANE	L	1.9813	<1%
94	3-ETHYLHEPTANE	L	1.9835	<3%
96	2,2-DIMETHYLHEPTANE	L	1.9488	<3%
100	3-METHYLUNDECANE	L	2.0245	<1%
107	ETHYLCYCLOPENTANE	L	2.0382	<10%
108	1,1-DIMETHYLCYCLOPENTANE	L	1.9963	<10%
109	cis-1,2-DIMETHYLCYCLOPENTANE	L	2.0388	<10%
110	trans-1,2-DIMETHYLCYCLOPENTANE	L	2.0053	<10%
111	cis-1,3-DIMETHYLCYCLOPENTANE	L	1.9896	<10%
112	trans-1,3-DIMETHYLCYCLOPENTANE	L	1.9992	<10%
114	n-PROPYLCYCLOPENTANE	L	2.0543	<10%
115	ISOPROPYLCYCLOPENTANE	L	2.0371	<10%
116	1-METHYL-1-ETHYLCYCLOPENTANE	L	2.0355	<10%

Table A.4 Con't

ChemID	Compound	Phase	Recommended	Unc
122	n-BUTYLCYCLOPENTANE	L	2.0653	<10%
140	ETHYLCYCLOHEXANE	L	2.0659	<10%
141	1,1-DIMETHYLCYCLOHEXANE	L	2.0321	<10%
142	cis-1,2-DIMETHYLCYCLOHEXANE	L	2.0676	<10%
143	trans-1,2-DIMETHYLCYCLOHEXANE	L	2.0330	<10%
144	cis-1,3-DIMETHYLCYCLOHEXANE	L	2.0203	<10%
145	trans-1,3-DIMETHYLCYCLOHEXANE	L	2.0499	<10%
146	cis-1,4-DIMETHYLCYCLOHEXANE	L	2.0455	<10%
147	trans-1,4-DIMETHYLCYCLOHEXANE	L	2.0108	<10%
148	1-trans-3,5-TRIMETHYLCYCLOHEXANE	L	2.0492	<10%
149	n-PROPYLCYCLOHEXANE	L	2.0737	<10%
150	ISOPROPYLCYCLOHEXANE	L	2.0784	<10%
151	1,2,3,4-TETRAMETHYLCYCLOHEXANE	L	2.1125	<10%
152	n-BUTYLCYCLOHEXANE	L	2.0827	<10%
155	BICYCLOHEXYL	L	2.1818	<3%
156	1,1-DIETHYLCYCLOHEXANE	L	2.1164	<10%
158	n-DECYLCYCLOHEXANE	L	2.1168	<10%
161	trans-1,4-DIETHYLCYCLOHEXANE	L	2.0746	<10%
190	2,2-DIMETHYL-3-ETHYLPENTANE	L	1.9555	<1%
192	2,4-DIMETHYL-3-ETHYLPENTANE	L	1.9786	<1%
203	1-TRIACONTENE	L	2.0969	<1%
210	cis-2-PENTENE	L	1.9731	<3%
211	trans-2-PENTENE	L	1.9194	<3%
217	cis-2-HEXENE	L	2.0714	<3%
221	2-METHYL-1-PENTENE	L	2.1140	<10%
222	3-METHYL-1-PENTENE	L	1.9934	<10%
223	4-METHYL-1-PENTENE	L	1.9975	<10%
224	2-METHYL-2-PENTENE	L	2.0661	<10%
225	3-METHYL-cis-2-PENTENE	L	2.0443	<10%
226	4-METHYL-1-HEXENE	L	1.9560	<10%
227	4-METHYL-cis-2-PENTENE	L	1.9305	<10%
228	4-METHYL-trans-2-PENTENE	L	1.9437	<10%
229	2-ETHYL-1-BUTENE	L	1.9572	<10%
230	2,3-DIMETHYL-1-BUTENE	L	1.9248	<10%
231	3,3-DIMETHYL-1-BUTENE	L	1.8681	<10%
232	2,3-DIMETHYL-2-BUTENE	L	2.0082	<10%
233	2-ETHYL-1-PENTENE	L	1.9806	<10%
235	cis-2-HEPTENE	L	2.0265	<3%
236	trans-2-HEPTENE	L	1.9798	<1%
237	trans-3-HEPTENE	L	1.9759	<1%
238	2-METHYL-1-HEXENE	L	2.1358	<10%
239	3-ETHYL-1-PENTENE	L	1.9500	<10%
240	3-METHYL-1-HEXENE	L	1.9501	<10%
241	3-ETHYL-1-HEXENE	L	2.0830	<5%
242	4-METHYL-1-HEPTENE	L	2.0812	<10%
243	1-TETRACONTENE	L	1.8865	<5%

Table A.4 Con't

ChemID	Compound	Phase	Recommended	Unc
244	cis-2-NONENE	L	2.0362	<3%
245	trans-2-NONENE	L	2.0123	<1%
248	2,3,3-TRIMETHYL-1-BUTENE	L	1.9438	<10%
249	cis-3-HEPTENE	L	2.0397	<1%
251	trans-2-OCTENE	L	1.9937	<1%
257	2,4,4-TRIMETHYL-2-PENTENE	L	1.9798	<5%
258	2-ETHYL-1-HEXENE	L	1.9930	<3%
264	1-TETRADECENE	L	2.2182	<3%
265	1-PENTADECENE	L	2.1928	<1%
266	1-HEXADECENE	L	2.1577	<1%
267	1-OCTADECENE	L	2.1629	<1%
268	6-METHYL-1-HEPTENE	L	1.9746	<10%
271	trans-2-EICOSENE	L	2.0461	<3%
272	trans-2-PENTADECENE	L	2.0617	<3%
274	CYCLOOCTENE	L	2.4838	<10%
276	cis-2-OCTENE	L	2.0891	<3%
281	1-HEPTADECENE	L	2.1837	<1%
283	1-NONADECENE	L	2.2027	<3%
284	1-EICOSENE	L	2.2054	<3%
285	VINYLCYCLOHEXENE	L	2.2455	<5%
286	1-METHYLCYCLOPENTENE	L	2.0826	<10%
287	3-METHYLCYCLOPENTENE	L	2.0386	<10%
288	4-METHYLCYCLOPENTENE	L	2.1837	<1%
289	2,3-DIMETHYL-1-HEXENE	L	1.9807	<3%
292	PROPENYL CYCLOHEXENE	L	2.1933	<10%
304	1,2-PENTADIENE	L	2.2140	<5%
306	trans-1,3-PENTADIENE	L	2.2197	<15%
308	2,3-PENTADIENE	L	2.1859	<10%
311	3-METHYL-1,2-BUTADIENE	L	2.2262	<15%
312	METHYLCYCLOPENTADIENE	L	2.4583	<15%
313	1,4-HEXADIENE	L	2.0013	<10%
315	CYCLOPENTADIENE	L	2.2881	<15%
316	DICYCLOPENTADIENE	L	2.3902	<3%
317	alpha-PHELLANDRENE	L	2.1636	<5%
318	beta-PHELLANDRENE	L	2.4360	<3%
320	cis,trans-2,4-HEXADIENE	L	2.2211	<5%
321	3-METHYL-1,4-PENTADIENE	L	2.0107	<3%
322	1,5,9-CYCLODODECATRIENE	L	2.2085	<10%
329	2,5-DIMETHYL-1,5-HEXADIENE	L	2.0315	<10%
330	2,5-DIMETHYL-2,4-HEXADIENE	L	2.1731	<10%
333	1,5-CYCLOOCTADIENE	L	2.4381	<10%
340	trans-1,3-HEXADIENE	L	2.1487	<1%
341	trans-2-METHYL-1,3-PENTADIENE	L	2.2846	<15%
342	1,9-DECADIENE	L	2.1639	<3%
343	1,3,5,7-CYCLOOCTATETRAENE	L	2.3761	<10%
404	DIMETHYLACETYLENE	L	3.6897	<10%

Table A.4 Con't

ChemID	Compound	Phase	Recommended	Unc
405	1-PENTYNE	L	2.3024	<10%
406	3-HEXYNE	L	2.0368	<10%
407	2-HEXYNE	L	2.2233	<10%
412	2-PENTYNE	L	2.2008	<10%
414	2-METHYL-1-BUTENE-3-YNE	L	2.1637	<10%
416	1-OCTYNE	L	2.3660	<10%
419	3-METHYL-1-BUTYNE	L	2.1597	<10%
420	1-PENTENE-3-YNE	L	2.4133	<10%
421	1-PENTENE-4-YNE	L	2.2766	<10%
424	DIPHENYLACETYLENE	L	2.4335	<3%
426	1-NONYNE	L	2.4384	<10%
427	1-DECYNE	L	2.4498	<10%
522	o-CYMENE	L	2.4083	<1%
523	m-CYMENE	L	2.2903	<3%
531	1,2,3,5-TETRAMETHYLBENZENE	L	2.4788	<10%
533	p-tert-BUTYL ETHYLBENZENE	L	2.1655	<3%
534	1,4-DI-tert-BUTYLBENZENE	L	2.1498	<10%
536	1,3,5-TRI-TERTBUTYLBENZENE	L	2.1816	<1%
537	1,3,5-TRIISOPROPYLBENZENE	L	2.0951	<5%
542	1,2,4,5-TETRAISOPROPYL BENZENE	L	2.1702	<10%
543	m-DIISOPROPYLBENZENE	L	2.2331	<5%
544	p-DIISOPROPYLBENZENE	L	2.1986	<1%
545	1,2,4-TRIETHYLBENZENE	L	2.2547	<1%
548	1,2,3-TRIETHYLBENZENE	L	2.4683	<10%
553	1,2,3,5-TETRAETHYLBENZENE	L	2.3785	<1%
554	n-DECYLBENZENE	L	2.2009	<3%
555	PENTAETHYLBENZENE	L	2.2986	<1%
556	HEXAETHYLBENZENE	L	2.1051	<3%
557	CYCLOHEXYLBENZENE	L	2.6090	<10%
559	p-TERPHENYL	L	2.4768	<3%
560	m-TERPHENYL	L	2.5277	<1%
561	o-TERPHENYL	L	2.3577	<5%
562	1,1-DIPHENYLETHANE	L	2.5042	<1%
566	2,4-DIPHENYL-4-METHYLPENTENE-1	L	2.4279	<1%
567	n-PENTYLBENZENE	L	2.2180	<3%
570	n-NONYLBENZENE	L	2.2067	<3%
571	n-UNDECYLBENZENE	L	2.2013	<3%
572	n-TRIDECYLBENZENE	L	2.1814	<5%
573	n-TETRADECYLBENZENE	L	2.1712	<5%
574	n-DODECYLBENZENE	L	2.1887	<5%
576	2-ETHYL-m-XYLENE	L	2.5630	<15%
577	2-ETHYL-p-XYLENE	L	2.3796	<10%
578	4-ETHYL-m-XYLENE	L	2.3702	<5%
579	4-ETHYL-o-XYLENE	L	2.4318	<10%
580	3-ETHYL-o-XYLENE	L	2.6141	<15%
582	2-PHENYLBUTENE-1	L	2.3187	<10%

Table A.4 Con't

ChemID	Compound	Phase	Recommended	Unc
583	cis-2-PHENYLBUTENE-2	L	2.5754	<10%
584	trans-2-PHENYLBUTENE-2	L	2.4584	<10%
585	1-METHYL-2-n-PROPYLBENZENE	L	2.4645	<10%
586	1-METHYL-3-n-PROPYLBENZENE	L	2.3643	<5%
587	1-METHYL-4-n-PROPYLBENZENE	L	2.2261	<1%
588	1,1,2-TRIPHENYLETHANE	L	2.4251	<3%
592	1,2-DIMETHYL-3-PROPYLBENZENE	L	2.4903	<3%
593	1,2,3-TRIMETHYL-4-ETHYLBENZENE	L	2.5632	<3%
594	1,2,4-TRIMETHYL-3-ETHYLBENZENE	L	2.4044	<1%
595	1,2,4-TRIMETHYL-5-ETHYLBENZENE	L	2.2975	<1%
596	1-(4-ETHYLPHENYL)-2-(4-ETHYLPHENYL)ETHANE	L	1.6068	<10%
597	2,2-DIPHENYL PROPANE	L	2.4719	<1%
602	o-METHYLSTYRENE	L	2.5985	<10%
603	m-METHYLSTYRENE	L	2.5238	<10%
605	o-ETHYLSTYRENE	L	2.5232	<10%
606	m-ETHYLSTYRENE	L	2.5406	<10%
612	p-METHYLSTYRENE	L	2.5593	<10%
614	m-DIVINYLBENZENE	L	2.4550	<10%
616	4-ISOBUTYLSTYRENE	L	2.5322	<10%
618	cis-1-PROPENYLBENZENE	L	2.6716	<10%
619	trans-1-PROPENYLBENZENE	L	2.6670	<10%
620	p-ISOPROPENYLSTYRENE	L	2.4878	<10%
621	p-tert-BUTYLSTYRENE	L	2.4413	<10%
704	1-ETHYLNAPHTHALENE	L	2.7458	<10%
709	2,6-DIMETHYLNAPHTHALENE	L	2.3637	<10%
710	1-PHENYLNAPHTHALENE	L	2.7707	<1%
711	1-n-NONYLNAPHTHALENE	L	2.4263	<10%
712	1-n-DECYLNAPHTHALENE	L	2.4051	<10%
713	1-n-BUTYLNAPHTHALENE	L	2.6874	<10%
714	1-n-HEXYLNAPHTHALENE	L	2.6226	<10%
715	2,7-DIMETHYLNAPHTHALENE	L	2.4900	<10%
716	1-n-HEXYL-1,2,3,4-TETRAHYDRONAPHTHALENE	L	2.5177	<10%
717	FLUORANTHENE	L	2.5640	<10%
718	1-n-PROPYLNAPHTHALENE	L	2.5336	<10%
719	2-ETHYLNAPHTHALENE	L	2.5625	<1%
723	1-METHYLINDENE	L	2.4519	<10%
724	2-METHYLINDENE	L	2.4866	<10%
725	1,2,3-TRIMETHYLINDENE	L	2.3814	<10%
726	METHYLCYCLOPENTADIENE DIMER	L	2.2800	<10%
728	1-PHENYLINDENE	L	2.7581	<10%
731	TRIPHENYLETHYLENE	L	2.3990	<5%
735	cis-STILBENE	L	2.5660	<3%
736	trans-STILBENE	L	2.5969	<5%
738	FLUORENE	L	2.6492	<10%
803	INDENE	L	2.8708	<10%
806	CHRYSENE	L	2.6631	<10%

Table A.4 Con't

ChemID	Compound	Phase	Recommended	Unc
807	PYRENE	L	3.0779	<10%
808	ACENAPHTHENE	L	2.6006	<10%
809	ACENAPHTHALENE	L	2.4445	<10%
810	ADAMANTANE	L	2.1513	<10%
811	VINYLNORBORNENE	L	2.8721	<10%
812	DIAMANTANE	L	1.9429	<10%
814	1,3-DIMETHYLADAMANTANE	L	2.1354	<10%
817	4-METHYLPHENANTHRENE	L	2.7886	<10%
818	METHYLNORBORNENE	L	2.2228	<10%
819	ETHYLNORBORNENE	L	2.2138	<10%
820	INDANE	L	2.6857	<10%
823	2-NORBORNENE	L	2.1539	<10%
824	5-ETHYLIDENE-2-NORBORNENE	L	2.4505	<10%
826	BENZANTHRACENE	L	3.2802	<10%
839	CAMPHENE	L	2.2282	<10%
1505	1,4-DICHLORO-trans-2-BUTENE	L	2.3482	<10%
1537	2,3-DICHLOROBUTANE	L	2.1443	<10%
1593	1,4-DICHLORO-cis-2-BUTENE	L	2.3476	<10%
1625	PERFLUORO-n-OCTANE	L	1.6778	<10%
1626	PERFLUORO-n-NONANE	L	1.6870	<10%
1627	PERFLUORO-n-DECANE	L	1.6778	<15%
1631	PERFLUORO-n-DODECANE	L	1.6971	<10%
1867	TRIETHYL ALUMINUM	L	3.3023	<10%
1869	TRIISOBUTYL ALUMINUM	L	1.8766	<10%
1884	TRIPHENYLPHOSPHINE	L	2.8638	<10%
2082	n-DOTRIACONTANE	L	2.0729	<3%
2086	n-HEXATRIACONTANE	L	2.0706	<3%
2095	2,3-DIMETHYLOCTANE	L	1.9944	<1%
2096	2,4-DIMETHYLOCTANE	L	1.9723	<3%
2097	2,5-DIMETHYLOCTANE	L	1.9803	<3%
2098	2,6-DIMETHYLOCTANE	L	1.9752	<3%
2226	3-METHYL-trans-2-PENTENE	L	2.0793	<10%
2240	5-METHYL-1-HEXENE	L	1.9471	<10%
2251	2-METHYL-1-OCTENE	L	1.9998	<10%
2252	2-METHYL-1-HEPTENE	L	1.9831	<10%
2285	1-METHYL-4-VINYLCYCLOHEXENE	L	2.1781	<10%
2310	1,2-HEXADIENE	L	2.0925	<15%
2414	1-HEPTYNE	L	2.3203	<10%
2522	1-ETHYL-2-ISOPROPYLBENZENE	L	2.2491	<1%
2575	n-PENTADECYLBENZENE	L	2.1643	<5%
2576	n-HEXADECYLBENZENE	L	2.1598	<5%
2577	n-HEPTADECYLBENZENE	L	2.1557	<5%
2578	n-OCTADECYLBENZENE	L	2.1528	<5%
2623	PERFLUORO-n-PENTANE	L	1.6059	<15%
2624	PERFLUORO-n-HEXADECANE	L	1.6807	<15%
2772	FUMARONITRILE	L	2.4426	<10%

Table A.4 Con't

ChemID	Compound	Phase	Recommended	Unc
2869	2-(2-(2-METHOXYETHOXY)ETHOXY)ETHANOL	L	2.2934	<10%
2925	ALUMINUM	L	37.2250	<10%
2930	MERCURY	L	6.3169	<10%
3251	7-METHYL-1-OCTENE	L	2.0109	<10%
3258	2-METHYL-1-NONENE	L	2.0273	<10%
3259	8-METHYL-1-NONENE	L	2.0595	<10%
3260	cis-2-DECENE	L	2.0866	<1%
3261	trans-2-DECENE	L	2.0398	<3%
3262	cis-2-DODECENE	L	2.1051	<1%
3263	trans-2-DODECENE	L	2.0623	<3%
3714	1-n-PENTYLNAPHTHALENE	L	2.4669	<10%
3730	TETRAMETHYLETHYLENEDIAMINE	L	2.0298	<10%
3922	TRIMETHYL INDIUM	L	2.3581	<10%
3923	TRIETHYL GALLIUM	L	2.4298	<10%
3969	TRIMETHYLALUMINUM	L	3.1757	<10%
3970	TRIMETHYLGALLIUM	L	2.2425	<10%
3971	TETRAETHYL LEAD	L	2.2223	<10%
20711	1-n-NONYLNAPHTHALENE_2004Review	L	2.5202	<10%
20712	1-n-DECYLNAPHTHALENE_2004Review	L	2.4969	<10%
21625	PERFLUORO-n-OCTANE_2004Review	L	1.6748	<10%
21627	PERFLUORO-n-DECANE_2004Review	L	1.6884	<10%
22623	PERFLUORO-n-PENTANE_2004Review	L	1.6167	<15%
22624	PERFLUORO-n-HEXADECANE_2004Review	L	1.7008	<15%
22869	2-(2-(2-METHOXYETHOXY)ETHOXY)ETHANOL_2004Review	L	2.2549	<10%

Bibliography

[1] Nelson, R. D., Lide, D. R. and Maryott, A. A., Selectred Values of Electric Dipole Moments for Molecules in the Gas Pase, NSRDS-NBS10, Washington, 1967.

[2] Pier L., S., Michele, P., Water Molecule Dipole in the Gas and in the Liquid Phase, **1999**, *Phys. Rev. Lett*. 82, 3308.

[3] Moore, W. J. Physical chemistry, 4th ed., Prentice-Hall, Englewood Cliffs, N.J., 1972.

[4] LeFevre, R. J. W., Dipole Moments, Their Measurement and Application in Chemistry, John Wiley and Sons, New York, 1953.

[5] Fishtine, S. H., Reliable Latent Heats of Vaporization. *Ind. Eng. Chem*., **1963**, 6, 47-56.

[6] Maryott, A., Birnbaum, G., *J. Chem. Phys*.,**1956**, 24, 1022.

[7] Boggs, J. E., Deam, A. P., *J. Chem. Phys*., **1960**, 32, 315.

[8] Higasi, K., Sci. Papers Inst. *Phys. Chem. Res.*, **1936**, 28, 284.

[9] Frank, F. C., *Proc. Roy. Soc*. 152 A, **1935**, 171.

[10] Rowley R. L., Wilding, W. V., Oscarson, J. L., Giles, N. F., *DIPPR® Data Compilation of Pure Chemical Properties*, Design Institute for Physical Properties, AIChE, New York, NY, 2009.

[11] Debye, P., Physik. Z., 13, 97 (1912); "Handbuch der Radiologie" (Marx), Akademische Verlagsgesellschaft m.b.H., Leipzig, 1925, VI, pp. 597-653; "Polar Molecules," Chemical Catalog, New York, 1929.

[12] Onsager, L., Electric Moments of Molecules in Liquids. *J. Am. Chem. Soc.* **1938**, *58*, 1486-1493.

[13] Maxwell, J. C., Treatise on Electricity, Oxford, London, vol, II, 1881.

[14] Kirkwood, J. G. The Dielectric Polarization of Polar Liquids. *J. Chem. Phys.* **1939**, *7*, 911.

[15] Kirkwood, J. G. *Ann. N. Y. Acad. Sci.*,**1940**, 40, 315; *Trans. Faraday Soc.* **1946**, *42A*, 7.

[16] Frohlich, H., Trans. *Faraday Soc.*, **1948**, 44, 238; Theory of Dielectrics, Oxford University Press, London, 1958.

[17] Heston, W. H., Hennelly, E. J., Smith, C. P., *J. Am. Chem. Soc*., **1950**, 72, 2071.

[18] Guggenheim, E. A., Trans. *Faraday Soc.,* **1949**, 45, 714.

[19] Guggenheim, E. A., Trans. *Faraday Soc.,* **1951**, 47, 573.

[20] Smith, J. W., Trans, *Faraday Soc*., **1950**, 46, 394.

[21] Smyth, C. P., *Dielectric Behaviour and Structure,* McGraw-Hill, N. Y., 1955.

[22] Debye, P., Physik. Z., **1912**,13, 97; "Handbuch der Radiologie" (Marx), Akademische Verlagsgesellschaft m.b.H., Leipzig, **1925**, VI, 597-653; "*Polar Molecules*," Chemical Catalog, New York, 1929.

[23] Onsager, L., *J. Am. Chem. Soc.*, **1938**, 58, 1486.

[24] Kirkwood, J. G., *J. Chem. Phys.*, **1939**, 7, 911.

[25] Ladanyi, B. M., Skaf, M. F., in: H. L. Strauss, G. T. Babcock, S. R. Leone (Eds.), *Ann. Rev. Phys. Chem*., Vol. 44, Annual Reviews, Palo alto, Ca, **1993**, 335-368.

[26] Tomasi J.; Mennucci, B.; Cappelli, C. In Handbook of Solvent; Wypych, G., Ed.; ChemTec Publishing: Toronto, 2001; Chapter 8, 487-489.

[27] Horvath, A. L., Molecular design: Chemical Structure Generation from the Properties of Pure Organic Compounds. Elserier, 1992.

[28] Papazian, H. A., *J. Am. Chem. Soc*., **1971**, 93, 5634-5641.

29 Holmes, C. F., *J. Am. Chem. Soc*., **1973**, 95, 1014-1016.

[30] Paruta, A. N., Sciarrone, B. J. and Lordi, N. G., *J. Pharm. Sci*., **1962**, 51, 704-705.

[31] Gorman, W. G. and Hall, G. D., *J. Pharm. Sci*.,**1964**,53, 1017-1020.

[32] Katritzky, A. R., Lobanov, V. S. and Karelson, M., *Chem. Soc. Rev*. **1995**, 24, 279.

[33] Katritzky, A. R., Maran, U., Lobanov, V.S. and Karelson, M. Structurally Diverse Quantitative Structure-Property Relationship Correlations of Technologically Relevant Physical Properties. *J. Chem. Inf. Comput. Sci*. **2000**, 40, 1-18.

[34] Schweitzer, R. C., Morris, J. B., *Anal. Chim. Acta*, **1999**, 394, 285-303.

[35] Cocchi, M., de Benedetti, P. G., Seeber, R., Tassi, L. and Ulrici, A., *J. Chem. Inf. Comput. Sci.*, **1999**, 39, 1190-1203.

[36] Sild, S. and Karelson, M., *J. Chem. Inf. Comput. Sci.*, **2002**, 42, 360-367.

[37] Lide, D. R., "Handbook of Chemistry and Physics, 88th ed.," CRC Press, LLC, 2007-2008

[38] CODESSA, Vesion 2.13, Semichem, http://www.semichem.com, 2008.

[39] Frisch, M. J., Trucks, G. W., Schlegel, H. B., et al., Gaussian98, Revision A.6, Gaussian, Inc., Pittsburgh, PA, 1998.

[40] Tsar QSAR, Accelrys Software, http://accelrys.com/products/accord/desktop/tsar.html, 2008.

[41] Bondi, A., *Physical Properties of Molecular Crystals, Liquids, and Glasses*, John Wiley, New York, 1968.

[42] Wesson, L. G., *Tables of electric dipole moments,* Massachusetts Institute of Technology, Technology Press, 1948.

[43] Riddick, J. A., Bunger, W. B. and Sakano, T., K., *Organic Solvents*, *4e*, John Wiley & Sons, New York, 1986.

[44] NIST Computational Chemistry Comparison and Benchmark DataBase, http://srdata.nist.gov/cccbdb/default.htm.

[45] Oster, G. The Dielectric Properties of Liquid Mixtures. *J. Am. Chem. Soc*. **1946**, 68, 2036-2041.

[46] Harvey, A. H., Prausnitz, J.M., Dielectric Constants of Fluid Mixtures over a Wide Range of Temperature and Density. *J. Solut. Chem*. **1987**, 16, 857–869.

[47] Buckingham, A. D., The Dielectric Constant of a Liquid. *Aust. J. Chem***. 1953**, 6, 93–103.

[48] Buckingham, A. D., The Calculation of True Dipole Moments from Solutions in Polar Solvents. *Aust. J. Chem*.*Aust. J. Chem*. **1953**, 6, 323–331.

[49] Wang, P. and Anderko, A., Computation of Dielectric Constants of Solvent Mixtures and Electrolyte Solutions. *Fluid Phase Equilib.* **2001**, 186, 103-122.

[50] Prestbo, E. W. and McHale, J. L., Static Dielectric Constants and Kirkwood Correlation Factors of Dimethyl Sulfoxide/Carbon Tetrachloride Solutions. *J. Chem. Eng. Data* **1984**, 29, 387-389.

[51] Renon H. and Prausnitz, J. M., *Ind. Eng. Chem Process Design Develop.,* **1969**, 8, 413.

[52] Rowley, R. L., A Local Composition Model for Multicomponent Liquid Mixture Thermal Conductivities. *Chem. Eng. Sci.* **1982**, 37, 897-904.

[53] Wei, I. C., Rowley, R. L., A Local Composition Model for Multicomponent Liquid Mixture Shear Viscosity. *Chem. Eng. Sci.* **1985**, 40, 401-408.

[54] Gmehling, J., Onken, W., Arlt, W. *Vapor-Liquid Equilibrium Data Collection;* DECHEMA Chemistry Data Series, DECHEMA, Frankfurt, Germany, 1982.

[55] Campbell, A. N. and Kartzmark, E. M., *J. Chem. Thermodyn*. **1973**, 5, 163–172.

[56] Åkerlöf, G., *J. Am. Chem. Soc*. **1932**, 54, 4125–4139.

[57] Sigvartsen, T., Songstad, J., Gestblom, B. and Norelan, E., *J. Solut. Chem*, **1991**, 20, 565–5582.

[58] Suryanarayana, C. V. and Somasundaram, K., M., *Acta Chim. Hung*. **1960**, 24, 31–53.

[59] Jain, D. V. S., Wadl, R. K., Saini, S. B. and Puri, K., *J. Chem. Thermodyn.* **1978**, 10, 707.

[60] Geddes, J. A., The Fluidity of Dioxane – Water Mixtures. *J. Am. Chem. Soc*. **1933**, 55, 4832-4837.

[61] Schrodle, S., Hefter, G., Buchner, R., Dielectric Spectroscopy of Hydrogen Bond Dynamics and Microheterogenity of Water þ Dioxane Mixtures. *J. Phys. Chem*. B **2007**, 111, 5946.

[62] Fredenslund, A., Gmehling, J. and Rasmussen, P., *Vapor-Liquid Equilibrium Using UNIFAC*; Elsevier, Amsterdam, **1977**.

[63] Kirkwood, J. G., *J. Chem. Phys.* **1939**, 7. 911.

[64] Frohlich, H., *Trans. Faraday Soc*., **1948**, 44, 238.

[65] Neumann, M., *Mol. Phys*. **1983**, 50, 841.

[66] Neumann, M. and Steinhauser, O., *Chem. Phys. Lett*., **1983**, 95, 417.

[67] Neumann, M. and Steinhauser, O., *Mol. Phys*. **1986**, 57, 97.

[68] de Leeuw, S. W., Perram, J. W., Smith, E. R., *Annu. Rev. Phys. Chem*., **1986**, 37, 245.

[69] Hunenberger, P. H. and van Gunsteren, W. F., *J. Chem. Phys*., **1998**, 108, 6117.

[70] Barker, J. A. and Watts, R. O., *Mol. Phys*, **1973**, 26, 789.

[71] Tironi, I. G., Sperb, R., Smith, P. E., van Gunsteren, W. F., *J. Chem. Phys*. **1995**, 102, 5451.

[72] Neumann, M., Steinhauser, O. and Pawley, G. S., *Mole. Phys*. **1984**, 52, 97.

[73] Burnham, C. J. and Wantheas, S. S., *J. Chem. Phys*. **2002**, 116, 5115.

[74] Jeon, J., Lefohn, A. E. and Voth, G. A., *J. Chem. Phys*, **2003**, 118, 7504.

[75] Berendsen, H, J. C., Postma, J. P. M., van Gunsteren, W. F. and Hermans, H., *Intermolecular Forces*, edited by B. Pullman, **1981**, 331.

[76] Berendsen, H. J. C. , Grigera, J. R. and Strastsma, T. P., *J. Phys. Chem*., **1987**, 91, 6269.

[77] Wu, Y. J., Tepper, H. L. and Voth, G. A., *J. Phys. Chem*, **2006**, 124, 2, 024503.

[78] Edberg, R., Evans, D. J. and Morriss, G. P., *J. Chem. Phys.*, **1986**, 84, 6933.

[79] Edberg, R., Morriss, G. P. and Evans, D. J., *J. Chem. Phys.,* **1987**, 86, 4555.

[80] Wheeler, D. R. and Rowley, R. L., *Molec. Phys.*, **1998**, 94, 555.

[81] Fuller, N. G. and Rowley, R. L., *Int. J. Thermophys.*, **1998**, 19, 1039.

[82] Allen,M.P., Tildesley, D.J., Computer Simulation of Liquids, Oxford Science, Oxford, **1987**.

[83] Thomas J. C. and Rowley, R. L., *J. Chem. Phys.*, **2011**, 134, 024526.

[84] Allen, M. P. and Tildesley, D. J., Compute Simulation of Liquids, Oxford University Press, Oxford, 1987, Chap. 5.

[85] Fuller, N. G.and Rowley, R. L., *Int. J. Thermophys.*, **2000**, 21, 45.

[86] Cabaco, M. I., Danten, Y., Besnard, M., Guissani, Y. and Guillot, B., *J. Phys. Chem*. B 101, **1997**, 6977.

[87] Jedlovszky, P. and Palinkas, G. **1995**, *Molec. Phys*, 84, 217.

[88] Richardi, J, Fries, P. H. , Fischer, R., Rast, S. and Krienke, H., **1998**, *Molec. Phys*., 93, 925.

[89] Easteal, A. J. and Woolf L.A., *J. Chem. Thermodynamics*. **1985**, 17, 69-82.

[90] Gotze, G. and Schneider, G. M., *J. Chem. Thermodynamics*, **1988**, 12, 661-672.

[91] Tolosa, S., Sanson, J. A. and Hidalgo, A., Theoretical–experimental study of the solvation enthalpy of binary liquid mixtures in dilute aqueous solution: Application to the acetone–water system. *Chem. Phys.,* **2005**.

[92] Tolosa, S., Sanson, J. A., Martin, N. and Hidalgo, A., Molecular dynamics simulation of aqueous solutions using interaction energy components: Application to the dielectric properties of the acetone–water system. *Molecular Simulation*, **2005**, 31, 549–553.

[93] Matsuoka, D., Clementi, E. and Yoshimina, M., CI study of the water dimer potential surface. *J. Chem. Phys*., **1976**, 64, 1351.

[94] Eliane C. and Kollman, K. A., Molecular dynamics studies of the properties of water around simple organic solutes. *J. Phys. Chem*., **1996**, 100, 11460-11470.